Coordinated Multi Point Transmission and Reception for Mixed-Delay Traffic

Homa Nikbakht, *Student Member, IEEE*, Michèle Wigger, *Senior Member, IEEE*, and Shlomo Shamai (Shitz), *Life Fellow, IEEE*

Abstract

This paper analyzes the multiplexing gains (MG) for simultaneous transmission of delay-sensitive and delay-tolerant data over interference networks. In the considered model, only delay-tolerant data can profit from coordinated multipoint (CoMP) transmission or reception techniques, because delay-sensitive data has to be transmitted without further delay. Transmission of delay-tolerant data is also subject to a delay constraint, which is however less stringent than the one on delay-sensitive data. Different coding schemes are proposed, and the corresponding MG pairs for delay-sensitive and delay-tolerant data are characterized for Wyner's linear symmetric network and for Wyner's two-dimensional hexagonal network with and without sectorization. Information-theoretic converses are established for all the three models. For Wyner's linear symmetric the bounds match whenever the cooperation rates are sufficiently large or the delay-sensitive MG is small or moderate. These results show that on Wyner's symmetric linear network and for sufficiently large cooperation rates, the largest MG for delay-sensitive data can be achieved without penalizing the maximum sum-MG of both delay-sensitive and delay-tolerant data. Our achievable schemes show that a similar conclusion holds for Wyner's hexagonal network only for the model with sectorization. In the model without sectorization, a penalty in sum-MG is incurred whenever one insists on a positive delay-sensitive MG.

H. Nikbakht and M. Wigger are with LTCI, Télécom Paris, IP Paris, 91120 Palaiseau, France. E-mails: {homa.nikbakht, michele.wigger}@telecom-paris.fr. S. Shamai, is with the Department of Electrical Engineering, Technion—Israel Institute of Technology, Technion City, 32000, Israel, e-mail: sshlomo@ee.technion.ac.il. Part of this work has been presented at IEEE SPAWC 2019 [33]. The work of H. Nikbakht and M. Wigger has been supported by the European Union's Horizon 2020 Research And Innovation Programme, grant agreement no. 715111. The work of S. Shamai has been supported by the European Union's Horizon 2020 Research And Innovation Programme, grant agreement no. 694630.

I. Introduction

One of the main challenges for future wireless communication systems is to accommodate heterogeneous data streams with different delay constraints. This is also the focus of various recent works, notably [1]–[7]. In particular, [1], [2] study a cloud radio access network (C-RAN) under mixed-delay-constraints traffic. Specifically, users close to base stations (BS) transmit delay-sensitive data, which is directly decoded at the BSs, and users that are further away send delay-tolerant data, which is decoded at the central processor. In this paper we refer to delay-tolerant data as *"slow" messages*, and to delay-sensitive data as *"fast" messages*. In [4], we extended above C-RAN model to allow each user to send both "fast" and "slow" messages, and to time-varying fading channels. The results in [4] show that at any "fast" rate, the stringent delay constraint on "fast" messages penalizes the overall performance (sum-rate) of the system.

The work in [5] proposes a superposition approach over a fading channel to communicate "fast" messages within single coherence blocks and "slow" messages over multiple blocks. In [6] a scheduling algorithm is proposed for a K-user broadcast network that gives preference to the communication of "fast" messages over "slow" messages. A related work was performed in [7], where "fast" messages can be stored in a buffer during a single scheduling period.

The focus of the current work is on the benefits of cooperation for mixed-delay traffics, assuming that only the transmissions of "slow" messages can profit from cooperation between terminals, but not "fast" messages. Networks with transmitter- (Tx) and/or receiver- (Rx) cooperation have been considered in many recent works including [8]–[18] but mostly only with a single type of messages, namely the messages that we call "slow" messages. Huleihel and Steinberg [8] considered two types of messages: one type that has to be decoded whether or not the Rx-cooperation link is present, and the other that only has to be decoded when the cooperation link is present. Inspired by this model, we studied Wyner's soft-handoff model [22], [23] with mixed-delay traffics in [19], where the Tx-cooperation messages can only depend on the "slow" messages in the system and not on the "fast" messages, and "fast" messages have to be decoded prior to the Rx-cooperation phase, whereas "slow" messages can be decoded thereafter. Moreover, in [19] the total number of Tx- and Rx- cooperation rounds is constrained also for the "slow" messages as proposed [18]. The problem setup that we consider in this paper is different from the setups in [9]–[18] as each Tx wishes to send both "fast" and "slow" messages, and is different from the setup in [19] as it covers networks with arbitrary interference

graphs whereas in [19], we focus on Wyner's soft-handoff model where the signal sent by each transmitter interferes only the observed signal by the receiver to its right. The results in [19] show that, in the high signal to noise ratio (SNR) regime, when both the Txs and the Rxs can cooperate, and for sufficiently large cooperation rates, it is possible to accommodate the largest possible rate for "fast" messages without penalizing the maximum sum-rate of both "fast" and "slow" messages. When only Txs or only Rxs can cooperate, transmitting also "fast" messages causes no penalty on the sum-rate at low "fast" rates, but the sum-rate decreases linearly at high "fast" rates. Notice that the standard approach to combine the transmissions of "slow" and "fast" messages is to time-share (schedule) the transmission of "slow" messages with the transmission of "fast" messages. In this approach, the sum-rate decreases linearly with the rate of the "fast" messages and attains the maximum sum-rate only when no "fast" messages are transmitted.

The focus of this paper is on the pairs of *Multiplexing Gains (MG)*, also called degrees of freedom or capacity prelogs, that are simultaneously achievable for "fast" and "slow" messages. We propose a general coding scheme for any interference network with Tx- and Rx-cooperation that simultaneously accommodates the transmissions of "slow" and "fast" messages, and characterize their achievable MG pairs for two specific cellular network models: Wyner's linear symmetric model [22], [23] and Wyner's two-dimensional hexagonal model [22] with and without sectorization. In Wyner's linear symmetric model, cells are aligned in a line and interference is short range, so that transmissions in a cell are interfered only by transmissions from the two neighbouring cells. Such a model is adequate for systems deployed along highways, railroads or long corridors, see also [41]. In Wyner's two-dimensional models, cells are of hexagonal shapes and transmissions in a cell are interfered by the transmissions in the six neighbouring cells. Sectorization occurs in this model if the BS employs directional antennas pointed to three different directions, so that transmissions in these sectors do not interfere. The hexagonal models are adequate for systems where BSs are spread in two dimensions. For all three considered models, in this paper we assume that the various users of the same cell are scheduled in different frequency bands. Interference thus occurs only from the mobile users in neighbouring cells that are scheduled on the same frequency band.

We establish information-theoretic converses for all three models. For Wyner's symmetric network the converse bound matches the proposed set of achievable MG pairs when the cooperation links are of sufficiently high prelogs or when the MG of "fast" messages is small. These results show that when the prelog of the cooperation links is sufficiently large, for

Wyner's linear symmetric model, as for Wyner's linear soft-handoff model [19], it is possible to accommodate the largest possible MG for "fast" messages without penalizing the maximum sum MG of both "fast" and "slow" messages. Our achievable schemes suggest that the same also holds for the sectorized hexagonal model considered in this paper where each cell is divided into three non-interfering sectors by employing directional antennas at the BSs [33]. In contrast, for the considered non-sectorized hexagonal model, there seems to be a penalty in maximum sum MG whenever the "fast" MG is larger than 0.

To achieve the described performances, we propose a novel coding scheme where we assign "fast" and "slow" messages to different sets of transmitters in a way that "fast" transmissions are interfered only by "slow" transmissions. Then we use precoding and successive interference cancellation techniques to transmit each of the "fast" messages at full MG without disturbing the transmission of "slow" messages. The transmission of "slow" messages can benefit from cooperation by applying CoMP reception/ transmission in small subnets to jointly decode/encode the "slow" messages at different Rxs/Txs. More specifically, in our coding scheme, we identify a set of the Txs whose signals do not interfere. The chosen Txs send "fast" messages and the others send "slow" messages or nothing. Communication of "fast" messages is thus only interfered by transmissions of "slow" messages and this interference can be described during the Tx-conferencing phase and precanceled at the "fast" Txs. Also, "fast" Rxs decode their messages immediately and can describe their decoded messages during the Rx-conferencing phase to their adjacent "slow" Rxs allowing them to subtract the interference from "fast" messages before decoding their own "slow" messages. As a result, "fast" messages can be decoded based on interference-free outputs and moreover, they do not disturb the transmission of "slow" messages. CoMP transmission or reception [20], [21] for limited clusters is then employed to convey the "slow" messages.

A. Organization

The rest of this paper is organized as follows. We end this section with some remarks on notation. The following Sections II and III consider general interference networks and describe the problem setup and the proposed coding scheme and its multiplexing gain region for such a general network. Sections IV–VI specialize the results to the symmetric linear Wyner model and to the two-dimensional hexagonal Wyner model. Section VII concludes the paper.

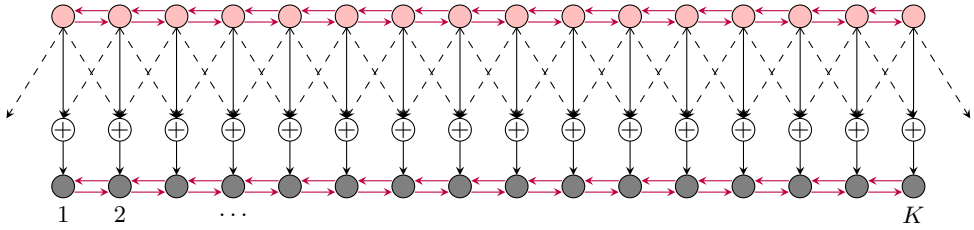

Fig. 1: Wyner's symmetric network. Black dashed arrows show interference links and purple arrows cooperation links.

B. Notation

We use the shorthand notations "Rx" for "Receiver" and "Tx" for "Transmitter". The set of all integers is denoted by $\mathbb{Z}$, the set of positive integers by $\mathbb{Z}^+$ and the set of real numbers by $\mathbb{R}$. For other sets we use calligraphic letters, e.g., $\mathcal{X}$. Random variables are denoted by uppercase letters, e.g., X, and their realizations by lowercase letters, e.g., x. For vectors we use boldface notation, i.e., upper case boldface letters such as $\mathbf{X}$ for random vectors and lower case boldface letters such as $\mathbf{x}$ for deterministic vectors.) Matrices are depicted with sans serif font, e.g., H. We use $[K]$ to denote the set $\{1, \ldots, K\}$. We also write X^n for the tuple of random variables $(X_1, \ldots, X_n)$ and $\mathbf{X}^n$ for the tuple of random vectors $(\mathbf{X}_1, \ldots, \mathbf{X}_n)$.

II. Problem Description

Consider a cellular interference network with K cells each consisting of one Tx and Rx pair. Txs and Rxs are equipped with L antennas and we assume a regular interference pattern except at the network borders. As an example, Fig. 1 shows Wyner's symmetric network where each cell corresponds to a Tx/Rx pair and the interference pattern is depicted with black dashed lines.

Each Tx $k \in [K]$ sends a pair of independent messages $M_k^{(F)}$ and $M_k^{(S)}$ to Rx $k \in [K]$. The "fast" message $M_k^{(F)}$ is uniformly distributed over the set $\mathcal{M}_k^{(F)} \triangleq \{1, \ldots, \lfloor 2^{nR_k^{(F)}} \rfloor\}$ and needs to be decoded subject to a stringent delay constraint, as we explain shortly. The "slow" message $M_k^{(S)}$ is uniformly distributed over $\mathcal{M}_k^{(S)} \triangleq \{1, \ldots, \lfloor 2^{nR_k^{(S)}} \rfloor\}$ and is subject to a less stringent decoding delay constraint. Here, n denotes the blocklength of transmission and $R_k^{(F)}$ and $R_k^{(S)}$ the rates of transmissions of the "fast" and "slow" messages.

We consider a cooperation scenario where neighbouring Txs cooperate during $\mathsf{D}_{\text{Tx}} > 0$ rounds and neighbouring Rxs during $\mathsf{D}_{\text{Rx}} > 0$ rounds. The total cooperation delay is constrained:

$$\mathsf{D}_{\text{Tx}} + \mathsf{D}_{\text{Rx}} \leq \mathsf{D}, \tag{1}$$

where $\mathrm{D} \geq 0$ is a given parameter of the system and the values of D_{Tx} and D_{Rx} are design parameters and can be chosen arbitrary such that (1) is satisfied.

To describe the encoding at the Txs, denote by $\mathcal{N}_{\mathrm{Tx}}(k)$ the set of all Txs that have a direct cooperation link with a given Tx $k \in [K]$. We refer to $\mathcal{N}_{\mathrm{Tx}}(k)$ as the *Tx-neighbouring set* of Tx k. Neighbouring Txs can communicate to each other during $\mathrm{D}_{\mathrm{Tx}} > 0$ rounds, where this communication can only depend on "slow" messages but not on "fast" messages. In each conferencing round $j \in \{1, \ldots, \mathrm{D}_{\mathrm{Tx}}\}$, Tx k sends a cooperation message $T_{k\to\ell}^{(j)}\Big(M_k^{(S)}, \{T_{\ell'\to k}^{(1)}, \ldots, T_{\ell'\to k}^{(j-1)}\}_{\ell' \in \mathcal{N}_{\mathrm{Tx}}(k)}\Big)$ to Tx ℓ if $\ell \in \mathcal{N}_{\mathrm{Tx}}(k)$. The cooperation communication is assumed noise-free but rate-limited:

$$\sum_{j=1}^{\mathrm{D}_{\mathrm{Tx}}} H(T_{k\to\ell}^{(j)}) \leq \mu_{\mathrm{Tx}} \cdot \frac{n}{2} \log(\mathsf{P}), \qquad k \in [K],\ \ell \in \mathcal{N}_{\mathrm{Tx}}(k), \tag{2}$$

for a given *Tx-conferencing prelog* $\mu_{\mathrm{Tx}} > 0$ and where $H(\cdot)$ denotes the entropy function and $\mathsf{P} > 0$ is the average block power constraint.

Tx k computes its channel inputs $\mathbf{X}_k^n = (\boldsymbol{X}_{k,1}, \ldots, \boldsymbol{X}_{k,n}) \in \mathbb{R}^{\mathsf{L}\times n}$ as a function of its "fast" and "slow" messages and of the $\mathrm{D}_{\mathrm{Tx}}|\mathcal{N}_{\mathrm{Tx}}(k)|$ obtained cooperation messages:

$$\mathbf{X}_k^n = f_k^{(n)}\Big(M_k^{(F)}, M_k^{(S)}, \{T_{\ell'\to k}^{(1)}, \ldots, T_{\ell'\to k}^{(\mathrm{D}_{\mathrm{Tx}})}\}_{\ell' \in \mathcal{N}_{\mathrm{Tx}}(k)}\Big). \tag{3}$$

The channel inputs have to satisfy the average block-power constraint almost surely:

$$\frac{1}{n}\sum_{t=1}^{n} ||\mathbf{X}_{k,t}||^2 \leq \mathsf{P}, \quad \forall\ k \in [K]. \tag{4}$$

To describe the decoding, denote the *Rx-neighbouring set* of a given Rx $k \in [K]$, i.e., the set of all receivers that can directly exchange cooperation messages with Rx k, by $\mathcal{N}_{\mathrm{Rx}}(k)$. Also, define the *interference set* $\mathcal{I}_k$ as the the set of all Txs whose signals interfere at Rx k.

Decoding takes place in two phases. During the *fast-decoding phase*, each Rx k decodes its "fast" message $M_k^{(F)}$ based on its channel outputs $\mathbf{Y}_k^n = (\boldsymbol{Y}_{k,1}, \ldots, \boldsymbol{Y}_{k,n}) \in \mathbb{R}^{\mathsf{L}\times n}$, where

$$\mathbf{Y}_k^n = \mathsf{H}_{k,k}\boldsymbol{X}_k^n + \sum_{\hat{k}\in\mathcal{I}_k} \mathsf{H}_{\hat{k},k}\boldsymbol{X}_{\hat{k}}^n + \boldsymbol{Z}_k^n, \tag{5}$$

and $\boldsymbol{Z}_{k,k}^n$ is i.i.d. standard Gaussian noise, and the fixed L-by-L full-rank matrix $\mathsf{H}_{\hat{k},k}$ models the channel from Tx $\hat{k}$ to the receiving antennas at Rx k. So, Rx k produces:

$$\hat{M}_k^{(F)} = g_k^{(n)}\big(\mathbf{Y}_k^n\big), \tag{6}$$

using some decoding function $g_k^{(n)}$ on appropriate domains. In the subsequent *slow-decoding phase*, each Rx $k \in [K]$ sends a conferencing message

$Q_{k\to\ell}^{(j)}\Big(\mathbf{Y}_k^n, \{Q_{\ell'\to k}^{(1)}, \ldots, Q_{\ell'\to k}^{(j-1)}\}_{\ell'\in\mathcal{N}_{\text{Rx}}(k)}\}\Big)$ during cooperation round $j \in \{1, \ldots, \mathrm{D}_{\text{Rx}}\}$ to Rx ℓ if $\ell \in \mathcal{N}_{\text{Rx}}(k)$. The cooperative communication is noise-free, but rate-limited:

$$\sum_{j=1}^{\mathrm{D}_{\text{Rx}}} H(Q_{k\to\ell}^{(j)}) \le \mu_{\text{Rx}} \cdot \frac{n}{2}\log(\mathsf{P}), \qquad k \in [K],\ \ell \in \mathcal{N}_{\text{Rx}}(k), \tag{7}$$

for given *Rx-conferencing prelog* $\mu_{\text{Rx}} > 0$. Each Rx k decodes its desired "slow" message as

$$\hat{M}_k^{(S)} = b_k^{(n)}\Big(\mathbf{Y}_k^n, \Big\{Q_{\ell'\to k}^{(1)}, \ldots, Q_{\ell'\to k}^{(\mathrm{D}_{\text{Rx}})}\Big\}_{\ell'\in\mathcal{N}_{\text{Rx}}(k)}\Big), \tag{8}$$

using some decoding function $b_k^{(n)}$ on appropriate domains.

Throughout this article we assume short range interference and thus:

$$\mathcal{I}_k \subseteq (\mathcal{N}_{\text{Rx}}(k) \cap \mathcal{N}_{\text{Tx}}(k)). \tag{9}$$

Given power $\mathsf{P} > 0$, maximum delay $\mathrm{D} \ge 0$, and cooperation prelogs $\mu_{\text{Rx}}, \mu_{\text{Tx}} \ge 0$, average rates $(\bar{R}_K^{(S)}(\mathsf{P}), \bar{R}_K^{(F)}(\mathsf{P}))$ are called achievable, if there exist rates $\{(R_k^{(F)}, R_k^{(S)})\}_{k=1}^K$ satisfying

$$\bar{R}_K^{(F)} := \frac{1}{K}\sum_{k=1}^K R_k^{(F)}, \quad \text{and} \quad \bar{R}_K^{(S)} := \frac{1}{K}\sum_{k=1}^K R_k^{(S)}, \tag{10}$$

and encoding, cooperation, and decoding functions for these rates satisfying constraints (1), (2), (4), and (7) and so that the probability of error vanishes:

$$p(\text{error}) \triangleq \mathbb{P}\Big[\bigcup_{k\in[K]}\Big(\big(\hat{M}_k^{(F)} \ne M_k^{(F)}\big) \cup \big(\hat{M}_k^{(S)} \ne M_k^{(S)}\big)\Big)\Big] \to 0 \quad \text{as} \quad n \to \infty. \tag{11}$$

An MG pair $(\mathsf{S}^{(F)}, \mathsf{S}^{(S)})$ is called *achievable*, if for every positive integer K and power $P > 0$ there exist achievable average rates $\{\bar{R}_K^{(F)}(\mathsf{P}), \bar{R}_K^{(S)}(\mathsf{P})\}_{\mathsf{P}>0}$ satisfying

$$\mathsf{S}^{(F)} \triangleq \varlimsup_{K\to\infty} \varlimsup_{\mathsf{P}\to\infty} \frac{\bar{R}_K^{(F)}(\mathsf{P})}{\frac{1}{2}\log(\mathsf{P})}, \quad \text{and} \quad \mathsf{S}^{(S)} \triangleq \varlimsup_{K\to\infty} \varlimsup_{\mathsf{P}\to\infty} \frac{\bar{R}_K^{(S)}(\mathsf{P})}{\frac{1}{2}\log(\mathsf{P})}. \tag{12}$$

The closure of the set of all achievable MG pairs $(\mathsf{S}^{(F)}, \mathsf{S}^{(S)})$ is called *optimal MG region* and denoted $\mathcal{S}^\star(\mu_{\text{Tx}}, \mu_{\text{Rx}}, \mathrm{D})$.

Remark 1: In (12), we let $K \to \infty$ to remove the boundary effects. The coding scheme proposed in the following Section III can be implemented for arbitrary values of K.

III. Coding Schemes and Achievable Multiplexing Gains

We describe various coding schemes that either transmit both "fast" and "slow" messages (Subsections III-A and III-B) or only "slow" messages (Subsection III-C), and a scheme that does not use any kind of cooperation (Subsection III-D).

An important building block in our coding schemes is CoMP transmission or CoMP reception. Depending on which of the two is used, the scheme requires more Tx- or Rx-cooperation rates. So, depending on the application, any of the two can be advantageous. In some applications, cooperation rates might however be too low to employ either of the two. In this case, the proposed schemes can be time-shared with alternative schemes that require less or no cooperation rates at all. Alternatively, the proposed schemes can be employed with a smaller number of cooperation rounds $\mathrm{D}' < \mathrm{D}$, which also reduces the required cooperation prelog in all our schemes.

A. Coding scheme to transmit both "fast" and "slow" messages with CoMP reception:

Split the total number of conferencing rounds between Tx- and Rx-conferencing as:

$$\mathrm{D}_{\mathrm{Tx}} = 1 \quad \text{and} \quad \mathrm{D}_{\mathrm{Rx}} = \mathrm{D} - 1. \tag{13}$$

1) Creation of subnets and message assignment: Each network is decomposed into three subsets of Tx/Rx pairs, $\mathcal{T}_{\text{silent}}$, $\mathcal{T}_{\text{fast}}$ and $\mathcal{T}_{\text{slow}}$, where

- Txs in $\mathcal{T}_{\text{silent}}$ are silenced and Rxs in $\mathcal{T}_{\text{silent}}$ do not take any action.
- Txs in $\mathcal{T}_{\text{fast}}$ send only "fast" messages. The corresponding Txs/Rxs are called "fast".
- Txs in $\mathcal{T}_{\text{slow}}$ send only "slow" messages. The corresponding Txs/Rxs are called "slow".

We choose the sets $\mathcal{T}_{\text{silent}}$, $\mathcal{T}_{\text{fast}}$ and $\mathcal{T}_{\text{slow}}$ in a way that:

- the signals sent by the "fast" Txs do not interfere; and
- silencing the Txs in $\mathcal{T}_{\text{silent}}$ decomposes the network into non-interfering subnets such that in each subnet there is a dedicated Rx, called *master Rx*, that can send a cooperation message to any other "slow" Rx in the same subnet in at most $\left\lfloor \frac{\mathrm{D}_{\mathrm{Rx}}-1}{2} \right\rfloor$ cooperation rounds.

For example, consider Wyner's symmetric model (described in detail in Section IV) where Txs and Rxs are aligned on a grid and cooperation is possible only between neighbouring Txs or Rxs. Interference at a given Rx is only from adjacent Txs. The network is illustrated in Figure 2. This figure also shows a possible decomposition of the Tx/Rx pairs into the sets $\mathcal{T}_{\text{silent}}$ (in white), $\mathcal{T}_{\text{fast}}$ (in yellow) and $\mathcal{T}_{\text{slow}}$ (in blue) when $\mathrm{D} = 6$. The proposed decomposition creates subnets

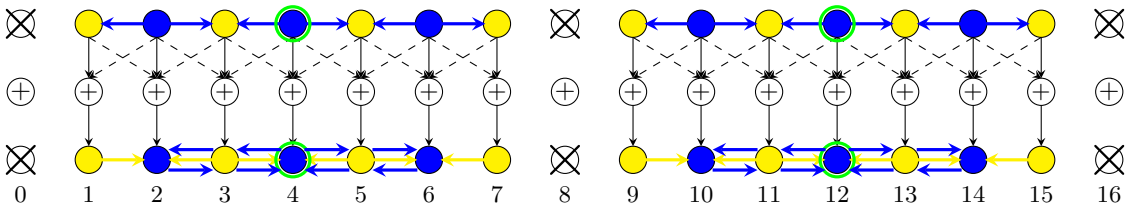

Fig. 2: Illustration of message assignment and cooperation in Wyner's symmetric network.

with 7 active Tx/Rx pairs where the Rx in the center of any subnet (e.g. Rx 4 in the first subnet) can serve as a master Rx as it reaches any slow (blue) Rx in the same subnet in at most $\lfloor \mathrm{D}_{\mathrm{Rx}} - 1/2 \rfloor = \lfloor (\mathrm{D}-2)/2 \rfloor = 2$ cooperation rounds. As required, transmissions from fast (yellow) Txs are only interfered by transmissions from slow (blue) Txs.

2) Precanceling of "slow" interference at "fast" Txs: Any "slow" Tx k' quantizes its pre-computed input signal $X_{k'}^n$ (how this signal is generated will be described under item 5)) and describes the quantised signal $\hat{X}_{k'}^n$ during the last Tx-cooperation round to all its neighbouring "fast" Txs, which then precancel this interference on their transmit signals. (Here, there is only a single Tx-cooperation round, but this item will be reused in later subsections where $\mathrm{D}_{\mathrm{Tx}} > 1$.) Fig. 2 illustrates the sharing of the described quantization information with neighbouring "fast" Txs for Wyner's symmetric model.

To describe this formally, for each $k \in \{1, \ldots, K\}$, we define the *"slow" interfering set*

$$\mathcal{I}_k^{(S)} \triangleq \mathcal{I}_k \cap \mathcal{T}_{\text{slow}}. \tag{14}$$

Also, we denote by $\boldsymbol{U}_k^n(M_k^{(F)})$ the non-precoded input signal precomputed at a given "fast" Tx k. (The following item 3) explains how to obtain $\boldsymbol{U}_k^n(M_k^{(F)})$.) Tx k sends the inputs

$$\boldsymbol{X}_k^n = \boldsymbol{U}_k^n(M_k^{(F)}) - \sum_{k' \in \mathcal{I}_k^{(S)}} \mathsf{H}_{k,k}^{-1} \mathsf{H}_{k',k} \hat{\boldsymbol{X}}_{k'}^n, \tag{15}$$

over the channel. Since each "fast" Rx k is not interfered by the signal sent at any other "fast" Tx, the precoding in (15) makes that a "fast" Rx k observes the almost interference-free signal

$$\boldsymbol{Y}_k^n = \mathsf{H}_{k,k} \boldsymbol{U}_k^n + \underbrace{\sum_{k' \in \mathcal{I}_k^{(S)}} \mathsf{H}_{k',k} (\boldsymbol{X}_{k'}^n - \hat{\boldsymbol{X}}_{k'}^n) + \boldsymbol{Z}_k^n}_{\text{disturbance}}, \tag{16}$$

where the variance of above disturbance is around noise level and does not grow with P.

3) Transmission of "fast" messages: Each "fast" Tx k encodes its desired message $M_k^{(F)}$ using a codeword $\mathbf{U}_k^{(n)}(M_k^{(F)})$ from a Gaussian point-to-point code of power P. The corresponding Rx k applies a standard point-to-point decoding rule to directly decode this "fast" codeword without Rx-cooperation from its "almost" interference-free outputs $\mathbf{Y}_k$, see (16).

4) Canceling "fast" interference at "slow" Rxs: According to the previous item 3), all "fast" messages are decoded directly from the outputs without any Rx-cooperation. During the first Rx-cooperation round, all "fast" Rxs can thus share their decoded messages with all their neighbouring "slow" Rxs, which can cancel the corresponding interference from their receive signals. More formally, we define the *fast interference set*

$$\mathcal{I}_k^{(F)} \triangleq \mathcal{I}_k \cap \mathcal{T}_{\text{fast}} \tag{17}$$

as the set of "fast" Txs whose signals interfere at Rx k. Each "slow" Rx k forms the new signal

$$\hat{\boldsymbol{Y}}_k^n := \boldsymbol{Y}_k^n - \sum_{\hat{k}\in\mathcal{I}_k^{(F)}} \mathsf{H}_{\hat{k},k}\boldsymbol{X}_{\hat{k}}^n(\hat{M}_{\hat{k}}^{(F)}), \tag{18}$$

and decodes its desired "slow" message based on this new signal following the steps described in the following item 5). Fig. 2 illustrates with yellow arrows the sharing of decoded "fast" messages with neighbouring "slow" Rxs in Wyner's symmetric model.

5) Transmission and reception of "slow" messages using CoMP reception: Each "slow" Tx k encodes its message $M_k^{(S)}$ using a codeword $\boldsymbol{X}_k^n(M_k^{(S)})$ from a Gaussian point-to-point code of power P. "Slow" messages are decoded based on the new outputs $\hat{\boldsymbol{Y}}_k^n$ in (18). CoMP reception is employed to decode all "slow" messages in a given subnet. That means, each "slow" Rx k applies a rate-$\frac{\mathsf{L}}{2}\log(1+\mathsf{P})$ quantizer to the new output signal $\hat{\boldsymbol{Y}}_k^n$, and sends the quantization information over the cooperation links to the master Rx in its subnet. Each master Rx reconstructs all the quantized signals and jointly decodes the "slow" messages, before sending them back to their intended Rxs. By item 4) the influence of "fast" transmissions has been canceled on the "slow" receive signals.

6) MG Analysis: In the described scheme, all transmitted "fast" and "slow" messages can be sent reliably at MG L because all interference is cancelled (up to noise level) either at the Tx or the Rx side, and because Txs and Rxs are equipped with L antennas each.

The presented coding scheme thus achieves the MG pair

$$\left(\mathsf{S}^{(F)} = \mathsf{S}_{\text{both}}^{(F)},\ \ \mathsf{S}^{(S)} = \mathsf{S}_{\text{both}}^{(S)}\right), \tag{19}$$

where

$$\mathsf{S}_{\text{both}}^{(F)} \triangleq \mathsf{L} \cdot \overline{\lim_{K\to\infty}} \frac{|\mathcal{T}_{\text{fast}}|}{K} \quad \text{and} \quad \mathsf{S}_{\text{both}}^{(S)} \triangleq \mathsf{L} \cdot \overline{\lim_{K\to\infty}} \frac{|\mathcal{T}_{\text{slow}}|}{K}. \tag{20}$$

The scheme we described so far requires different cooperation rates on the various Tx- or Rx-cooperation links. To evenly balance the load on the Tx-cooperation links and on the Rx-cooperation links, different versions of the scheme with different choices of the sets $\mathcal{T}_{\text{silent}}$, $\mathcal{T}_{\text{fast}}$ and $\mathcal{T}_{\text{slow}}$ and different cooperation routes can be time-shared. The main quantity of interest is then the *average cooperation load*, which for the scheme above is characterized as follows. During the single Tx-cooperation round, each "fast" Tx k receives a quantised version of the transmit signal of each of its "slow" interferers $\hat{k} \in \mathcal{I}_k^{(S)}$. Since each quantisation message is of prelog L, the average required Tx-cooperation prelog equals

$$\mu_{\text{Tx,both}}^{(\text{r})} \triangleq \mathsf{L} \cdot \overline{\lim_{K\to\infty}} \frac{\sum_{k\in\mathcal{T}_{\text{fast}}} |\mathcal{I}_k^{(S)}|}{\mathcal{Q}_{K,\text{Tx}}}, \tag{21}$$

where $\mathcal{Q}_{K,\text{Tx}}$ denotes the total number of Tx-cooperation links in the network.

There are three types of Rx-cooperation messages. In the first Rx-cooperation round, each "slow" Rx k obtains a decoded message from each of its "fast" interferers $\hat{k} \in \mathcal{I}_k^{(F)}$. The total number of messages sent in this first round is thus $\sum_{k\in\mathcal{T}_{\text{slow}}} |\mathcal{I}_k^{(F)}|$ and each is of prelog L. In Rx-cooperation rounds $2, \ldots, \lfloor \frac{\mathsf{D}_{\text{Rx}}-1}{2} \rfloor + 1$, "slow" Rxs send quantized versions of their output signals to the master Rx in the same network. Each of these messages is of prelog L and the total number of such messages equals $\sum_{k\in\mathcal{T}_{\text{slow}}} \gamma_{\text{Rx},k}$, where $\gamma_{\text{Rx},k}$ denotes the number of cooperation rounds required for "slow" Rx k to reach the master Rx in its subnet. In rounds $\lfloor \frac{\mathsf{D}_{\text{Rx}}-1}{2} \rfloor + 2, \ldots, \mathsf{D}_{\text{Rx}}$, the master Rx sends the decoded messages to all the "slow" Rxs in the subnet. Each of these messages is again of prelog L and the total number of such messages is again $\sum_{k\in\mathcal{T}_{\text{slow}}} \gamma_{\text{Rx},k}$. To summarize, each of the transmitted messages is of prelog L and thus the average cooperation prelog required per Rx-cooperation link is:

$$\mu_{\text{Rx,both}}^{(\text{r})} \triangleq \mathsf{L} \cdot \overline{\lim_{K\to\infty}} \frac{\sum_{k\in\mathcal{T}_{\text{slow}}} \left(|\mathcal{I}_k^{(F)}| + 2\gamma_{\text{Rx},k}\right)}{\mathcal{Q}_{K,\text{Rx}}}, \tag{22}$$

where $\mathcal{Q}_{K,\text{Rx}}$ denotes the total number of Rx-cooperation links in the network.

Remark 2: If the master Rx of a subnet is a "fast" Rx, it does not have to send its decoded message to its "slow" neighbours, because it decodes all "slow" messages jointly. In this case, less Rx-cooperation prelog is required.

B. Coding scheme to transmit both "fast" and "slow" messages with CoMP transmission:

This second scheme splits the total number of cooperation rounds D as:

$$\mathrm{D_{Tx}} = \mathrm{D} - 1 \quad \text{and} \quad \mathrm{D_{Rx}} = 1. \tag{23}$$

Similarly to the previous Subsection III-A, the scheme is described by 5 items:

1) Creation of subnets and message assignment: This item is similar to item 1) of Subsection III-A, but the sets $\mathcal{T}_{\text{silent}}$, $\mathcal{T}_{\text{fast}}$ and $\mathcal{T}_{\text{slow}}$ are chosen in a way that:

- as before, the signals sent by the "fast" Txs do not interfere; and
- silencing the Txs in $\mathcal{T}_{\text{silent}}$ decomposes the network into non-interfering subnets so that in each subnet there is a dedicated *master Tx* that can send a cooperation message to any other "slow" Tx in the same subnet in at most $\left\lfloor \frac{\mathrm{D_{Tx}}-1}{2} \right\rfloor$ cooperation rounds.

Items 2)-4) remain as described in Subsection III-A. Item 5) is replaced by the following item.

5) Transmission and reception of "slow" messages using CoMP transmission: "Slow" messages are transmitted using standard CoMP transmission techniques that can ignore interference from "fast" Txs (due to the post-processing in item 4)) but account for the modified interference graph and the modified channel matrix between slow messages caused by the precanceling performed under item 2). The receivers decode based on the new outputs $\hat{\boldsymbol{Y}}_k^n$ in (18).

We describe CoMP transmission in this context more formally. During the first $\left\lfloor \frac{\mathrm{D_{Tx}}-1}{2} \right\rfloor$ Tx-cooperation rounds, each "slow" Tx of a subnet, sends its message to the master Tx of the subnet. This latter encodes all received "slow" messages using individual Gaussian codebooks and precodes them so as to cancel all the interference from other "slow" messages at the corresponding Rxs. I.e., it produces signals so that when they are transmitted over the active antennas in the cell, the signal observed at each "slow" Rx only depends on the "slow" message sent by the corresponding Tx but not on the other "slow" messages. The master Tx applies a Gaussian vector quantizer on these precoded signals and sends the quantization information over the cooperation links to the corresponding Txs during the Tx-cooperation rounds $\left\lfloor \frac{\mathrm{D_{Tx}}-1}{2} \right\rfloor + 1$ to $\mathrm{D_{Tx}} - 1$. This is possible by the way we defined the master Txs. All "slow" Txs reconstruct the quantized signals $\hat{\boldsymbol{X}}_k^n$ intended for them and send them over the network: $\boldsymbol{X}_k^n \triangleq \hat{\boldsymbol{X}}_k^n$.

Each "slow" Rx k decodes its desired message from the modified output sequence $\hat{\boldsymbol{Y}}_k^n$ defined in (18) using a standard point-to-point decoder.

Analysis: Similarly to Subsection III-A, each transmitted message can be sent reliably at MG L, and thus the scheme achieves the MG pair in (19).

The load on the different cooperation links is again unevenly distributed across links, and thus, by time-sharing and symmetry arguments, the average Rx- and Tx-cooperation rates are the limiting quantities. The required average Rx-cooperation rate is easily characterized as:

$$\mu_{\text{Rx,both}}^{(\text{t})} \triangleq \mathsf{L} \cdot \overline{\lim_{K\to\infty}} \frac{\sum_{k\in\mathcal{T}_{\text{slow}}} |\mathcal{I}_k^{(F)}|}{\mathcal{Q}_{K,\text{Rx}}}, \tag{24}$$

because Rx-cooperation takes place in a single round, during which each "slow" Rx k learns all decoded "fast" messages that interfere their receive signals and these messages are of MG L. To calculate the required average Tx-cooperation rate, define for each $k \in \mathcal{T}_{\text{slow}}$ the positive parameter $\gamma_{\text{Tx},k}$ to be the number of cooperation hops required from Tx k to reach the master Tx in its subnet. During the first $\lfloor \frac{\text{D}_{\text{Tx}}-1}{2} \rfloor$ Tx-cooperation rounds, a total of $\sum_{k\in\mathcal{T}_{\text{slow}}} \gamma_{\text{Tx},k}$ cooperation messages of MG L are transmitted from the "slow" Txs to the master Txs in their subnet. The same number of Tx-cooperation messages, all of MG L, is also conveyed during rounds $\lfloor \frac{\text{D}_{\text{Tx}}-1}{2} \rfloor + 1, \ldots, 2\lfloor \frac{\text{D}_{\text{Tx}}-1}{2} \rfloor$, now from the master Tx to the "slow" Txs in the subnet. During the last round, "slow" Txs convey their messages to the adjacent "fast" Txs that are interfered by their signals. Some of these signals, however have already been shared during Tx-cooperation rounds $\lfloor \frac{\text{D}_{\text{Tx}}-1}{2} \rfloor + 1, \ldots, 2\lfloor \frac{\text{D}_{\text{Tx}}-1}{2} \rfloor$, and thus do not have to be sent again. The total number of cooperation messages during the last Tx-cooperation rounds is thus only equal to $\sum_{k\in\mathcal{T}_{\text{fast}}} |\mathcal{I}_k^{(S)}| - q$, where q denotes the number of the messages that have already been sent in previous rounds. We will chracterize the value of q when we analyze specific networks. To summarize, the average required Tx-cooperation rate of our scheme is:

$$\mu_{\text{Tx,both}}^{(\text{t})} \triangleq \mathsf{L} \cdot \overline{\lim_{K\to\infty}} \frac{\sum_{k\in\mathcal{T}_{\text{slow}}} 2\gamma_{\text{Tx},k} + \sum_{k\in\mathcal{T}_{\text{fast}}} |\mathcal{I}_k^{(S)}| - q}{\mathcal{Q}_{K,\text{Tx}}}. \tag{25}$$

C. Coding scheme to transmit only "slow" messages with CoMP reception and transmission:

In principle, since any "fast" message satisfies the constraints on "slow" messages, we can use the schemes provided in Subsections III-A and III-B to send only "slow" messages. Sometimes, the following scheme however performs better because it requires less Tx- or Rx-cooperation rates. Choose a set $\mathcal{T}_{\text{silent}} \subseteq [K]$ and silence the Txs in this set, which decomposes the network in non-interfering subnets. The remaining Txs in $\mathcal{T}_{\text{slow}} := [K] \backslash \mathcal{T}_{\text{silent}}$ send only "slow" messages using CoMP transmission or reception. The set $\mathcal{T}_{\text{silent}}$ thus has to be chosen such that in each subnet there is a dedicated *master Rx* (or *master Tx*), which can be reached by any other Rx (Tx) in the subnet in at most $\lfloor \frac{\text{D}}{2} \rfloor$ cooperation rounds. Both versions achieve the MG pair

$$\left(\mathsf{S}^{(F)} = 0, \;\; \mathsf{S}^{(S)} = \mathsf{S}_{\max}^{(S)}\right), \tag{26}$$

where

$$\mathsf{S}_{\max}^{(S)} \triangleq \mathsf{L} \cdot \varlimsup_{K\to\infty} \frac{|\mathcal{T}_{\text{slow}}|}{K}. \tag{27}$$

The CoMP-reception scheme requires no Tx-cooperation but average Rx-cooperation prelog

$$\mu_{\text{Rx},\mathsf{S}}^{(\text{r})} \triangleq \mathsf{L} \cdot \varlimsup_{K\to\infty} \frac{\sum_{k\in\mathcal{T}_{\text{slow}}} 2\gamma_{\text{Rx},k}}{\mathcal{Q}_{K,\text{Rx}}}, \tag{28}$$

and the CoMP-transmission scheme no Tx-cooperation but average Tx-cooperation rate

$$\mu_{\text{Tx},\mathsf{S}}^{(\text{t})} \triangleq \mathsf{L} \cdot \varlimsup_{K\to\infty} \frac{\sum_{k\in\mathcal{T}_{\text{slow}}} 2\gamma_{\text{Tx},k}}{\mathcal{Q}_{K,\text{Tx}}}, \tag{29}$$

where recall that $\gamma_{\text{Rx},k}, \gamma_{\text{Tx},k} \in \{1, \ldots, \lfloor \frac{\mathsf{D}}{2} \rfloor\}$ denote the number of cooperation hops required from a Rx k or a Tx k to reach the master Rx or the master Tx in its subnet.

D. Coding scheme without cooperation:

Choose a set of Txs $\mathcal{T}_{\text{silent}} \subseteq [K]$ so that the remaining Txs $\mathcal{T}_{\text{active}} := [K]\backslash\mathcal{T}_{\text{silent}}$ do not interfere, and send "slow" or "fast" over the resulting interference-free links. The scheme requires no cooperation and achieves for any $\beta \in [0,1]$ the MG pair

$$\left(\mathsf{S}^{(F)} = \beta\mathsf{S}_{\text{no-coop}},\ \ \mathsf{S}^{(S)} = (1-\beta)\mathsf{S}_{\text{no-coop}}\right), \tag{30}$$

where

$$\mathsf{S}_{\text{no-coop}} \triangleq \mathsf{L} \cdot \varlimsup_{K\to\infty} \left(1 - \frac{|\mathcal{T}_{\text{silent}}|}{K}\right). \tag{31}$$

IV. Wyner's Symmetric Linear Model

Consider Wyner's symmetric linear cellular model where cells are aligned in a single dimension and signals of users that lie in a given cell interfere only with signals sent in the two adjacent cells. See Figure 1 where the interference pattern is illustrated by black dashed lines. We assume that the various mobile users in a cell are scheduled on different frequency bands, and focus on a single mobile user per cell (i.e., on a single frequency band). We shall further assume that the number of cells K and the maximum delay D are even.

The input-output relation of the network is

$$\boldsymbol{Y}_{k,t} = \mathsf{H}_{k,k}\boldsymbol{X}_{k,t} + \mathsf{H}_{k-1,k}\boldsymbol{X}_{k-1,t} + \mathsf{H}_{k+1,k}\boldsymbol{X}_{k+1,t} + \boldsymbol{Z}_{k,t}, \tag{32}$$

where $\boldsymbol{X}_{0,t} = \mathbf{0}$ for all t, and the interference set at a given user k is

$$\mathcal{I}_k = \{k-1, k+1\}, \tag{33}$$

where indices out of the range $[K]$ should be ignored. In this model, Rxs and Txs can cooperate with the two Rxs and Txs in the adjacent cells, so

$$\mathcal{N}_{\text{Tx}}(k) = \{k-1, k+1\} \quad \text{and} \quad \mathcal{N}_{\text{Rx}}(k) = \{k-1, k+1\}. \tag{34}$$

Fig. 1 illustrates the interference pattern of the network and the available cooperation links. As can be seen from this figure, Txs 1 and K and Rxs 1 and K have a single outgoing cooperation link and all other Txs and Rxs in this network have two outgoing cooperation links. Thus, the total numbers of Tx- and of Rx-cooperation links both are

$$\mathcal{Q}_{K,\text{Tx}} = \mathcal{Q}_{K,\text{Rx}} = 2K - 2. \tag{35}$$

A. Choice of Tx/Rx Sets for the Schemes in Section III

1) "Fast" and "slow" messages with CoMP reception: For the mixed-delay scheme, choose the Tx/Rx set association in Fig. 2, where "fast" Tx/Rx pairs are in yellow, "slow" in blue, and silenced in white. I.e., set

$$\mathcal{T}_{\text{silent}} = \left\{ \ell\,(\mathsf{D}+2) : \ell = 1, \ldots, \left\lfloor \frac{K}{\mathsf{D}+2} \right\rfloor \right\}, \tag{36a}$$

$$\mathcal{T}_{\text{fast}} = \{1, 3, \ldots, K-1\}, \tag{36b}$$

$$\mathcal{T}_{\text{slow}} = \{1, \ldots, K\} \backslash \{\mathcal{T}_{\text{silent}}, \mathcal{T}_{\text{fast}}\}. \tag{36c}$$

For this choice, transmissions of "fast" messages are interfered only by transmissions of "slow" messages and for any ℓ, the Tx/Rx pairs in

$$\mathcal{T}_\ell \triangleq \{\ell(\mathsf{D}+2)+1, \ldots, (\ell+1)(\mathsf{D}+2)-1\} \tag{37}$$

form a subnet for which Rx $\ell(\mathsf{D}+2) + \mathsf{D}/2 + 1$ can act as the master Rx because it can be reached by any *"slow" Rx (i.e., even Rx)* in its subnet in at most $(\mathsf{D}_{\text{Rx}} - 1)/2$ cooperation hops.

By (20) and (36), the scheme achieves the MG pair $(\mathsf{S}^{(F)} = \mathsf{S}^{(F)}_{\text{both}}, \mathsf{S}^{(S)} = \mathsf{S}^{(S)}_{\text{both}})$ where

$$\mathsf{S}^{(F)}_{\text{both}} \triangleq \frac{\mathsf{L}}{2} \quad \text{and} \quad \mathsf{S}^{(S)}_{\text{both}} \triangleq \mathsf{L} \cdot \frac{\mathsf{D}}{2(\mathsf{D}+2)}. \tag{38}$$

To analyze the required cooperation prelogs of the scheme, $\mu^{(\text{r})}_{\text{Tx,both}}$ and $\mu^{(\text{r})}_{\text{Rx,both}}$, we evaluate the formulas in (21) and (22). We have for each subnet $\ell \in \{1, \ldots, \lfloor K/(\mathsf{D}+2) \rfloor\}$:

$$\sum_{k \in \mathcal{T}_{\text{fast}} \cap \mathcal{T}_\ell} |\mathcal{I}^{(S)}_k| = 2 + 2(\mathsf{D}/2 - 1) = \mathsf{D}. \tag{39}$$

In the limit $K \to \infty$, we obtain

$$\mu^{(\mathrm{r})}_{\mathrm{Tx,both}} = \mathsf{L} \cdot \frac{\mathrm{D}}{2(\mathrm{D}+2)}. \tag{40}$$

To calculate the required Rx-cooperation prelog $\mu^{(\mathrm{r})}_{\mathrm{Rx,both}}$, notice that $|\mathcal{I}_k^{(F)}| = 2$. Since there are $\mathrm{D}/2$ "slow" Rxs in each subnet $\mathcal{T}_\ell$:

$$\sum_{k \in \mathcal{T}_{\mathrm{slow}} \cap \mathcal{T}_\ell} |\mathcal{I}_k^{(F)}| = 2 \cdot \frac{\mathrm{D}}{2} = \mathrm{D}. \tag{41}$$

In addition, Rxs also exchange cooperation messages to enable CoMP reception. Thereby, the quantization message produced by a "slow" Rx $k = \ell(\mathrm{D}+2) + i$, for $i \in \{2, 4, \ldots, \mathrm{D}-2\}$, has to propagate over $\gamma_{\mathrm{Rx},k} = |\mathrm{D}/2 + 1 - i|$ hops to reach the subnet's master Rx. If $\mathrm{D}/2+1$ is even,

$$\sum_{k \in \mathcal{T}_{\mathrm{slow}} \cap \mathcal{T}_\ell} \gamma_{\mathrm{Rx},k} = \sum_{i \in \{2,4,\ldots,\mathrm{D}/2-1\}} 2 \cdot (\mathrm{D}/2 + 1 - i) = \frac{1}{2}\left(\frac{\mathrm{D}^2}{4} - 1\right). \tag{42}$$

Then, according to (22), (35), (41), and (42), when $\mathrm{D}/2 + 1$ is even, in the limit as $K \to \infty$:

$$\mu^{(\mathrm{r})}_{\mathrm{Rx,both}} = \mathsf{L} \cdot \frac{\mathrm{D} + \frac{\mathrm{D}^2}{4} - 1}{2(\mathrm{D}+2)}, \quad \text{for } \mathrm{D}/2 + 1 \text{ even}. \tag{43}$$

When $\mathrm{D}/2 + 1$ is odd, the sum in (42) evaluates to $\frac{\mathrm{D}^2}{8}$. Moreover, in this case, the master Rx is a "fast" Rx. It does not have to send its decoded message to any neighbour, as it locally decodes all "slow" messages of the subnet. So, (see also Remark 2), the nominator in (22) can be reduced by 2. Putting all these together, we obtain $\mu^{(\mathrm{r})}_{\mathrm{Rx,both}} = \mathsf{L} \cdot \frac{\mathrm{D}+\frac{\mathrm{D}^2}{4}-2}{2(\mathrm{D}+2)}$ when $\mathrm{D}/2+1$ is odd.

2) "Fast" and "slow" messages with CoMP transmission: Choose the same cell association as for the CoMP reception scheme described in (36) and depicted in Fig. 2. Under this cell association, Tx $\mathrm{D}/2+1$ can act as a master Tx because it can be reached by any "slow" (even) Tx in its subnet in at most $(\mathrm{D}_{\mathrm{Tx}} - 1)/2$ cooperation rounds. Since the same cell partitioning is used, namely (36), this scheme achieves the same MG pair as with CoMP reception, see (38). Moreover, by (24) and (41) in the limit as $K \to \infty$, the required average Rx-cooperation prelog is

$$\mu^{(\mathrm{t})}_{\mathrm{Rx,both}} = \mathsf{L} \cdot \frac{\mathrm{D}}{2(\mathrm{D}+2)}. \tag{44}$$

Similarly, consider (25) and (39) and notice that for $\mathrm{D}/2 + 1$ even,

$$\sum_{k \in \mathcal{T}_{\mathrm{slow}} \cap \mathcal{T}_\ell} \gamma_{\mathrm{Tx},k} = \sum_{i \in \{2,4,\ldots,\mathrm{D}/2-1\}} 2(\mathrm{D}/2 + 1 - i) = \frac{1}{2}\left(\frac{\mathrm{D}^2}{4} - 1\right), \tag{45}$$

whereas for $\mathrm{D}/2 + 1$ odd, this sum evaluates to $\frac{\mathrm{D}^2}{8}$. We consider the q-term in (25), which characterizes the number of quantization messages describing the "slow" signals that are counted

twice: once for the CoMP transmission and once for the interference mitigation at "fast" transmitters. In each subnet, $\mathrm{D}/2-1$ such messages are double-counted, when $\mathrm{D}/2+1$ is even, and $\mathrm{D}/2$ messages are double-counted when $\mathrm{D}/2+1$ is odd. Therefore, and according to (25), (39), (45), when $K\to\infty$, the average Tx-cooperation prelog required by the scheme is

$$\mu^{(\mathrm{t})}_{\mathrm{Tx,both}}=\mathsf{L}\cdot\frac{\mathrm{D}+\frac{\mathrm{D}^2}{4}-1-\mathrm{D}/2+1}{2(\mathrm{D}+2)}=\mathsf{L}\cdot\frac{\mathrm{D}}{8}, \tag{46}$$

irrespective of whether $\mathrm{D}/2+1$ is even or odd.

3) Transmitting only "slow" messages with CoMP reception and transmission: Consider the scheme in Subsection III-C that transmits only "slow" messages, either using CoMP transmission or CoMP reception. For both schemes we regularly silence every $\mathrm{D}+2$nd Tx, i.e., as in the two previous subsections, $\mathcal{T}_{\text{silent}}\triangleq\left\{\ell(D+2)\colon \ell=1,\ldots,\lfloor\frac{K}{\mathrm{D}+2}\rfloor\right\}$. Also, we set $\mathcal{T}_{\text{slow}}=[K]\backslash\mathcal{T}_{\text{silent}}$. These choices are permissible, because all Txs (or Rxs) in a subnet $\mathcal{T}_\ell=\{(\ell-1)(\mathrm{D}+2)+1,\ldots,\ell(\mathrm{D}+2)-1\}$ can reach the subnet's central Tx $(\ell-1)(\mathrm{D}+2)+\mathrm{D}+1$ (or Rx $(\ell-1)(\mathrm{D}+2)+\mathrm{D}+1$) in at most $\mathrm{D}/2$ cooperation hops.

By (27), the scheme in Subsection III-C achieves the MG pair $(\mathsf{S}^{(F)}=0,\ \mathsf{S}^{(S)}=\mathsf{S}^{(S)}_{\text{max}})$ where

$$\mathsf{S}^{(S)}_{\text{max}}\triangleq\mathsf{L}\cdot\frac{\mathrm{D}+1}{\mathrm{D}+2}. \tag{47}$$

With CoMP reception, this scheme does not use any Tx-cooperation. To calculate the Rx-cooperation prelog, we use the fact that Rx $k=\ell(\mathrm{D}+2)+i$, for positive integers ℓ and $i\le\mathrm{D}+1$, reaches the master Rx in its subnet in $\gamma_{\mathrm{Rx},k}=|\mathrm{D}/2+1-i|$ hops. Since:

$$2\sum_{k\in\mathcal{T}_\ell}\gamma_{\mathrm{Rx},k}=4\sum_{i=1}^{\mathrm{D}/2}i=\frac{\mathrm{D}(\mathrm{D}+2)}{2}, \tag{48}$$

by (28), in the limit as $K\to\infty$, the average Rx-cooperation prelog tends to

$$\mu^{(\mathrm{r})}_{\mathrm{Rx,S}}=\mathsf{L}\cdot\frac{\mathrm{D}}{4}. \tag{49}$$

Similar conclusions show that when CoMP transmission is used instead of CoMP reception, the scheme requires zero Rx-cooperation prelog and a Tx-cooperation prelog of $\mu^{(\mathrm{t})}_{\mathrm{Tx,S}}=\mu^{(\mathrm{r})}_{\mathrm{Rx,S}}$.

4) No-cooperation scheme: Consider the no-cooperation scheme in Subsection III-D. For Wyner's symmetric network we create non-interfering point-to-point links by silencing all even Txs in the network, i.e., by choosing $\mathcal{T}_{\text{silent}}\triangleq\{2,4,\ldots 2\lfloor\frac{K}{2}\rfloor\}$. Since all odd receivers remain active, the sum-prelog in (31) for this network evaluates to

$$\mathsf{S}_{\text{no-coop}}\triangleq\frac{\mathsf{L}}{2}. \tag{50}$$

B. Achievable MG Regions

Recall the definitions of $\mathsf{S}^{(F)}_{\text{both}}$, $\mathsf{S}^{(S)}_{\text{both}}$, $\mathsf{S}^{(S)}_{\text{max}}$, $\mathsf{S}_{\text{no-coop}}$ in (38), (47), and (50) and the definitions of $\mu^{(\text{r})}_{\text{Tx,both}}, \mu^{(\text{r})}_{\text{Rx,both}}, \mu^{(\text{t})}_{\text{Rx,both}}, \mu^{(\text{t})}_{\text{Tx,both}}$ in (40), (43), (46), and (44). Define further

$$\alpha \triangleq \max\left\{\min\left\{\frac{\mu_{\text{Tx}}}{\mu^{(\text{r})}_{\text{Tx,both}}}, \frac{\mu_{\text{Rx}}}{\mu^{(\text{r})}_{\text{Rx,both}}}\right\}, \min\left\{\frac{\mu_{\text{Tx}}}{\mu^{(\text{t})}_{\text{Tx,both}}}, \frac{\mu_{\text{Rx}}}{\mu^{(\text{t})}_{\text{Rx,both}}}\right\}\right\}, \tag{51}$$

and

$$\mathsf{S}^{(S)}_{\text{sym},1}(\alpha) \triangleq \alpha \mathsf{S}^{(S)}_{\text{max}} + (1-\alpha)\mathsf{S}_{\text{no-coop}} \tag{52}$$

$$\mathsf{S}^{(F)}_{\text{sym},2}(\alpha) \triangleq \alpha \mathsf{S}^{(F)}_{\text{both}} + (1-\alpha)\mathsf{S}_{\text{no-coop}} \qquad \text{and} \qquad \mathsf{S}^{(S)}_{\text{sym},2}(\alpha) \triangleq \alpha \mathsf{S}^{(S)}_{\text{both}} \tag{53}$$

$$\mathsf{S}^{(F)}_{\text{sym},3}(\alpha) \triangleq \alpha \mathsf{S}^{(F)}_{\text{both}} \qquad \text{and} \qquad \mathsf{S}^{(S)}_{\text{sym},3}(\alpha) \triangleq \alpha \mathsf{S}^{(S)}_{\text{both}} + (1-\alpha)\mathsf{S}^{(S)}_{\text{max}}. \tag{54}$$

According to the arguments in the previous subsection, the following regions of MG pairs are achievable depending on the available cooperation prelogs μ_{Tx} and μ_{Rx}.

Theorem 1 (Achievable MG Region: Wyner's Symmetric Model): Assume $\text{D} \geq 2$ and even.

When $\mu_{\text{Rx}} \geq \mu^{(\text{r})}_{\text{Rx,both}}$ and $\mu_{\text{Tx}} \geq \mu^{(\text{r})}_{\text{Tx,both}}$; or when $\mu_{\text{Rx}} \geq \mu^{(\text{t})}_{\text{Rx,both}}$ and $\mu_{\text{Tx}} \geq \mu^{(\text{t})}_{\text{Tx,both}}$:

$$\text{convex hull}\Big((0,0),\ (0,\mathsf{S}^{(S)}_{\text{max}}),\ (\mathsf{S}^{(F)}_{\text{both}},\mathsf{S}^{(S)}_{\text{both}}),\ (\mathsf{S}_{\text{no-coop}},0)\Big) \subseteq \mathcal{S}^{\star}(\mu_{\text{Tx}},\mu_{\text{Rx}},\text{D}). \tag{55}$$

When $\mu_{\text{Rx}} \geq \mu^{(\text{r})}_{\text{Rx},\mathsf{S}}$ and $\mu_{\text{Tx}} < \mu^{(\text{r})}_{\text{Tx,both}}$; or when $\mu_{\text{Tx}} \geq \mu^{(\text{t})}_{\text{Tx},\mathsf{S}}$ and $\mu_{\text{Rx}} < \mu^{(\text{t})}_{\text{Rx,both}}$:

$$\text{convex hull}\Big((0,0),\ (0,\mathsf{S}^{(S)}_{\text{max}}),\ (\mathsf{S}^{(F)}_{\text{sym},3}(\alpha),\mathsf{S}^{(S)}_{\text{sym},3}(\alpha)),\ (\mathsf{S}^{(F)}_{\text{sym},2}(\alpha),\mathsf{S}^{(S)}_{\text{sym},2}(\alpha)),\ (\mathsf{S}_{\text{no-coop}},0)\Big) \subseteq \mathcal{S}^{\star}(\mu_{\text{Tx}},\mu_{\text{Rx}},\text{D}). \tag{56}$$

When $\mu_{\text{Rx}} < \mu^{(\text{r})}_{\text{Rx,both}}$ or when $\mu_{\text{Tx}} < \mu^{(\text{t})}_{\text{Tx,both}}$:

$$\text{convex hull}\Big((0,0),\ (0,\mathsf{S}^{(S)}_{\text{sym},1}(\alpha)),\ (\mathsf{S}^{(F)}_{\text{sym},2}(\alpha),\mathsf{S}^{(S)}_{\text{sym},2}(\alpha)),\ (\mathsf{S}_{\text{no-coop}},0)\Big) \subseteq \mathcal{S}^{\star}(\mu_{\text{Tx}},\mu_{\text{Rx}},\text{D}). \tag{57}$$

Proposition 1 (Outer Bound on the MG Region: Wyner's Symmetric Model): Any MG pair $(\mathsf{S}^{(F)},\mathsf{S}^{(S)})$ in $\mathcal{S}^{\star}(\mu_{\text{Tx}},\mu_{\text{Rx}},\text{D})$ satisfies

$$\mathsf{S}^{(F)} \leq \frac{\mathsf{L}}{2}, \tag{58}$$

$$\mathsf{S}^{(F)} + \mathsf{S}^{(S)} \leq \mathsf{L} \cdot \frac{\text{D}+1}{\text{D}+2}. \tag{59}$$

Proof: Follows by specializing the *MAC-Lemma for interference networks with conferencing* [18, Lemma 1] to Wyner's symmetric network and to the choices

$$\mathcal{J}_{\text{outputs}} \triangleq \bigcup_{\ell \in \{1,\ldots,\lceil \frac{K}{2(\text{D}+2)} \rceil\}} \{2+(\ell-1)(2\text{D}+4),\ldots,\ell(2\text{D}+4)-1\}, \tag{60}$$

$$\mathcal{J}_{\text{inputs}} \triangleq \bigcup_{\ell \in \{1,\ldots,\lceil \frac{K}{2(\mathsf{D}+2)} \rceil\}} \{\mathsf{D}+2+(\ell-1)(2\mathsf{D}+4), \ldots, \mathsf{D}+3+(\ell-1)(2\mathsf{D}+4)\}\,, \tag{61}$$

$$\mathcal{J}_{\text{messages}} \triangleq \bigcup_{\ell \in \{1,\ldots,\lceil \frac{K}{2(\mathsf{D}+2)} \rceil\}} \{\mathsf{D}+2-\mathsf{D}_{\text{Tx}}+(\ell-1)(2\mathsf{D}+4), \ldots, \mathsf{D}+3+\mathsf{D}_{\text{Tx}}+(\ell-1)(2\mathsf{D}+4)\}\,. \tag{62}$$

■

Corollary 1: If

$$\left(\mu_{\text{Rx}} \geq \mu^{(\text{r})}_{\text{Rx,both}} \quad \text{and} \quad \mu_{\text{Tx}} \geq \mu^{(\text{r})}_{\text{Tx,both}}\right) \quad \text{or} \quad \left(\mu_{\text{Rx}} \geq \mu^{(\text{t})}_{\text{Rx,both}} \quad \text{and} \quad \mu_{\text{Tx}} \geq \mu^{(\text{t})}_{\text{Tx,both}}\right), \tag{63}$$

the optimal MG region $\mathcal{S}^{\star}(\mu_{\text{Tx}}, \mu_{\text{Rx}}, \mathsf{D})$ coincides with the trapezoid in (55).

Proof: Follows directly by Theorem 1 and Proposition 1. ■

By Corollary 1, for large cooperation prelogs μ_{Tx} and μ_{Rx}, imposing a stringent delay constraint on the "fast" messages never penalizes the maximum achievable sum-MG of the system: the same sum-MG can be achieved as if only "slow" messages were sent.

The next corollary characterizes the optimal MG region $\mathcal{S}^{\star}(\mu_{\text{Tx}}, \mu_{\text{Rx}}, \mathsf{D})$ when one of the two cooperation prelogs (μ_{Tx} or μ_{Rx}) is small and the other large, and when $\mathsf{S}^{(F)}$ lies below a certain threshold. The corollary shows that also in this regime the same maximum sum-MG can be achieved as if only "slow" messages were sent. When $\mathsf{S}^{(F)}$ exceeds this threshold, our achievable MG region in (56) shows a penalty in sum-MG which increases linearly with the "fast" MG. In this regime we do not have a matching converse result.

Corollary 2: Assume that

$$\left(\mu_{\text{Rx}} \geq \mu^{(\text{r})}_{\text{Rx},\mathsf{S}} \quad \text{and} \quad \mu_{\text{Tx}} < \mu^{(\text{r})}_{\text{Tx,both}}\right) \qquad \text{or} \qquad \left(\mu_{\text{Tx}} \geq \mu^{(\text{t})}_{\text{Tx},\mathsf{S}} \quad \text{and} \quad \mu_{\text{Rx}} < \mu^{(\text{t})}_{\text{Rx,both}}\right). \tag{64}$$

For any $\mathsf{S}^{(F)} \in [0, \alpha \cdot \frac{\mathsf{L}}{2}]$, where α is defined in (51), the pair $(\mathsf{S}^{(F)}, \mathsf{S}^{(S)})$ lies in the optimal MG region $\mathcal{S}^{\star}(\mu_{\text{Tx}}, \mu_{\text{Rx}}, \mathsf{D})$ if, and only if, it is in the trapezoid described on the LHS of (56).

Proof: Follows directly by Theorem 1, see (56), and by Proposition 1, and because the sum $\mathsf{S}^{(F)}_{\text{sym},3}(\alpha) + \mathsf{S}^{(S)}_{\text{sym},3}(\alpha) = \mathsf{L} \cdot \frac{\mathsf{D}+1}{\mathsf{D}+2}$ coincides with the maximum sum MG. ■

Figures 3 and 4 illustrate the inner and outer bounds (Theorem 1 and Proposition 1) on the MG region with $\mathsf{D} = 6$ and $\mathsf{D} = 10$, and different values of μ_{Rx} and μ_{Tx}. As can be seen in Figure 3 and as also explained in Corollary 1, when $\mu_{\text{Rx}} \geq 2.625$ and $\mu_{\text{Tx}} \geq 1.125$, or when $\mu_{\text{Rx}} \geq 1.125$ and $\mu_{\text{Tx}} \geq 2.25$ the inner bound in (55) and the outer bound match. In the former case, the inner bound is achievable using the scheme in Subsection IV-A1 based on CoMP reception, and in the latter case it is achievable using the scheme in Subsection IV-A2 based on CoMP transmission. As explained in Corollary 2, when only one of the two cooperation prelogs

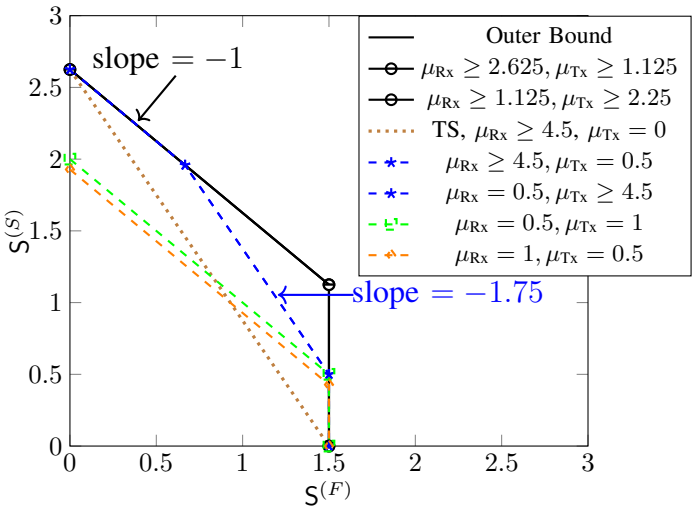

Fig. 3: Inner and outer bounds on $\mathcal{S}^\star(\mu_{\text{Tx}}, \mu_{\text{Rx}}, \mathsf{D})$ for the symmetric Wyner network for different values of μ_{Rx} and μ_{Tx}, and for $\mathsf{L} = 3$ and $\mathsf{D} = 6$. The brown dotted line is the time-sharing region.

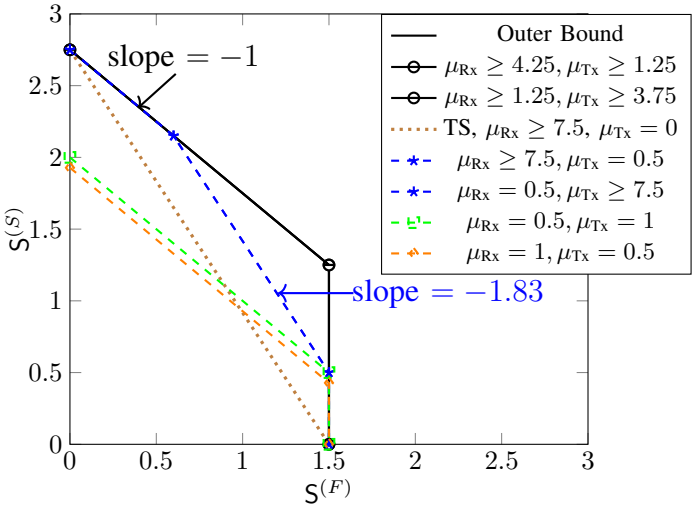

Fig. 4: Inner and outer bounds on $\mathcal{S}^\star(\mu_{\text{Tx}}, \mu_{\text{Rx}}, \mathsf{D})$ for the symmetric Wyner network for different values of μ_{Rx} and μ_{Tx}, and for $\mathsf{L} = 3$ and $\mathsf{D} = 10$. The brown dotted line is the time-sharing region.

is large and the other small (e.g., $\mu_{\text{Rx}} \geq 4.5$ and $\mu_{\text{Tx}} = 0.5$; or $\mu_{\text{Tx}} \geq 4.5$ and $\mu_{\text{Rx}} = 0.5$) the inner bound in (56) matches the outer bound of Proposition 1 only for $\mathsf{S}^{(F)} < \alpha \cdot \frac{\mathsf{L}}{2}$, where α is defined in (51). For larger values of $\mathsf{S}^{(F)}$, the maximum "slow" MG $\mathsf{S}^{(S)}$ achieved by our schemes decreases linearly with $\mathsf{S}^{(F)}$. For example, for $\mathsf{D} = 6$ and $(\mu_{\text{Rx}} \geq 4.5, \mu_{\text{Tx}} = 0.5)$ or

$(\mu_{\text{Tx}} \geq 4.5, \mu_{\text{Rx}} = 0.5)$ when $\mathsf{S}^{(F)} \geq \alpha \cdot \frac{\mathsf{L}}{2}$ increases by Δ then $\mathsf{S}^{(S)}$ decreases by approximately 1.75Δ and the sum-MG by 0.75Δ. The behaviour changes again when both μ_{Rx} and μ_{Tx} are moderate or small, e.g., $\mu_{\text{Rx}} = 0.5$ and $\mu_{\text{Tx}} = 1$ or $\mu_{\text{Rx}} = 1$ and $\mu_{\text{Tx}} = 0.5$. In this case, the sum-MG achieved by our inner bound is constant over all regimes of $\mathsf{S}^{(F)}$. We finally notice that in these small cooperation-prelog regimes our inner bounds remain unchanged for $\text{D} = 6, 8, 10$. The reason is that in this regime, even when $\text{D} > 6$, it is more advantageous to reduce the number of cooperation rounds to 6 in order to satisfy the cooperation prelogs than to time-share different schemes with $\text{D} > 6$ cooperation rounds. The brown dotted line is the the result of time-sharing the scheme in Subsection IV-A3 that transmit only "slow" messages with the scheme in Subsection IV-A4 when only "fast" messages are transmitted. The scheme in Subsection IV-A3 is based on CoMP reception and to achieve the maximum "slow" MG requires $\mu_{\text{Rx}} \geq 4.5$ for $\text{D} = 6$ and $\mu_{\text{Rx}} \geq 7.5$ for $\text{D} = 10$. The sum-MG in this scheme decreases linearly with the "fast" MG.

V. Hexagonal Network

Consider a network with K hexagonal cells, where each cell consists of one single mobile user (MU) and one BS. The signals of users that lie in a given cell interfere with the signals sent in the 6 adjacent cells. The interference pattern of our network is depicted by the black dashed lines in Fig. 5, i.e., the interference set $\mathcal{I}_k$ contains the indices of the 6 neighbouring cells whose signals interfere with cell k. The input-output relation of the network is as in (89).

Each Rx k (BS of a cell) can cooperate with the six Rxs in the adjacent cells, i.e., $|\mathcal{N}_{\text{Rx}}(k)| = 6$. Thus, the number of Rx-cooperation links $\mathcal{Q}_{K,\text{Rx}}$ in this network is approximately equal to $6K$ (up to edge effects). Similarly, each Tx (MU of a cell) can cooperate with the six Txs in the adjacent cells and thus $|\mathcal{N}_{\text{Tx}}(k)| = 6$ and $\mathcal{Q}_{K,\text{Tx}} \approx 6K$.

To describe the setup and our schemes in detail, we parametrize the locations of the Tx/Rx pair in the k-th cell by a number o_k in the complex plane $\mathbb{C}$. Introducing the coordinate vectors

$$\mathbf{e}_x = \frac{\sqrt{3}}{2} - \frac{1}{2}i \quad \text{and} \quad \mathbf{e}_y = i, \tag{65}$$

as in Figure 5, the position o_k of Tx/Rx pair k can be associated with integers (a_k, b_k) satisfying

$$o_k \triangleq a_k \cdot \mathbf{e}_x + b_k \cdot \mathbf{e}_y. \tag{66}$$

The interference set $\mathcal{I}_k$ and the neighbouring sets can then be expressed as

$$\mathcal{N}_{\text{Tx}}(k) = \mathcal{N}_{\text{Rx}}(k) = \mathcal{I}_k = \big\{k' \colon \quad |a_k - a_{k'}| = 1 \quad \text{and} \quad |b_k - b_{k'}| = 1$$

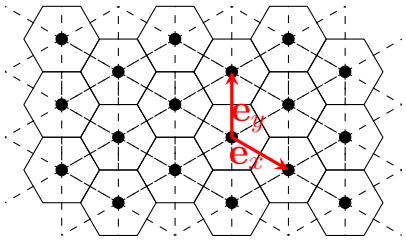

Fig. 5: Illustration of the hexagonal network. Small circles indicate Txs and Rxs, black solid lines the cell borders, and black dashed lines interference between cells.

$$\text{and} \quad |a_k - a_{k'} - b_k + b_{k'}| = 1\big\}. \quad (67)$$

For simplicity we assume an even-valued D satisfying

$$\frac{\mathsf{D}}{2} - 1 \mod 3 = 0. \quad (68)$$

Other cases can be treated in a similar way.

We specify the Tx/Rx set associations for the schemes in Section III. See Appendix A for a detailed analysis. For the no-cooperation scheme in Subsection III-D choose

$$\mathcal{T}_{\text{active}} = \{k \in [K]\colon \quad (a_k + b_k) \mod 3 = 0\} \quad (69)$$

and $\mathcal{T}_{\text{silent}} = [K] \backslash \mathcal{T}_{\text{active}}$. The corresponding cell association is shown in Figure 6a where active cells are in yellow and silenced in white. By (31), the sum-MG achieved by this scheme is

$$\mathsf{S}_{\text{no-coop}} = \frac{\mathsf{L}}{3}. \quad (70)$$

We next explain the Tx/Rx set association for sending only "slow" messages as in Subsection III-C, see also [37]. Set $\tau = \frac{\mathsf{D}}{2} + 1$ and choose Tx k (Rx k) as a master Tx (Rx), if it belongs to

$$\mathcal{T}_{\text{master}} = \{k \in [K]\colon (a_k \mod \tau = 0) \text{ and } (b_k \mod \tau = 0) \text{ and } (|a_k + b_k| \mod 3\tau = 0)\}. \quad (71)$$

To describe the silenced $\mathcal{T}_{\text{silent}}$, we define for any integers x and $\tau \geq 0$:

$$x_{[-\tau,2\tau]} \triangleq ((x + \tau) \mod 3\tau) - \tau, \quad (72)$$

where $\mod$ denotes the standard modulo operator. In fact, the operator $x_{[-\tau,2\tau]}$ ressembles the standard $\mod 3\tau$ operator, but it shifts every number into the interval $[-\tau, 2\tau)$ and not into $[0, 3\tau)$. We then set

$$\mathcal{T}_{\text{silent}} = \big\{k\colon \max\{|a_{k[-\tau,2\tau)}|, |b_{k[-\tau,2\tau)}|, |a_{k[-\tau,2\tau)} - b_{k[-\tau,2\tau)}|\} = \tau\big\} \quad (73)$$

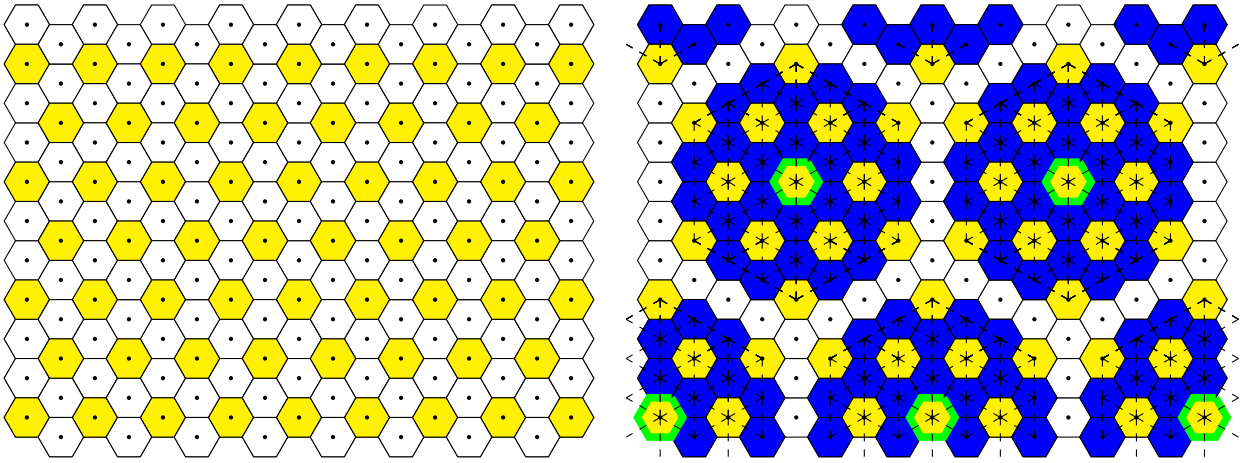

(a) No-cooperation scheme (b) Cooperative scheme

Fig. 6: Cell associations for the schemes in the hexagonal network.

and $\mathcal{T}_{\text{slow}} = [K] \backslash \mathcal{T}_{\text{silent}}$. Figure 6b shows the proposed cell association for $\mathrm{D} = 6$: blue or yellow are the active "slow" cells and white the silenced cells. Master Txs (Rxs) are depicted with green borders. We observe that the choice in (73) silences all Tx/Rx pairs which lie $\frac{\mathrm{D}}{2} + 1$ hops away from a master Tx/Rx pair. As we detail out in Appendix A, by (26) and (27), this choice establishes an achievable MG pair of $(\mathsf{S}^{(F)} = 0, \mathsf{S}^{(S)} = \mathsf{S}^{(S)}_{\text{max}})$, where

$$\mathsf{S}^{(S)}_{\text{max}} \triangleq \mathsf{L} \cdot \frac{4 + 3\mathrm{D}(\mathrm{D}+2)}{3(\mathrm{D}+2)^2}. \tag{74}$$

Moreover, by (28) and (29), with CoMP reception or CoMP transmission the scheme requires average Rx- or Tx-cooperation prelogs equal to

$$\mu^{(\mathrm{t})}_{\text{Tx,S}} = \mu^{(\mathrm{r})}_{\text{Rx,S}} = \mathsf{L} \cdot \frac{\mathrm{D}(\mathrm{D}+1)}{9(\mathrm{D}+2)}. \tag{75}$$

Finally, we turn to the scheme that sends both "fast" and "slow" messages in Subsections III-A and III-B. Here, we set $\tau = \frac{\mathrm{D}}{2}$ and choose the set of master Txs (Rxs) as in (71), but for this new value of τ. Similarly, we choose the silenced set $\mathcal{T}_{\text{silent}}$ as in (73) but again for the new value $\tau = \frac{\mathrm{D}}{2}$. The "fast" transmit set $\mathcal{T}_{\text{fast}}$ is chosen in the same way as $\mathcal{T}_{\text{active}}$ in (69), and $\mathcal{T}_{\text{slow}} = [K] \backslash \{\mathcal{T}_{\text{silent}} \cup \mathcal{T}_{\text{fast}}\}$. The cell association is depicted in Figure 6b for $\mathrm{D} = 8$, where "fast" cells are in yellow, "slow" cells in blue, and master cells are designated with green borders. As detailed out in Appendix A, by (20), the proposed cell association achieves the MG pair $(\mathsf{S}^{(F)} = \mathsf{S}^{(F)}_{\text{both}}, \mathsf{S}^{(S)} = \mathsf{S}^{(S)}_{\text{both}})$ where

$$\mathsf{S}^{(F)}_{\text{both}} \triangleq \frac{\mathsf{L}}{3}\left(1 - \frac{2(\mathrm{D}-2)}{\mathrm{D}^2}\right) \quad \text{and} \quad \mathsf{S}^{(S)}_{\text{both}} \triangleq \frac{2\mathsf{L}}{3}\left(1 - \frac{2}{\mathrm{D}}\right), \tag{76}$$

and by (21) and (22) the average Tx- and Rx-cooperation prelogs with CoMP reception are

$$\mu^{(\mathrm{r})}_{\mathrm{Tx,both}} \triangleq \mathsf{L} \cdot \frac{(\mathrm{D}-2)(3\mathrm{D}-4)}{9\mathrm{D}^2} \quad \text{and} \quad \mu^{(\mathrm{r})}_{\mathrm{Rx,both}} \triangleq \mathsf{L} \cdot \frac{2\mathrm{D}^3+3\mathrm{D}^2-30\mathrm{D}+32}{27\mathrm{D}^2}, \tag{77}$$

and with CoMP transmission they are

$$\mu^{(\mathrm{t})}_{\mathrm{Tx,both}} \triangleq \mathsf{L} \cdot \frac{2\mathrm{D}^3-12\mathrm{D}-28}{27\mathrm{D}^2} \quad \text{and} \quad \mu^{(\mathrm{t})}_{\mathrm{Rx,both}} \triangleq \mathsf{L} \cdot \frac{(\mathrm{D}-2)(3\mathrm{D}-4)}{9\mathrm{D}^2}. \tag{78}$$

A. Achievable MG Region

Recall the definitions of $\mathsf{S}_{\text{no-coop}}$, $\mathsf{S}^{(S)}_{\max}$, $\mathsf{S}^{(F)}_{\text{both}}$, $\mathsf{S}^{(S)}_{\text{both}}$ in (70), (74), and (76), and the definitions of $\mu^{(\mathrm{r})}_{\mathrm{Tx,both}}$, $\mu^{(\mathrm{r})}_{\mathrm{Rx,both}}$, $\mu^{(\mathrm{t})}_{\mathrm{Tx,both}}$ and $\mu^{(\mathrm{t})}_{\mathrm{Rx,both}}$ in (77) and (78). Define

$$\alpha_1 \triangleq \max\left\{\min\left\{\frac{\mu_{\mathrm{Tx}}}{\mu^{(\mathrm{r})}_{\mathrm{Tx,both}}}, \frac{\mu_{\mathrm{Rx}}}{\mu^{(\mathrm{r})}_{\mathrm{Rx,both}}}\right\}, \min\left\{\frac{\mu_{\mathrm{Tx}}}{\mu^{(\mathrm{t})}_{\mathrm{Tx,both}}}, \frac{\mu_{\mathrm{Rx}}}{\mu^{(\mathrm{t})}_{\mathrm{Rx,both}}}\right\}\right\}, \quad \alpha_2 \triangleq \max\left\{\frac{\mu_{\mathrm{Tx}}}{\mu^{(\mathrm{t})}_{\mathrm{Tx,S}}}, \frac{\mu_{\mathrm{Rx}}}{\mu^{(\mathrm{r})}_{\mathrm{Rx,S}}}\right\}. \tag{79}$$

Also, define

$$\mathsf{S}^{(F)}_{\text{hexa},1}(\alpha_1) \triangleq \alpha_1 \mathsf{S}^{(F)}_{\text{both}}, \qquad \mathsf{S}^{(S)}_{\text{hexa},1}(\alpha_1) \triangleq \alpha_1 \mathsf{S}^{(S)}_{\text{both}} + (1-\alpha_1)\mathsf{S}^{(S)}_{\max}, \tag{80}$$

$$\mathsf{S}^{(F)}_{\text{hexa},2}(\alpha_1) \triangleq \alpha_1 \mathsf{S}^{(F)}_{\text{both}} + (1-\alpha_1)\mathsf{S}_{\text{no-coop}}, \qquad \mathsf{S}^{(S)}_{\text{hexa},2}(\alpha_1) \triangleq \alpha_1 \mathsf{S}^{(S)}_{\text{both}}, \tag{81}$$

$$\mathsf{S}^{(S)}_{\text{hexa}}(\alpha_2) \triangleq \alpha_2 \mathsf{S}^{(S)}_{\max} + (1-\alpha_2)\mathsf{S}_{\text{no-coop}}. \tag{82}$$

Theorem 2 (Achievable MG Region: Hexagonal Model): Assume $\mathrm{D} \geq 2$, even, and $\frac{\mathrm{D}}{2} - 1 \mod 3 = 0$.

When $\mu_{\mathrm{Rx}} \geq \max\{\mu^{(\mathrm{r})}_{\mathrm{Rx,both}}, \mu^{(\mathrm{r})}_{\mathrm{Rx,S}}\}$ and $\mu_{\mathrm{Tx}} \geq \mu^{(\mathrm{r})}_{\mathrm{Tx,both}}$; or when $\mu_{\mathrm{Tx}} \geq \max\{\mu^{(\mathrm{t})}_{\mathrm{Tx,both}}, \mu^{(\mathrm{t})}_{\mathrm{Tx,S}}\}$ and $\mu_{\mathrm{Rx}} \geq \mu^{(\mathrm{t})}_{\mathrm{Rx,both}}$; then:

$$\text{convex hull}\Big((0,0),\ (0,\mathsf{S}^{(S)}_{\max}),\ (\mathsf{S}^{(F)}_{\text{both}}, \mathsf{S}^{(S)}_{\text{both}}),\ (\mathsf{S}_{\text{no-coop}}, 0)\Big) \subseteq \mathcal{S}^{\star}(\mu_{\mathrm{Tx}}, \mu_{\mathrm{Rx}}, \mathrm{D}). \tag{83}$$

When $\mu^{(\mathrm{r})}_{\mathrm{Rx,both}} \leq \mu_{\mathrm{Rx}} < \mu^{(\mathrm{r})}_{\mathrm{Rx,S}}$ and $\mu_{\mathrm{Tx}} \geq \mu^{(\mathrm{r})}_{\mathrm{Tx,both}}$; or when $\mu^{(\mathrm{t})}_{\mathrm{Tx,both}} \leq \mu_{\mathrm{Tx}} < \mu^{(\mathrm{t})}_{\mathrm{Tx,S}}$ and $\mu_{\mathrm{Rx}} \geq \mu^{(\mathrm{t})}_{\mathrm{Rx,both}}$; then:

$$\text{convex hull}\Big((0,0),\ (0,\mathsf{S}^{(F)}_{\text{both}} + \mathsf{S}^{(S)}_{\text{both}}),\ (\mathsf{S}^{(F)}_{\text{both}}, \mathsf{S}^{(S)}_{\text{both}}),\ (\mathsf{S}_{\text{no-coop}}, 0)\Big) \subseteq \mathcal{S}^{\star}(\mu_{\mathrm{Tx}}, \mu_{\mathrm{Rx}}, \mathrm{D}). \tag{84}$$

When $\mu_{\mathrm{Rx}} \geq \mu^{(\mathrm{r})}_{\mathrm{Rx,S}}$ and $\mu_{\mathrm{Tx}} < \mu^{(\mathrm{r})}_{\mathrm{Tx,both}}$; or when $\mu_{\mathrm{Tx}} \geq \mu^{(\mathrm{t})}_{\mathrm{Tx,S}}$ and $\mu_{\mathrm{Rx}} < \mu^{(\mathrm{t})}_{\mathrm{Rx,both}}$; then:

$$\begin{aligned}\text{convex hull}\Big((0,0),\ (0,\mathsf{S}^{(S)}_{\max}),\ &(\mathsf{S}^{(F)}_{\text{hexa},1}(\alpha_1), \mathsf{S}^{(S)}_{\text{hexa},1}(\alpha_1)),\\ &(\mathsf{S}^{(F)}_{\text{hexa},2}(\alpha_1), \mathsf{S}^{(S)}_{\text{hexa},2}(\alpha_1)),\ (\mathsf{S}_{\text{no-coop}}, 0)\Big) \subseteq \mathcal{S}^{\star}(\mu_{\mathrm{Tx}}, \mu_{\mathrm{Rx}}, \mathrm{D}).\end{aligned} \tag{85}$$

When $\mu_{\mathrm{Rx}} < \mu^{(\mathrm{r})}_{\mathrm{Rx,both}}$ or when $\mu_{\mathrm{Tx}} < \mu^{(\mathrm{t})}_{\mathrm{Tx,both}}$, then:

$$\text{convex hull}\Big((0,0),\ (0,\mathsf{S}^{(S)}_{\text{hexa}}(\alpha_2)),\ (\mathsf{S}^{(F)}_{\text{hexa},2}(\alpha_1), \mathsf{S}^{(S)}_{\text{hexa},2}(\alpha_1)),\ (\mathsf{S}_{\text{no-coop}}, 0)\Big) \subseteq \mathcal{S}^{\star}(\mu_{\mathrm{Tx}}, \mu_{\mathrm{Rx}}, \mathrm{D}). \tag{86}$$

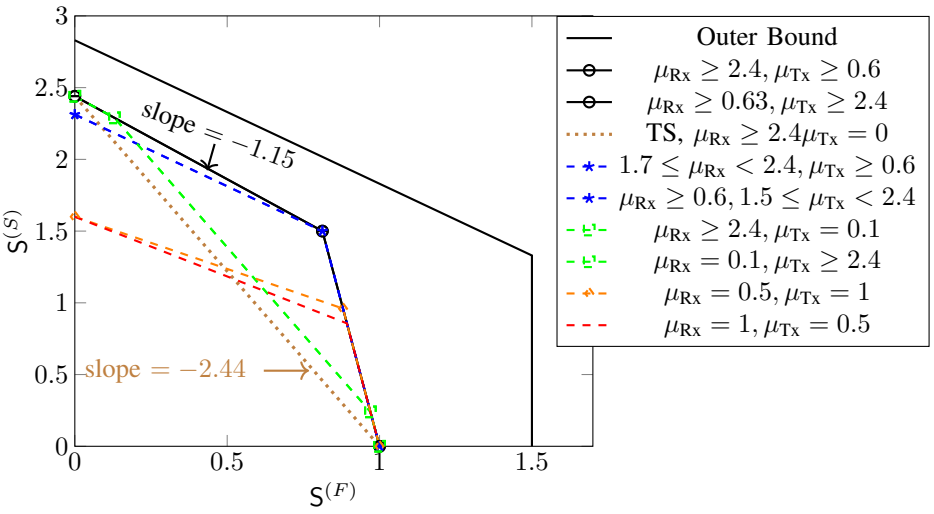

Fig. 7: Inner and outer bounds on $\mathcal{S}^\star(\mu_{\text{Tx}}, \mu_{\text{Rx}}, \mathsf{D})$ for the hexagonal model for $\mathsf{D} = 8$, $\mathsf{L} = 3$ and different values of μ_{Rx} and μ_{Tx}. The dotted brown line shows the time-sharing line.

Proposition 2 (Outer Bound on The MG Region: Hexagonal Model): Any MG pair $(\mathsf{S}^{(F)}, \mathsf{S}^{(S)})$ in $\mathcal{S}^\star(\mu_{\text{Tx}}, \mu_{\text{Rx}}, \mathsf{D})$ satisfies

$$\mathsf{S}^{(F)} \leq \frac{\mathsf{L}}{2}, \tag{87}$$

$$\mathsf{S}^{(F)} + \mathsf{S}^{(S)} \leq \min\left\{\frac{\mathsf{L}}{2} + 2\mu_{\text{Rx}} + 2\mu_{\text{Tx}},\ \mathsf{L}\left(1 - \frac{1}{2(1+\mathsf{D})}\right)\right\}. \tag{88}$$

Proof: Follows by extending the converse in [37, Theorem 2] to the hexagonal model without sectors and with both Tx- and Rx-cooperation. See Appendix C for details. ■

Figure 7 illustrates the inner and outer bounds (Theorem 2 and Proposition 2) on the MG region for $\mathsf{D} = 8$, and different values of μ_{Rx} and μ_{Tx}. We observe that, unlike Wyner's symmetric model, the sum-MG of this network always decreases as $\mathsf{S}^{(F)}$ increases, irrespective of the cooperation prelogs $\mu_{\text{Tx}}, \mu_{\text{Rx}}$. Moreover, maximum $\mathsf{S}^{(F)} = \frac{1}{3}$ in our bound is only achieved for $\mathsf{S}^{(S)} = 0$. We remark here that for certain channel matrices (in fact for many but not for all) "fast" MG $\mathsf{S}^{(F)}$ is achievable using interference alignment [38]–[40]. For these channel matrices of course our inner bound can be improved accordingly.

In Figure 7, we can distinguish 4 behaviours for the achieved MG region: 1) If both μ_{Rx} and μ_{Tx} are above given thresholds, for $\mathsf{D} = 8$ and either $(\mu_{\text{Tx}} \geq 0.6, \mu_{\text{Rx}} \geq 2.4)$ or $(\mu_{\text{Tx}} \geq 0.63, \mu_{\text{Rx}} \geq 2.4)$, then the points $(0, \mathsf{S}^{(S)}_{\max})$ and $(\mathsf{S}^{(F)}_{\text{both}}, \mathsf{S}^{(F)}_{\text{both}})$ are both achievable. 2) When one of the two cooperation prelogs remains very high (μ_{Rx} or μ_{Tx} larger than 2.4) but the other one

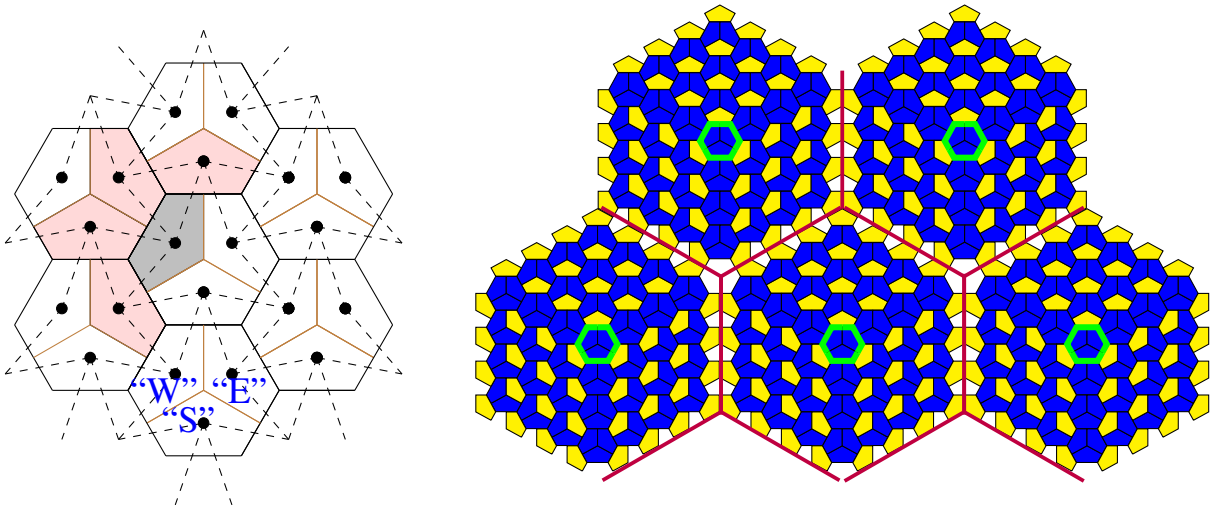

(a) (b) D = 8

Fig. 8: Illustration of sectorized hexagonal network. (a) Dashed lines indicate interference between sectors and thick lines cell borders. (b) Txs in white sectors are deactivated, Txs in yellow sectors send "fast" messages and Txs in blue sectors send "slow" messages.

becomes relatively small, only $(0, \mathsf{S}_{\text{max}}^{(S)})$ is achievable, but not $(\mathsf{S}_{\text{both}}^{(F)}, \mathsf{S}_{\text{both}}^{(F)})$. The largest achievable $\mathsf{S}^{(S)}$ is thus not reduced as long as $\mathsf{S}^{(F)}$ remains small; for larger values of $\mathsf{S}^{(F)}$ the maximum achievable $\mathsf{S}^{(S)}$ however suffers significantly. The reason is that our schemes that send both "fast" and "slow" messages inherently require both Tx- *and* Rx-cooperation of sufficiently high cooperation prelogs. As a consequence, the maximum $\mathsf{S}^{(S)}$ that our schemes achieve for large $\mathsf{S}^{(F)}$ highly depends on the smaller of the two cooperation prelogs μ_{Tx} and μ_{Rx}. 3) When both $\mu_{\text{Tx}}, \mu_{\text{Rx}}$ are moderate, we can still achieve the MG pair $(\mathsf{S}_{\text{both}}^{(F)}, \mathsf{S}_{\text{both}}^{(F)})$ but not $(0, \mathsf{S}_{\text{max}}^{(S)})$. In the regime of small $\mathsf{S}^{(F)}$ there is thus a penalty in $\mathsf{S}^{(S)}$ and sum MG compared to the case of high cooperation prelogs but not in the regime of large $\mathsf{S}^{(F)}$. 4) Finally, when both cooperation prelogs become small then neither of the two points $(0, \mathsf{S}_{\text{max}}^{(S)})$ and $(\mathsf{S}_{\text{both}}^{(F)}, \mathsf{S}_{\text{both}}^{(F)})$ is achievable anymore.

The brown dotted line is the resulting region under the traditional scheduling scheme that time-shares the scheme achieving the point $(0, \mathsf{S}_{\text{max}}^{(S)})$ with the scheme achieving the point $(\mathsf{S}_{\text{no-coop}}, 0)$. To achieve the point $(0, \mathsf{S}_{\text{max}}^{(S)})$, this scheme requires $\mu_{\text{Rx}} \geq 2.4$ and $\mu_{\text{Tx}} = 0$ while using CoMP reception, and $\mu_{\text{Rx}} = 0$ and $\mu_{\text{Tx}} \geq 2.4$ while using CoMP transmission. Comparing the slope of this line with the slopes of the regions achieved under our proposed scheme show that the penalty of transmitting "fast" messages on sum-MG is very large in this scheme.

VI. Sectorized Hexagonal Model

Reconsider the cellular network with K hexagonal cells and cell coordinate system spanned by the vectors $\mathbf{e}_x$ and $\mathbf{e}_y$ introduced in the previous section. Here, each cell consists of three sectors denoted by "S", "W", and "E", see Figure 8a, and we also number the sectors from 1 to $3K$. A single $3\mathsf{L}$-antenna Rx (BS) is associated to each *cell* and a single L-antenna Tx to each *sector*. Each Rx decodes the 3 "slow" and the 3 "fast" messages of the Txs in the 3 sectors corresponding to its cell. Rxs are equipped with directional antennas, where each set of L antennas at a given Rx (BS) points to one of the three sectors of its cell. Therefore, communications from different sectors in the same cell do not interfere, see Fig. 8a where interference is depicted by dashed lines. Interference is short-range, and transmission in the grey-shaded sector of Fig. 8a is, e.g., interfered by the transmissions in the four adjacent pink-shaded sectors. The interference set $\mathcal{I}_{\text{Tx},k'}$ of sector k' is thus the set of indices of the 4 adjacent sectors that lie in a different cell.

For the purpose of this section, we thus modify the setup in Section II in that we have $3K$ Txs and K Rxs and each Rx k observes the output signals $\mathbf{Y}_k^n := (\mathbf{Y}_{k_1}^n, \mathbf{Y}_{k_2}^n, \mathbf{Y}_{k_3}^n)$, where k_1, k_2, k_3 denote the three sectors in cell k, and

$$\mathbf{Y}_{k_i}^n = \mathsf{H}_{k_i,k_i}\boldsymbol{X}_{k_i}^n + \sum_{\hat{k}\in\mathcal{I}_{k_i}} \mathsf{H}_{\hat{k},k_i}\boldsymbol{X}_{\hat{k}}^n + \boldsymbol{Z}_{k_i}^n, \qquad i \in \{1,2,3\}. \tag{89}$$

We consider *per-sector MGs*, and accordingly the average rates in (10) are normalized with respect to $3K$ and not K. All other definitions of Section II remain unchanged.

Each Rx k (BS of a cell) can cooperate with the Rxs in the six adjacent cells, i.e., $|\mathcal{N}_{\text{Rx}}(k)| = 6$ and $\mathcal{Q}_{K,\text{Rx}} \approx 6K$. Each Tx (MU of a cell) can cooperate with the four Txs in the adjacent sectors of different cells, i.e. $|\mathcal{N}_{\text{Tx}}(k)| = 4$ and since there are $3K$ Txs, $\mathcal{Q}_{K,\text{Tx}} \approx 12K$. Assume D even.

The coding schemes and results in Section III apply also to this modified setup, if $\mathcal{T}_{\text{silent}}, \mathcal{T}_{\text{active}}, \mathcal{T}_{\text{fast}}, \mathcal{T}_{\text{slow}} \subseteq [3K]$ and the MG results (20), (27), and (31) are normalized with respect to $3K$ and not K. We only consider CoMP reception, and thus $\mathcal{T}_{\text{master}} \subseteq [K]$.

A. Tx/Rx Set Associations and MG Region

We specify the Tx/Rx set associations for our schemes of Section III. For the no cooperation scheme, define the active set $\mathcal{T}_{\text{active}}$ as the set of either the "W" sectors, the "E" sectors, or the "S" sectors of all cells. This achieves the sum-MG

$$\mathsf{S}_{\text{no-coop}} \triangleq \frac{\mathsf{L}}{3}. \tag{90}$$

For the cooperative schemes, we pick the set of *master cells* $\mathcal{T}_{\text{master}}$ as in (71) for $\tau = \frac{\mathrm{D}}{2}$. Unlike in the hexagonal model in Section V, it suffices to silence certain sectors of layer $\mathrm{D}/2$ around each master cell. Consider the subnet that has its master cell k_{master} at the origin $a_{k_{\text{master}}} = b_{k_{\text{master}}} = 0$, for which we keep active all 3 sectors of the corner cells in layer $\mathrm{D}/2$ that have coordinates $(a_k = \mathrm{D}/2, b_k = 0)$, $(a_k = 0, b_k = \mathrm{D}/2)$, and $(a_k = -\mathrm{D}/2, b_k = -\mathrm{D}/2)$, and we silence all 3 sectors of the remaining 3 corner cells of this layers, which have coordinates $(a_k = \mathrm{D}/2, b_k = \mathrm{D}/2)$, $(a_k = -\mathrm{D}/2, b_k = 0)$, and $(a_k = 0, b_k = -\mathrm{D}/2)$. We further silence in this layer $\mathrm{D}/2$ the "S" sector of all non-corner cells with coordinates $|b_k| = \mathrm{D}/2$ and $\text{sign}(a_k) = \text{sign}(b_k)$; the "E" sector of all non-corner cells with coordinates $|a_k| = \mathrm{D}/2$ and $\text{sign}(a_k) = \text{sign}(b_k)$; and the "W" sector of all non-corner cells with coordinates $\text{sign}(a_k) \neq \text{sign}(b_k)$. As for the hexagonal model, all Txs that lie less than $\mathrm{D}/2$ cell hops from a master cell are kept active. The proposed sector association splits the entire network into equal non-interfering subnets (up to edge effects that vanish as $K \to \infty$), each consisting of a master cell, all sectors of the cells in the $\mathrm{D}/2 - 1$ surrounding layers, and none or one sector in each cell of layer $\mathrm{D}/2$. The proposed cell and sector association is shown in Figure 8b for $\mathrm{D} = 8$, where yellow and blue sectors are active and white are silenced. The borders of the subnets are shown by red lines.

As shown in Appendix B, when sending only "slow" messages the proposed sector association achieves $(\mathsf{S}^{(F)} = 0, \mathsf{S}^{(S)} = \mathsf{S}^{(S)}_{\text{max}})$ where

$$\mathsf{S}^{(S)}_{\text{max}} \triangleq \mathsf{L} \cdot \frac{3\mathrm{D} - 2}{3\mathrm{D}}, \tag{91}$$

and it requires an average Rx-cooperation prelog of

$$\mu^{(\text{r})}_{\text{Rx},\mathsf{S}} = \mathsf{L} \cdot \frac{(\mathrm{D} - 1)}{3}. \tag{92}$$

In the scheme sending both "fast" and "slow" messages, the Txs in the "yellow" sectors of Figure 8b send "fast" messages and the Txs in the "blue" sectors send "slow" messages. We describe the cell association more formally for a subnet whose master cell is at the origin. All other subnets are equal. All active sectors in layer-$\mathrm{D}/2$ of this subnet send "fast" messages, but all sectors in the cells satisfying one of the three following conditions only send "slow" messages: ($a_k \geq 0$ and $b_k = 0$) or ($a_k = 0$ and $b_k \geq 0$) or ($a_k = b_k \leq 0$). All other cells have exactly one "fast" sector and two "slow" sectors. Specifically, cells with $a_k, b_k > 0$ send a "fast" message in their "W" sector; cells with $a_k < 0$ and $b_k > a_k$ send a "fast" message in their "S" sector; and cells with $b_k < 0$ and $a_k > b_k$ send a "fast" message in their "E" sector.

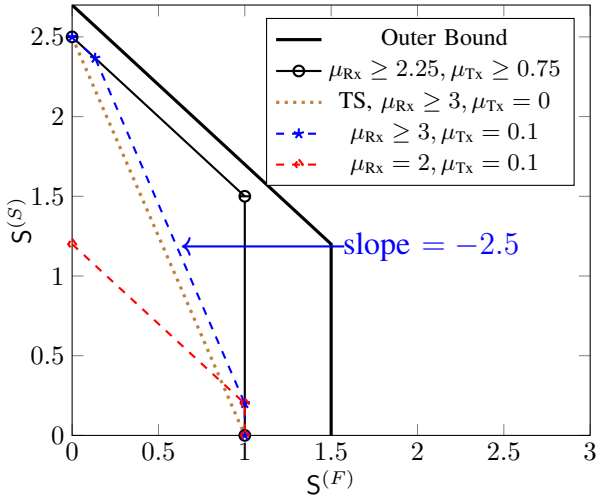

Fig. 9: Inner and outer bounds on $\mathcal{S}^{\star}(\mu_{\text{Tx}}, \mu_{\text{Rx}}, \mathsf{D})$ for the sectorized hexagonal model for $\mathsf{D} = 4$, $\mathsf{L} = 3$ and different values of μ_{Rx} and μ_{Tx}. The brown dotted line is the time-sharing region.

We prove in Appendix B that the proposed sector association achieves the MG pair

$$\mathsf{S}^{(F)}_{\text{both}} \triangleq \frac{\mathsf{L}}{3}, \quad \text{and} \quad \mathsf{S}^{(S)}_{\text{both}} \triangleq \mathsf{L} \cdot \frac{2\mathsf{D}-2}{3\mathsf{D}}, \tag{93}$$

and requires average Tx- and Rx-cooperation prelogs

$$\mu^{(\text{r})}_{\text{Tx,both}} \triangleq \mathsf{L} \cdot \frac{(\mathsf{D}-1)}{3\mathsf{D}} \quad \text{and} \quad \mu^{(\text{r})}_{\text{Rx,both}} \triangleq \mathsf{L} \cdot \frac{2\mathsf{D}^2-5}{9\mathsf{D}}. \tag{94}$$

Recall definitions (90)–(93) and define

$$\alpha_1 \triangleq \frac{\mu_{\text{Tx}}}{\mu^{(\text{r})}_{\text{Tx,both}}} \quad \text{and} \quad \alpha_2 \triangleq \min\left\{\frac{\mu_{\text{Tx}}}{\mu^{(\text{r})}_{\text{Tx,both}}}, \frac{\mu_{\text{Rx}}}{\mu^{(\text{r})}_{\text{Rx,both}}}\right\}, \tag{95}$$

$$\mathsf{S}^{(F)}_{\text{sec}}(\alpha_1) \triangleq \alpha_1 \mathsf{S}^{(F)}_{\text{both}}, \qquad \mathsf{S}^{(S)}_{\text{sec}}(\alpha_1) \triangleq \alpha_1 \mathsf{S}^{(S)}_{\text{both}} + (1-\alpha_1)\mathsf{S}^{(S)}_{\text{max}}, \tag{96}$$

$$\mathsf{S}^{(F)}_{\text{sec},1}(\alpha_2) \triangleq \alpha_2 \mathsf{S}^{(F)}_{\text{both}} + (1-\alpha_2)\mathsf{S}_{\text{no-coop}}, \qquad \mathsf{S}^{(S)}_{\text{sec},1}(\alpha_2) \triangleq \alpha_2 \mathsf{S}^{(S)}_{\text{both}}, \tag{97}$$

$$\mathsf{S}^{(S)}_{\text{sec},2}(\alpha_2) \triangleq \alpha_2 \mathsf{S}^{(S)}_{\text{max}} + (1-\alpha_2)\mathsf{S}_{\text{no-coop}}. \tag{98}$$

The following theorem is proved in Appendix B.

Theorem 3 (Achievable MG Region: Sectorized Hexagonal Model): Assume $\mathsf{D} \geq 2$ and even.

- When $\mu_{\text{Rx}} \geq \mu^{(\text{r})}_{\text{Rx,both}}$ and $\mu_{\text{Tx}} \geq \mu^{(\text{r})}_{\text{Tx,both}}$;

$$\text{convex hull}\Big((0,0),\ (0,\mathsf{S}^{(S)}_{\text{max}}),\ (\mathsf{S}^{(F)}_{\text{both}},\mathsf{S}^{(S)}_{\text{both}}),\ (\mathsf{S}_{\text{no-coop}},0)\Big) \subseteq \mathcal{S}^{\star}(\mu_{\text{Tx}},\mu_{\text{Rx}},\mathsf{D}). \tag{99}$$

- When $\mu_{\text{Rx}} \geq \mu^{(\text{r})}_{\text{Rx,S}}$ and $\mu_{\text{Tx}} < \mu^{(\text{r})}_{\text{Tx,both}}$;

$$\text{convex hull}\Big((0,0),\ (0,\mathsf{S}^{(S)}_{\text{max}}),\ (\mathsf{S}^{(F)}_{\text{sec}}(\alpha_1),\mathsf{S}^{(S)}_{\text{sec}}(\alpha_1)),$$

$$\left(\mathsf{S}_{\text{sec},1}^{(F)}(\alpha_2), \mathsf{S}_{\text{sec},1}^{(S)}(\alpha_2)\right),\ (\mathsf{S}_{\text{no-coop}}, 0)\Big) \subseteq \mathcal{S}^{\star}(\mu_{\text{Tx}}, \mu_{\text{Rx}}, \mathrm{D}). \quad (100)$$

- When $\mu_{\text{Rx}} < \mu_{\text{Rx,both}}^{(\text{r})}$ and $\mu_{\text{Tx}} < \mu_{\text{Tx,both}}^{(\text{r})}$;

$$\text{convex hull}\Big((0,0),\ (0, \mathsf{S}_{\text{sec},2}^{(S)}(\alpha_2)),\ \left(\mathsf{S}_{\text{sec},1}^{(F)}(\alpha_2), \mathsf{S}_{\text{sec},1}^{(S)}(\alpha_2)\right),\ (\mathsf{S}_{\text{no-coop}}, 0)\Big) \subseteq \mathcal{S}^{\star}(\mu_{\text{Tx}}, \mu_{\text{Rx}}, \mathrm{D}). \quad (101)$$

Proposition 3 (Outer Bound on The MG Region: Sectorized Hexagonal Model): Any MG pair $(\mathsf{S}^{(F)}, \mathsf{S}^{(S)})$ in $\mathcal{S}^{\star}(\mu_{\text{Tx}}, \mu_{\text{Rx}}, \mathrm{D})$ satisfies

$$\mathsf{S}^{(F)} \leq \frac{\mathsf{L}}{2}, \quad (102)$$

$$\mathsf{S}^{(F)} + \mathsf{S}^{(S)} \leq \min\left\{\frac{\mathsf{L}}{2} + \frac{2\mu_{\text{Rx}} + 4\mu_{\text{Tx}}}{3}, \mathsf{L}\left(1 - \frac{1}{2(1+\mathrm{D})}\right)\right\}. \quad (103)$$

Proof: Follows by an extension of the converse in [37, Theorem 2] to both Tx- and Rx-cooperation. See Appendix D for details. ■

Figure 9 illustrates the inner and outer bounds (Theorem 3 and Proposition 3) on the MG region for $\mathrm{D} = 4$, and different values of μ_{Rx} and μ_{Tx}. As can be seen from this figure, when $\mu_{\text{Rx}} \geq 2.25$ and $\mu_{\text{Tx}} \geq 0.75$, there is no penalty in sum MG even at maximum "fast" MG. It also can be seen from this figure that transmitting "fast" messages using the traditional time-sharing scheme (brown dotted line) at any "fast" MG has a penalty on sum-MG.

VII. Conclusions

We proposed a coding scheme for general interference networks that accommodates the transmission of both delay-sensitive and delay-tolerant messages. We characterized the MG region of Wyner's symmetric network for certain parameters and derived inner bounds on the achievable MG region for general parameters, as well as for the sectorized and non-sectorized hexagonal model. The results for Wyner's symmetric model showed that it is possible to accommodate the largest possible MG for delay-sensitive messages, without penalizing the maximum sum MG of both delay-sensitive and delay-tolerant messages. Our proposed scheme suggests a similar behaviour for the sectorized hexagonal model, when one restricts to one-shot interference alignment. For the non-sectorized hexagonal model this does not seem to be the case, and our results always show a penalty in sum MG whenever the delay-sensitive MG is not zero. These results indicate that each network needs to be carefully analyzed to determine whether a sum MG penalty exists under mixed-delay traffics. Nevertheless, in this paper we proposed a joint coding scheme for mixed-delay traffics that significantly improves the sum MG compared to a classical scheduling approach.

Our proposed coding schemes suggest that in the regime of high delay-sensitive MGs, it is important to have sufficiently high cooperation prelogs both at the Tx- and the Rx-side to attain the same sum MG as when only delay-tolerant messages are sent. Moreover, in this regime, Tx-cooperation seems to be slightly more beneficial under mixed-delay traffics than Rx-cooperation.

An interesting line of future research is to analyze the effect of delay-sensitive messages on generalized Wyner models with fading coefficients and finite precision channel state information. Here also the notion of generalized degrees of freedom (GDoF) is of interest, see also [36].

APPENDIX A
ANALYSES FOR THE HEXAGONAL MODEL

We prove that the Tx/Rx set associations proposed in Section V are permissible and we provide details on how to compute the corresponding MG pairs and cooperation prelogs.

A. No Cooperation Scheme

Fig. 6a shows the active Txs in yellow and the silenced Txs in white. It is easily seen that transmissions in yellow cells do not interfere, as they pertain to non-neighbouring cells.

More formally, we consider two different Txs k and k' in the active set $\mathcal{T}_{\text{active}}$ defined in (69), and we prove by contradiction that Tx k' cannot be in the neighbouring set $\mathcal{I}_k$ of Tx k. Assume that $k' \in \mathcal{I}_k$. Then, by (67), either $(a_{k'} = a_k + 1, b_{k'} = b_k + 1)$ or $(a_{k'} = a_k - 1, b_{k'} = b_k - 1)$. Each of these two cases however violates the active set condition (69), which implies

$$(a_k + b_k) \mod 3 = 0 \quad \text{and} \quad (a_{k'} + b_{k'}) \mod 3 = 0. \tag{104}$$

We thus obtained the desired contradiction.

To see that the scheme achieves a sum-MG of $\mathsf{S}_{\text{no-coop}}$ we notice that in the limit as $K \to \infty$, the active set $\mathcal{T}_{\text{active}}$ defined in (69) includes a third of all Txs simply because a third of the integer pairs (a, b) satisfy $(a + b) \mod 3 = 0$ and because for each integer pair (a, b) corresponds a Tx.

B. Coding scheme to transmit only "slow" messages with CoMP reception or transmission

As mentioned in the main body, and as is easily seen in Figure 6b, the silenced set $\mathcal{T}_{\text{silent}}$ consists of all cells that are exactly $\frac{\mathrm{D}}{2} + 1$ cell hops away from the next master cell. All other cells have a master cell that lies less than $\frac{\mathrm{D}}{2} + 1$ cell hops away. In other words, each master

cell is surrounded by $\mathrm{D}/2$ layers of active cells sending "slow" messages, where in total these $\mathrm{D}/2$ layers contain $\sum_{i=1}^{\mathrm{D}/2} 6i = \frac{3}{4}\mathrm{D}(\mathrm{D}+2)$ cells. Such a subnet is then surrounded by a layer of $6 \cdot (\frac{\mathrm{D}}{2}+1) = 3\mathrm{D}+6$ silenced cells, each lying $\mathrm{D}/2+1$ cell hops away from the master cell. Among these layer-$(\mathrm{D}/2+1)$ cells, 6 of them (namely the corner cells) belong to the silenced layer of three different master cells, and the remaining $3\mathrm{D}$ belong to the silenced layer of two master cells. One can therefore add a set of $(6/3+3\mathrm{D}/2)$ silenced cells (2 corner cells and $3\mathrm{D}/2$ non-corner cells) to each of the subnets to partition the entire network of K cells into subsets of size

$$s \triangleq 1 + \frac{3}{4}\mathrm{D}(\mathrm{D}+2) + (6/3+3\mathrm{D}/2) = \frac{3(\mathrm{D}+2)^2}{4}. \tag{105}$$

By these considerations, and because master cells themselves also send "slow" messages,

$$\lim_{K\to\infty} \frac{|\mathcal{T}_{\text{slow}}|}{K} = \frac{1+\frac{3}{4}\mathrm{D}(\mathrm{D}+2)}{\frac{3}{4}(\mathrm{D}+2)} = \frac{4+3\mathrm{D}(\mathrm{D}+2)}{3(\mathrm{D}+2)^2}, \tag{106}$$

and as a result, by (26) and (27), the proposed cell association achieves the MG pair $(\mathsf{S}^{(F)} = 0, \mathsf{S}^{(S)} = \mathsf{S}^{(S)}_{\max})$ with $\mathsf{S}^{(S)}_{\max}$ defined in (74).

With CoMP reception, the scheme does not send any Tx-cooperation messages but only Rx-cooperation messages. To calculate the Rx-cooperation prelog, notice that for each Rx k we have $\gamma_{\text{Rx},k} = i \in \{1,\ldots,\mathrm{D}/2\}$ if Rx k lies i hops away from the next master cell. Fix a master cell $k_{\text{master}} \in \mathcal{T}_{\text{master}}$ and define $\mathcal{T}_{\text{subnet}}$ as the set including this master cell as well as the $\mathrm{D}/2$ layers around it:

$$\mathcal{T}_{\text{subnet}} \triangleq \left\{ k\colon \max\{|a_k - a_{k_{\text{master}}}|,\ |b_k - b_{k_{\text{master}}}|,\ |a_k - a_{k_{\text{master}}} - b_k + b_{k_{\text{master}}}|\} \le \frac{\mathrm{D}}{2} \right\}. \tag{107}$$

Since in this subnet $\mathcal{T}_{\text{subnet}}$ there are $6i$ Rxs with $\gamma_{\text{Rx},k} = i$, for each $i = 1,\ldots,\mathrm{D}/2$:

$$2\sum_{k\in\mathcal{T}_{\text{subnet}}} \gamma_{\text{Rx},k} = 2\sum_{i=1}^{\mathrm{D}/2} 6i^2 = \frac{\mathrm{D}(\mathrm{D}+2)(\mathrm{D}+1)}{2}, \tag{108}$$

and since by a sandwiching argument $K^{-1}\sum_{k\in\mathcal{T}_{\text{slow}}} \gamma_{\text{Rx},k} \to s^{-1}\sum_{k\in\mathcal{T}_{\text{subnet}}} \gamma_{\text{Rx},k}$ as $K\to\infty$:

$$\lim_{K\to\infty} \frac{2\sum_{k\in\mathcal{T}_{\text{slow}}} \gamma_{\text{Rx},k}}{K} = \frac{2\sum_{k\in\mathcal{T}_{\text{subnet}}} \gamma_{\text{Rx},k}}{s} \tag{109}$$

$$= \frac{\mathrm{D}(\mathrm{D}+2)(\mathrm{D}+1)/2}{\frac{3}{4}(\mathrm{D}+2)^2} = \frac{2\mathrm{D}(\mathrm{D}+1)}{3(\mathrm{D}+2)}. \tag{110}$$

Finally, because $\lim_{K\to\infty} \frac{\mathcal{Q}_{K,\text{Rx}}}{K} = 6$, according to (28) the required Rx-cooperation prelog equals

$$\mu^{(\text{r})}_{\text{Rx},\mathsf{S}} = \mathsf{L} \cdot \frac{\mathrm{D}(\mathrm{D}+1)}{9(\mathrm{D}+2)}. \tag{111}$$

With CoMP transmission, this scheme does not require any Rx-cooperation messages and consumes a Tx-cooperation prelog of $\mu^{(\text{t})}_{\text{Tx},\mathsf{S}} = \mu^{(\text{r})}_{\text{Rx},\mathsf{S}}$.

C. Coding Scheme to transmit both "fast" and "slow" messages with CoMP reception

Consider the cell association described for this scheme in the main body of the paper. That means,

$$\mathcal{T}_{\text{silent}} = \left\{ k\colon \max\{|a_{k[-\tau,2\tau)}|, |b_{k[-\tau,2\tau)}|, |a_{k[-\tau,2\tau)} - b_{k[-\tau,2\tau)}|\} = \frac{\mathrm{D}}{2} \right\}, \tag{112}$$

where the operator $x \mapsto x_{[-\tau,2\tau]}$ is defined in (72). Similarly, the set of master cells is given by

$$\mathcal{T}_{\text{master}} = \left\{ k \in [K]\colon \left(a_k \mod \frac{\mathrm{D}}{2} = 0 \right) \text{ and } \left(b_k \mod \frac{\mathrm{D}}{2} = 0 \right) \right.$$
$$\left. \text{and } \left(|a_k + b_k| \mod \frac{3\mathrm{D}}{2} = 0 \right) \right\}. \tag{113}$$

This choice decomposes the network into equal subnets of active cells, each one surrounding one of the master cells. For a given master cell k_{master}, the subnet is given by:

$$\mathcal{T}_{\text{subnet}} \triangleq \left\{ k\colon \max\{|a_k - a_{k_{\text{master}}}|,\ |b_k - b_{k_{\text{master}}}|,\ |a_k - a_{k_{\text{master}}} - b_k + b_{k_{\text{master}}}|\} \leq \frac{\mathrm{D}}{2} - 1 \right\}. \tag{114}$$

Notice that the subnet is defined in a similar way as in (107) in the preceding subsection, except that D is replaced by $\mathrm{D} - 2$. That means, it contains the master cell k_{master} and the $\mathrm{D}/2 - 1$ cell layers (i.e., the cells with $\gamma_{\text{Rx},k} = 1, \ldots, \mathrm{D}/2 - 1$) surrounding it. Therefore:

$$|\mathcal{T}_{\text{subnet}}| = 1 + \sum_{i=1}^{\frac{\mathrm{D}}{2}-1} 6i = 1 + \frac{3}{4}\mathrm{D}(\mathrm{D} - 2) \tag{115}$$

Cell-layer $\mathrm{D}/2$ (the cells with $\gamma_{\text{Rx},k} = \mathrm{D}/2$) around each master cell is silenced. It consists of 6 corner cells, which are $\mathrm{D}/2$ cell hops away from 3 different master cells, and of $3\mathrm{D} - 6$ non-corner cells, which lie $\mathrm{D}/2$ cell hops away from two different master cells. Similarly to the previous section, one can build a cell partitioning by simply associating a third of the corner cells and half of the non-corner cells of layer $\mathrm{D}/2$ to each master cell. Any subset of such a partition is then of size (up to some edge effects that vanish as $K \to \infty$)

$$s \triangleq \left(1 + \frac{3}{4}\mathrm{D}(\mathrm{D} - 2)\right) + \left(2 + \frac{3\mathrm{D} - 6}{2}\right) = \frac{3}{4}\mathrm{D}^2. \tag{116}$$

Recall further that we chose $\mathcal{T}_{\text{fast}} = \{k\colon (a_k + b_k) \mod 3 = 0\}$ and $\mathcal{T}_{\text{slow}} = [K] \backslash (\mathcal{T}_{\text{fast}} \cup \mathcal{T}_{\text{silent}})$.

Since all subnets are equal (there can be some edge effects that vanish as $K \to \infty$), by some sandwiching arguments, we obtain that $K^{-1}|\mathcal{T}_{\text{fast}}| \to s^{-1}|\mathcal{T}_{\text{subnet}} \cap \mathcal{T}_{\text{fast}}|$ and $K^{-1}|\mathcal{T}_{\text{slow}}| \to s^{-1}|\mathcal{T}_{\text{subnet}} \cap \mathcal{T}_{\text{slow}}|$ as $K \to \infty$. By the following Lemma 1, we then obtain the asymptotic ratios:

$$\lim_{K\to\infty} \frac{|\mathcal{T}_{\text{fast}}|}{K} = \frac{|\mathcal{T}_{\text{subnet}} \cap \mathcal{T}_{\text{fast}}|}{s} = \frac{\mathrm{D}^2 - 2\mathrm{D} + 4}{3\mathrm{D}^2} \tag{117}$$

$$\lim_{K\to\infty}\frac{|\mathcal{T}_{\text{slow}}|}{K}=\frac{|\mathcal{T}_{\text{subnet}}\cap\mathcal{T}_{\text{slow}}|}{s}=\frac{2\mathrm{D}-4}{3\mathrm{D}}. \tag{118}$$

By (20), this establishes the achievability of the desired MG pair in (76).

Lemma 1: The number of "fast" Txs in $\mathcal{T}_{\text{subnet}}$ equals

$$|\mathcal{T}_{\text{fast}}\cap\mathcal{T}_{\text{subnet}}|=\frac{\mathrm{D}^2}{4}-\frac{\mathrm{D}}{2}+1, \tag{119}$$

and the number of "slow" Txs in $\mathcal{T}_{\text{subnet}}$ equals

$$|\mathcal{T}_{\text{slow}}\cap\mathcal{T}_{\text{subnet}}|=\frac{\mathrm{D}^2}{2}-\mathrm{D}. \tag{120}$$

Proof: For ease of notation, assume that $k_{\text{master}}=0$.

Define the sector of the subnet $\mathcal{T}_{\text{subnet}}$ with positive coordinates $a_k>0$ and $b_k\geq 0$ (recall that we assume $k_{\text{master}}=0$):

$$\mathcal{T}^{+}_{\text{subnet}}\triangleq\left\{k\colon 0<a\leq\frac{\mathrm{D}}{2}-1,\ 0\leq b\leq\frac{\mathrm{D}}{2}-1\right\}\subseteq\mathcal{T}_{\text{subnet}}. \tag{121}$$

Since the angle between the coordinate vectors $\mathbf{e}_x$ and $\mathbf{e}_y$ is $\frac{2\pi}{3}$ and the sets $\mathcal{T}_{\text{fast}}$ and $\mathcal{T}_{\text{subnet}}$ are rotationally-invariant with respect to this angle,

$$|\mathcal{T}_{\text{subnet}}\cap\mathcal{T}_{\text{fast}}|=3|\mathcal{T}^{+}_{\text{subnet}}\cap\mathcal{T}_{\text{fast}}|+1, \tag{122}$$

where the 1 has to be added to account for the "fast" master cell at the origin.

To calculate the size of the set $\mathcal{T}^{+}_{\text{subnet}}\cap\mathcal{T}_{\text{fast}}$, notice that by Assumption (68), $\frac{\mathrm{D}}{2}-1$ is a multiple of 3 and thus for each value of $b\in\{0,1,\ldots,\frac{D}{2}-1\}$ there are exactly $\frac{\frac{\mathrm{D}}{2}-1}{3}$ values $a\in\{1,\ldots,\frac{\mathrm{D}}{2}-1\}$ so that the sum $a+b$ is a multiple of 3. Therefore,

$$|\mathcal{T}_{\text{fast}}\cap\mathcal{T}^{+}_{\text{subnet}}|=\frac{\mathrm{D}}{2}\cdot\frac{\frac{\mathrm{D}}{2}-1}{3}, \tag{123}$$

and

$$|\mathcal{T}_{\text{fast}}\cap\mathcal{T}_{\text{subnet}}|=3|\mathcal{T}_{\text{fast}}\cap\mathcal{T}^{+}_{\text{subnet}}|+1=\frac{\mathrm{D}^2}{4}-\frac{\mathrm{D}}{2}+1. \tag{124}$$

Since all cells in $\mathcal{T}_{\text{subnet}}$ that are not elements of $\mathcal{T}_{\text{fast}}$ belong to $\mathcal{T}_{\text{slow}}$, we obtain by (115) and (124) that

$$|\mathcal{T}_{\text{slow}}\cap\mathcal{T}_{\text{subnet}}|=|\mathcal{T}_{\text{subnet}}|-|\mathcal{T}_{\text{fast}}\cap\mathcal{T}_{\text{subnet}}|=\left(1+\frac{3}{4}\mathrm{D}(\mathrm{D}-2)\right)-\left(\frac{\mathrm{D}^2}{4}-\frac{\mathrm{D}}{2}+1\right)=\frac{\mathrm{D}^2}{2}-\mathrm{D} \tag{125}$$

■

We analyze the required cooperation prelogs. As in the previous subsection, $\gamma_{\text{Tx},k}=\gamma_{\text{Rx},k}=i$ for every cell k that lies i cell hops away from its next master cell, for $i=1,\ldots,\mathrm{D}/2-1$.

Moreover, for each "fast" Tx k with $\gamma_{\text{Tx},k} \in \{1, \ldots, \mathrm{D}/2-2\}$ the size of the "slow" interfering set $\mathcal{I}_k^{(S)}$ is equal to 6, and when $\gamma_{\text{Tx},k} = \mathrm{D}/2-1$ the size of this set is equal to 3 for the corner "fast"-cells and it is equal to 4 for the other "fast"-cells of this layer. By Assumption (68), the 6 corner cells are all "fast" cells. In fact, they are given by $(a_k = \frac{\mathrm{D}}{2}-1, b_k = 0)$, $(a_k = \frac{\mathrm{D}}{2}-1, b_k = \frac{\mathrm{D}}{2}-1)$, $(a_k = 0, b_k = \frac{\mathrm{D}}{2}-1)$, $(a_k = -\frac{\mathrm{D}}{2}+1, b_k = 0)$, $(a_k = -\frac{\mathrm{D}}{2}+1, b_k = -\frac{\mathrm{D}}{2}+1)$, $(a_k = 0, b_k = -\frac{\mathrm{D}}{2}+1)$, for which $a_k + b_k$ is a multiple of $\frac{\mathrm{D}}{2}-1$ and by (68) divisible by 3. Between any two corner cells there are $\frac{\mathrm{D}}{2}-2$ cells with $\gamma_{\text{Tx},k} = \frac{\mathrm{D}}{2}-1$, and $(\frac{\mathrm{D}}{2}-4)/3$ of them are fast cells. (This can be seen by the previously mentioned rotation invariance of both sets $\mathcal{T}_{\text{subnet}}$ and $\mathcal{T}_{\text{fast}}$ with respect to the angle $\frac{2\pi}{3}$, and because the non-corner cells in $\mathcal{T}_{\text{subnet}}^{+}$ with $\gamma_{\text{Tx},k} = \frac{\mathrm{D}}{2}-1$ either have coordinates $a_k = \frac{\mathrm{D}}{2}-1$ and $b_k = 1, \ldots, \frac{\mathrm{D}}{2}-2$ or they have coordinates $a_k = 1, \ldots, \frac{\mathrm{D}}{2}-2$ and $b_k = \frac{\mathrm{D}}{2}-1$. It is easily seen that since $\frac{\mathrm{D}}{2}-1$ is a multiple of 3, a total number of $2\big(\frac{\mathrm{D}}{2}-4\big)/3$ of these cells have sum $a_k + b_k$ that is divisible by 3.)

Since there are 6 "fast" corner cells with $\gamma_{\text{Tx},k} = \mathrm{D}/2-1$, we conclude that there are $6 \cdot \big(\frac{\mathrm{D}}{2}-4\big)/3$ "fast" non-corner cells with $\gamma_{\text{Tx},k} = \mathrm{D}/2-1$. Combining these considerations with (124), we conclude that

$$\begin{aligned}
&\sum_{k \in \mathcal{T}_{\text{fast}} \cap \mathcal{T}_{\text{subnet}}} \left|\mathcal{I}_k^{(S)}\right| \\
&\quad = \sum_{\substack{k \in \mathcal{T}_{\text{fast}} \cap \mathcal{T}_{\text{subnet}}: \\ \gamma_{\text{Tx},k} \neq \frac{\mathrm{D}}{2}-1}} 6 + \sum_{\substack{k \in \mathcal{T}_{\text{fast}} \cap \mathcal{T}_{\text{subnet}}: \\ \gamma_{\text{Tx},k} = \frac{\mathrm{D}}{2}-1 \\ k \text{ a non-corner cell}}} 4 + \sum_{\substack{k \in \mathcal{T}_{\text{fast}} \cap \mathcal{T}_{\text{subnet}}: \\ \gamma_{\text{Tx},k} = \frac{\mathrm{D}}{2}-1 \\ k \text{ a corner cell}}} 3 \qquad (126) \\
&\quad = 6 \cdot |\mathcal{T}_{\text{fast}} \cap \mathcal{T}_{\text{subnet}}| - 2 \cdot \left| \left\{ k \in \mathcal{T}_{\text{fast}} \cap \mathcal{T}_{\text{subnet}} \colon \gamma_{\text{Tx},k} = \frac{\mathrm{D}}{2}-1 \text{ and } k \text{ a non-corner cell} \right\} \right| \\
&\qquad -3 \cdot \left| \left\{ k \in \mathcal{T}_{\text{fast}} \cap \mathcal{T}_{\text{subnet}} \colon \gamma_{\text{Tx},k} = \frac{\mathrm{D}}{2}-1 \text{ and } k \text{ a corner cell} \right\} \right| \qquad (127) \\
&\quad = 6 \cdot \left(\frac{\mathrm{D}^2}{4} - \frac{\mathrm{D}}{2} + 1 \right) - 2 \cdot 6 \cdot \frac{\frac{\mathrm{D}}{2}-4}{3} - 3 \cdot 6 \qquad (128) \\
&\quad = \frac{(3\mathrm{D}-4)(\mathrm{D}-2)}{2} = \frac{3\mathrm{D}^2}{2} - 5\mathrm{D} + 4. \qquad (129)
\end{aligned}$$

Since $\frac{\mathcal{Q}_{K,\text{Rx}}}{K} \to 6$ and since, by a sandwiching argument, $\frac{1}{K}\sum_{k \in \mathcal{T}_{\text{fast}}} |\mathcal{I}_k^{(S)}| \to s^{-1}\sum_{k \in \mathcal{T}_{\text{fast}} \cap \text{subnet}} |\mathcal{I}_k^{(S)}|$ as $K \to \infty$:

$$\lim_{K\to\infty} \frac{\sum_{k \in \mathcal{T}_{\text{fast}}} \left|\mathcal{I}_k^{(S)}\right|}{\mathcal{Q}_{K,\text{Rx}}} = \lim_{K\to\infty} \frac{\sum_{k \in \mathcal{T}_{\text{fast}} \cap \mathcal{T}_{\text{subnet}}} \left|\mathcal{I}_k^{(S)}\right|}{s\mathcal{Q}_{K,\text{Rx}}/K} = \frac{\frac{(3\mathrm{D}-4)(\mathrm{D}-2)}{2}}{\frac{3}{4}\mathrm{D}^2 \cdot 6} = \frac{(3\mathrm{D}-4)(\mathrm{D}-2)}{9\mathrm{D}^2}. \qquad (130)$$

Then, by (21):

$$\mu_{\text{Tx,both}}^{(\mathsf{r})} = \mathsf{L} \cdot \frac{(3\mathrm{D}-4)(\mathrm{D}-2)}{9\mathrm{D}^2}. \qquad (131)$$

To calculate the Rx-cooperation prelog, we notice that for each "slow" cell k with $\gamma_{\text{Rx},k} \in \{1,\ldots,\mathrm{D}/2-2\}$ the "fast" interfering set $\mathcal{I}_k^{(F)}$ is of size 3, and for each "slow" cell k with $\gamma_{\text{Rx},k} = \mathrm{D}/2-1$ it is of size 2. As explained previously, among the $6\cdot\left(\frac{\mathrm{D}}{2}-1\right)$ cells with $\gamma_{\text{Rx},k} = \frac{\mathrm{D}}{2}-1$, there are 6 "fast" corner cells and $\mathrm{D}-8$ "fast" non-corner cells. The remaining are "slow" cells, and therefore

$$\sum_{k\in\mathcal{T}_{\text{slow}}\cap\mathcal{T}_{\text{subnet}}} |\mathcal{I}_k^{(F)}| = 3|\mathcal{T}_{\text{slow}}\cap\mathcal{T}_{\text{subnet}}| - |\{k\in(\mathcal{T}_{\text{slow}}\cap\mathcal{T}_{\text{subnet}})\colon \gamma_{\text{Tx},k}=\mathrm{D}/2-1\}| \tag{132}$$

$$= 3\left(\frac{\mathrm{D}^2}{2}-\mathrm{D}\right) - \left(6\cdot\left(\frac{\mathrm{D}}{2}-1\right)-6-(\mathrm{D}-8)\right) = \frac{3\mathrm{D}^2}{2}-5\mathrm{D}+4. \tag{133}$$

To calculate the sum $\sum_{k\in\mathcal{T}_{\text{slow}}\cap\mathcal{T}_{\text{subnet}}}\gamma_{\text{Rx},k}$, we first characterize the number of "fast" cells in the sector $\mathcal{T}^+_{\text{subnet}}$ that have $\gamma_{\text{Rx},k}=i$, for $i=1,\ldots\mathrm{D}/2-1$. A cell $k\in\mathcal{T}^+_{\text{subnet}}$ has $\gamma_{\text{Rx},k}=i$ if it has coordinates of the form $a_k=i$ and $b_k=0,\ldots,i-1$ or $a_k=1,\ldots,i$ and $b_k=i$. To count the number of "fast" cells in this set, we distinguish different cases for $i \mod 3$:

- If $i \mod 3=0$, then there are $2i/3$ "fast" cells among these cells (namely the cells $(a_k=i,b_k=0)$, $(a_k=i,b_k=3),\ldots,(a_k=i,b_k=i)$, $(a_k=i-3,b_k=i),\ldots,(a_k=3,b_k=i)$) and the remaining $4i/3$ cells are "slow" cells.
- If $i \mod 3=1$, then there are $2(i-1)/3$ "fast" cells among these cells (namely the cells $(a_k=i,b_k=2)$, $(a_k=i,b_k=5),\ldots,(a_k=i,b_k=i-2),(a_k=i-2,b_k=i),\ldots,(a_k=2,b_k=i)$) and the remaining $2(2i+1)/3$ cells are "slow" cells.
- If $i \mod 3=2$, then there are $2(i+1)/3$ "fast" cells among these cells (namely the cells $(a_k=i,b_k=1)$, $(a_k=i,b_k=4),\ldots,(a_k=i,b_k=i-1),(a_k=i-1,b_k=i),\ldots,(a_k=1,b_k=i)$) and the remaining $2(2i-1)/3$ cells are "slow" cells.

By the rotation invariance of all relevant sets with respect to the angle $2\pi/3$, we conclude that

$$|\{k\in\mathcal{T}_{\text{slow}}\cap\mathcal{T}_{\text{subnet}}:\gamma_{\text{Rx},k}=i\}| = \begin{cases} 4i & i \mod 3=0,\\ 4i+2 & i \mod 3=1,\\ 4i-2 & i \mod 3=2.\end{cases} \tag{134}$$

and since $\frac{\mathrm{D}}{2}-1$ is a multiple of 3, see (68):

$$\sum_{k\in\mathcal{T}_{\text{slow}}\cap\mathcal{T}_{\text{subnet}}}\gamma_{\text{Rx},k} = \sum_{i=1}^{\frac{\mathrm{D}}{2}-1} 4i^2 + 2\sum_{j=1}^{\frac{\frac{\mathrm{D}}{2}-1}{3}}(3j-2) - 2\sum_{j=1}^{\frac{\frac{\mathrm{D}}{2}-1}{3}}(3j-1) \tag{135}$$

$$= \frac{\mathrm{D}^3-3\mathrm{D}^2+4}{6}. \tag{136}$$

Putting (129) and (136) together, we obtain:

$$\sum_{k\in\mathcal{T}_{\text{slow}}\cap\mathcal{T}_{\text{subnet}}}\left(|\mathcal{I}_k^{(F)}|+2\gamma_{\text{Rx},k}\right)=\frac{3\mathrm{D}^2}{2}-5\mathrm{D}+4+2\cdot\left(\frac{\mathrm{D}^3-3\mathrm{D}^2+4}{6}\right) \tag{137}$$

$$=\frac{2\mathrm{D}^3+3\mathrm{D}^2-30\mathrm{D}+32}{6}. \tag{138}$$

Since $\frac{\mathcal{Q}_{K,\text{Rx}}}{K}\to 6$ and, by a sandwiching argument, $K^{-1}\sum_{k\in\mathcal{T}_{\text{slow}}}|\mathcal{I}_k^{(F)}|\to s^{-1}\sum_{k\in\mathcal{T}_{\text{slow}}\cap\mathcal{T}_{\text{subnet}}}|\mathcal{I}_k^{(F)}|$ as $K\to\infty$:

$$\lim_{K\to\infty}\frac{\sum_{k\in\mathcal{T}_{\text{slow}}}\left|\mathcal{I}_k^{(F)}\right|+2\gamma_{\text{Rx},k}}{\mathcal{Q}_{K,\text{Rx}}}=\lim_{K\to\infty}\frac{\sum_{k\in\mathcal{T}_{\text{fast}}\cap\mathcal{T}_{\text{subnet}}}\left|\mathcal{I}_k^{(S)}\right|+2\gamma_{\text{Rx},k}}{s\mathcal{Q}_{K,\text{Rx}}/K}$$

$$=\frac{2\mathrm{D}^3+3\mathrm{D}^2-30\mathrm{D}+32}{6\cdot\frac{3}{4}\mathrm{D}^2\cdot 6} \tag{139}$$

$$=\frac{2\mathrm{D}^3+3\mathrm{D}^2-30\mathrm{D}+32}{27\mathrm{D}^2}. \tag{140}$$

By (22), the average Rx-cooperation prelog is

$$\mu_{\text{Rx,both}}^{(\text{r})}=\mathsf{L}\cdot\frac{2\mathrm{D}^3+3\mathrm{D}^2-30\mathrm{D}+32}{27\mathrm{D}^2}. \tag{141}$$

D. Coding scheme to transmit both "fast" and "slow" messages with CoMP transmission

We choose the same cell association as in the previous subsection. Consequently, the scheme achieves the same MG pair and the single-round Rx-cooperation prelog coincides with the single-round Tx-cooperation prelog in the previous Subsection A-C (see (131)):

$$\mu_{\text{Rx,both}}^{(\text{t})}=\mu_{\text{Tx,both}}^{(\text{r})}. \tag{142}$$

To calculate the average Tx-cooperation prelog, we first consider the q-term in (25), which characterizes the number of quantization messages describing the "slow" signals that are counted twice: once for the CoMP transmission and once for the interference mitigation at "fast" Txs. Since the master Tx is a "fast"-Tx, all 6 incoming messages are counted twice. Moreover, for each "fast"-Tx k in layer i (i.e., with $\gamma_{\text{Tx},k}=i$), for $i\in\{1,\dots,\frac{\mathrm{D}}{2}-2\}$, there are 2 neighbouring "slow" Txs in the subsequent layer $i+1$. Thus for each such "fast" Tx, there are 2 messages that are double-counted. Repeating the arguments that justify (128), we obtain that

$$|\{k\in\mathcal{T}_{\text{subnet}}\cap\mathcal{T}_{\text{fast}}\colon\gamma_{\text{Tx},k}=i\}|=\left(\frac{\mathrm{D}^2}{4}-\mathrm{D}\right)-(6+\mathrm{D}-8)=\frac{\mathrm{D}^2}{4}-\frac{3\mathrm{D}}{2}+2. \tag{143}$$

Therefore,

$$q_{\text{subnet}}=6+2\left(\frac{\mathrm{D}^2-6\mathrm{D}+12}{4}-1\right)=\frac{\mathrm{D}^2}{2}-3\mathrm{D}+10. \tag{144}$$

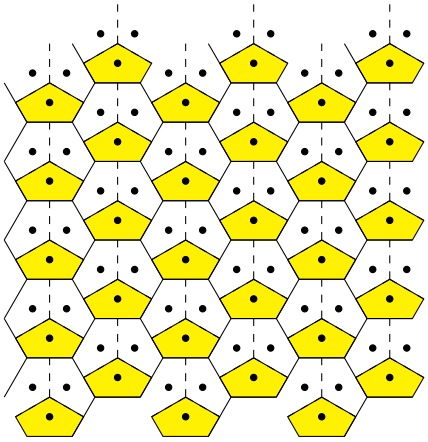

Fig. 10: Illustration of the scheme without cooperation in the sectorized hexagonal network.

The sum $\sum_{k\in\mathcal{T}_{\text{slow}}\cap\mathcal{T}_{\text{subnet}}} 2\gamma_{\text{Tx},k}+\sum_{k\in\mathcal{T}_{\text{fast}}\cap\mathcal{T}_{\text{subnet}}} |\mathcal{I}_k^{(S)}|$ can be calculated as in the previous subsection for the scheme with CoMP reception. Specifically, since $\gamma_{\text{Tx},k} = \gamma_{\text{Rx},k}$, the sum $\sum_{k\in\mathcal{T}_{\text{slow}}\cap\mathcal{T}_{\text{subnet}}} \gamma_{\text{Tx},k}$ is given by the right-hand side of (138). The sum $\sum_{k\in\mathcal{T}_{\text{fast}}\cap\mathcal{T}_{\text{subnet}}} |\mathcal{I}_k^{(S)}|$ is calculated in (129). This establishes:

$$\sum_{k\in\mathcal{T}_{\text{slow}}\cap\mathcal{T}_{\text{subnet}}} 2\gamma_{\text{Tx},k} + \sum_{k\in\mathcal{T}_{\text{fast}}\cap\mathcal{T}_{\text{subnet}}} |\mathcal{I}_k^{(S)}| - q_{\text{subnet}} = \frac{2\mathsf{D}^3 - 12\mathsf{D} - 28}{6}. \tag{145}$$

By now standard asymptotic arguments and by (25), the average Tx-cooperation prelog is then obtained by dividing (145) by $s = \frac{3}{4}\mathsf{D}^2$ and multiplying it by the number of antennas L:

$$\mu_{\text{Tx,both}}^{(\text{t})} = \mathsf{L} \cdot \frac{2\mathsf{D}^3 - 12\mathsf{D} - 28}{27\mathsf{D}^2}. \tag{146}$$

APPENDIX B
CODING SCHEMES AND ANALYSIS IN THE SECTORIZED HEXAGONAL MODEL

In this appendix we prove that the Tx/Rx set associations proposed in Subsection VI are permissible and we provide details on how to compute the corresponding MG pairs and cooperation prelogs.

A. No cooperation scheme

Figure 10 shows the active Txs in yellow and the silenced Txs in white. It is easily seen that transmissions in yellow sectors do not interfere, as they pertain to non-neighbouring sectors. This scheme requires no cooperation messages and achieves the sum MG in (90).

B. Coding scheme to transmit only "slow" messages with CoMP reception

As explained in the main body of the paper, the proposed cell association splits the network into non-interfering subnets. Moreover, in layer $\mathrm{D}/2$ 3 corner cells are completely silenced and each of the remaining cells contains exactly one active sector pertaining to the subnet. The total number of active sectors per cell is thus

$$s_{\text{active}} = 3 + 3 \sum_{i=1}^{\mathrm{D}/2-1} 6i + (3\mathrm{D} - 3) = 9\mathrm{D}^2/4 - 3\mathrm{D}/2. \tag{147}$$

A valid sector partitioning can be obtained by associating all sectors of the cell partitioning proposed for the hexagonal model to the same subset, which then contains (by (116) and because each cell contains 3 sectors):

$$s_{\text{sectors}} = 3\frac{3}{4}\mathrm{D}^2. \tag{148}$$

By these considerations

$$\lim_{K\to\infty} \frac{|\mathcal{T}_{\text{slow}}|}{K} = \frac{s_{\text{active}}}{s_{\text{sectors}}} = \frac{9\mathrm{D}^2/4 - 3\mathrm{D}/2}{9\mathrm{D}^2/4} = \frac{3\mathrm{D}-2}{3\mathrm{D}}, \tag{149}$$

and as a result, by (26) and (27), the proposed cell association achieves the MG pair $(\mathsf{S}^{(F)} = 0, \mathsf{S}^{(S)} = \mathsf{S}^{(S)}_{\text{max}})$ with $\mathsf{S}^{(S)}_{\text{max}}$ defined in (91).

With CoMP reception, this scheme does not use any Tx-cooperation messages and $\mu^{(\mathrm{r})}_{\text{Tx},\mathsf{S}} = 0$. To calculate the required Rx-cooperation prelog, notice that for each $k \in \mathcal{T}_{\text{subnet}}$, $\gamma_{\text{Rx},k} = i$ if k lies in the i-th layer around the master cell. Since in each layer $i \in \{1, \dots, \mathrm{D}/2-1\}$ there are $6i$ cells and thus $18i$ sectors and in layer $\mathrm{D}/2$ there are $3\mathrm{D}-3$ active sectors as explained above,

$$2\sum_{k\in\mathcal{T}_{\text{subnet}}} \gamma_{\text{Rx},k} = 2 \cdot \left(\sum_{i=1}^{\mathrm{D}/2-1} (18i)\cdot i + (3\mathrm{D}-3)\cdot \mathrm{D}/2 \right) = \frac{3\mathrm{D}^2(\mathrm{D}-1)}{2}. \tag{150}$$

and by a sandwiching argument

$$\lim_{K\to\infty} \frac{2\sum_{k\in\mathcal{T}_{\text{slow}}} \gamma_{\text{Rx},k}}{K} = \frac{2\sum_{k\in\mathcal{T}_{\text{subnet}}} \gamma_{\text{Rx},k}}{s_{\text{sector}}} = \frac{(3\mathrm{D}^2(\mathrm{D}-1))/2}{\frac{3\mathrm{D}^2}{4}} = 2(\mathrm{D}-1). \tag{151}$$

Since $\lim_{K\to\infty} \frac{\mathcal{Q}_{K,\text{Rx}}}{K} = 6$, according to (28) the required Rx-cooperation prelog equals

$$\mu^{(\mathrm{r})}_{\text{Rx},\mathsf{S}} = \mathsf{L} \cdot \frac{(\mathrm{D}-1)}{3}. \tag{152}$$

C. Coding scheme to transmit both "fast" and "slow" messages with CoMP reception

Consider the cell and sector association for this network described in the main body of the paper and illustrated in Fig. 8b for $\mathrm{D} = 8$ where white sectors are deactivated, Txs in yellow sectors send "fast" messages, and Txs in blue sectors send "slow" messages. As explained in the preceeding subsection, the network is split into subnets and the total number of active sectors in a subnet is $9\mathrm{D}^2/4 - 3\mathrm{D}/2$, see (147).

We count the number of "fast" sectors in a subnet $\mathcal{T}_{\text{subnet}}$ surrounding a master cell at the origin. Notice that all subnets are symmetric and have same number of "fast" and "slow" sectors. As explained in the main body of the paper, each cell in layer $\mathrm{D}/2$ has 1 active "fast" sector pertaining to the subnet, except for 3 three corner cells that are completely desactivated. The number of "fast" sectors in layer $\mathrm{D}/2$ is thus $3\mathrm{D} - 3$. In each layer-i with $i \in \{1, \ldots, \frac{\mathrm{D}}{2} - 1\}$, each cell has exactly one "fast' sector, except the cells with coordinates satisfying one of the three conditions: ($a_k = 0$ and $b_k > 0$) or ($a_k > 0$ and $b_k = 0$) or ($a_k = b_k < 0$). There are $3(\mathrm{D}/2 - 1)$ such cells, and thus the total number of "fast" sectors in layers $i = 1, \ldots, \mathrm{D}/2 - 1$ is:

$$\sum_{i=1}^{\mathrm{D}/2-1} 6i - 3(\mathrm{D}/2 - 1) = 3\frac{\mathrm{D}(\mathrm{D}-2)}{4} - \frac{3\mathrm{D}}{2} + 3 = \frac{3}{4}\mathrm{D}^2 - 3\mathrm{D} + 3. \tag{153}$$

Since the master cell sends "slow" messages only, we obtain that the number of "fast" sectors in subnet $\mathcal{T}_{\text{subnet}}$ equals

$$|\mathcal{T}_{\text{fast}} \cap \mathcal{T}_{\text{subnet}}| = (3\mathrm{D} - 3) + \left(\frac{3}{4}\mathrm{D}^2 - 3\mathrm{D} + 3\right) = \frac{3}{4}\mathrm{D}^2. \tag{154}$$

Since the total number of active Txs in this subnet equals $s_{\text{active}} = \frac{9\mathrm{D}^2}{4} - \frac{3\mathrm{D}}{2}$, see (147), the subnet's number of "slow" Txs is:

$$|\mathcal{T}_{\text{slow}} \cap \mathcal{T}_{\text{subnet}}| = \frac{6\mathrm{D}^2}{4} - \frac{3\mathrm{D}}{2}. \tag{155}$$

We notice that similarly to the previous subsection, one can obtain a valid cell partitioning by associating a subset of $s = 3\frac{3}{4}\mathrm{D}^2$ cells to each master cell. Since each cell has 3 sectors and because all subnets are equal, applying standard sandwiching arguments to eliminitate edge effects for finite number of users K, we obtain:

$$\lim_{K\to\infty} \frac{|\mathcal{T}_{\text{fast}}|}{K} = \frac{|\mathcal{T}_{\text{fast}} \cap \mathcal{T}_{\text{subnet}}|}{3s} = \frac{\frac{3\mathrm{D}^2}{4}}{\frac{9\mathrm{D}^2}{4}} = \frac{1}{3} \tag{156}$$

and

$$\lim_{K\to\infty} \frac{|\mathcal{T}_{\text{slow}}|}{K} = \frac{|\mathcal{T}_{\text{slow}} \cap \mathcal{T}_{\text{subnet}}|}{3s} = \frac{\frac{6\mathrm{D}^2}{4} - \frac{3\mathrm{D}}{2}}{\frac{9\mathrm{D}^2}{4}} = \frac{2\mathrm{D} - 2}{3\mathrm{D}}. \tag{157}$$

By (19) and (20), this establishes the achievability of the MG pair (93).

To analyze the cooperation prelog of the sector association, notice that for each "fast" Tx/Rx k with $\gamma_{\text{Rx},k} \in \{1, \ldots, \mathrm{D}/2-1\}$ the size of the "slow" interfering set $\mathcal{I}_k^{(S)}$ is equal to 4, and when $\gamma_{\text{Rx},k} = \mathrm{D}/2$ the size of this set is equal to 2 for the three active corner cells and equal to 3 for the other non-corner cells. Considering the fact that the number of "fast" Txs with $\gamma_{\text{Rx},k} = \frac{\mathrm{D}}{2}$ equals $3\mathrm{D}-3$, then by (154) we conclude that

$$\sum_{k \in \mathcal{T}_{\text{fast}} \cap \mathcal{T}_{\text{subnet}}} |\mathcal{I}_k^{(S)}| = 4\left(\frac{3\mathrm{D}^2}{4} - (3\mathrm{D}-3)\right) + 2 \cdot 3 + 3(3\mathrm{D}-6) = 3\mathrm{D}(\mathrm{D}-1). \tag{158}$$

According to (21), the average Tx-cooperation prelog required for the scheme is

$$\mu_{\text{Tx,both}}^{(\text{r})} = \mathsf{L} \cdot \frac{(\mathrm{D}-1)}{9\mathrm{D}}. \tag{159}$$

Fig. 8b also shows that the size of the "fast" interference set $\mathcal{I}_k^{(F)}$ is equal to 2 for each "slow" Tx k. To precisely calculate the number of required Rx-cooperation messages, notice that each non-corner "fast"-Rx k with $\gamma_{\text{Rx},k} = \frac{\mathrm{D}}{2}$ sends its decoded message to two of its neighbours and each corner "fast"-Rx k with $\gamma_{\text{Rx},k} = \frac{\mathrm{D}}{2}$ sends its decoded message to only one neighbouring Rx. As there are $3\mathrm{D}-6$ non-corner Rxs and 3 active corner Rxs in this layer, then the total number of cooperation messages by these Rxs equals $6\mathrm{D}-9$. Any other "fast" Rx who is not in this layer has to send its decoded messages to 3 of its neighbours. By (154), thus these "fast" Rxs send in total $3(\frac{3\mathrm{D}^2}{4} - (3\mathrm{D}-3))$ cooperation messages to their neighbours. Each Rx decoding a "slow" message also sends the quantized version of its channel outputs to the next master Rx. Among the Rxs with $\gamma_{\text{Rx},k} = i$, there are $6i-3$ Rxs observing two "slow" signals and 3 Rxs observing 3 "slow" signals. To sum up, the total number of Rx-cooperation messages transmitted in this scheme is

$$\begin{aligned}\sum_{k \in \mathcal{T}_{\text{slow}} \cap \mathcal{T}_{\text{subnet}}} |\mathcal{I}_k^{(F)}| + 2\gamma_{\text{Rx},k} &= 6\mathrm{D} - 9 + 3(\frac{3\mathrm{D}^2}{4} - (3\mathrm{D}-3)) + 4\sum_{i=1}^{\frac{\mathrm{D}}{2}-1} i(6i-3) + 6\sum_{i=1}^{\frac{\mathrm{D}}{2}-1} 3i \\ &= \frac{\mathrm{D}(2\mathrm{D}^2-5)}{2}.\end{aligned} \tag{160}$$

Thus according to (22), the average Rx-cooperation prelog required by the scheme is

$$\mu_{\text{Rx,both}}^{(\text{r})} = \mathsf{L} \cdot \frac{2\mathrm{D}^2-5}{9\mathrm{D}}. \tag{161}$$

APPENDIX C
PROOF OF PROPOSITION 2

The proof idea of our upper bounds is similar to [18, Lemma 1]. While [18, Lemma 1] is for Wyner's linear soft-handoff model, here we prove a similar result for the hexagonal model. Technically, the main novelty is in identifying appropriate cell partitionings based on which the genie information will be defined.

We first prove

$$\mathsf{S}^{(F)} + \mathsf{S}^{(S)} \leq \frac{\mathsf{L}}{2} + 2(\mu_{\text{Tx}} + \mu_{\text{Rx}}). \tag{162}$$

Partition the cells of the network alternately into red and white cells as depicted in Figure 11, and define

$$\mathbb{M}_{\text{red}} := \{(M_k^{(S)}, M_k^{(F)})\colon k \text{ is a red cell}\} \tag{163}$$

$$\mathbb{X}_{\text{red}} := \{\mathbf{X}_k^n\colon k \text{ is a red cell}\} \tag{164}$$

$$\mathbb{Y}_{\text{red}} := \{\mathbf{Y}_k^n\colon k \text{ is a red cell}\} \tag{165}$$

$$\mathbb{Y}_{\text{white}} := \{\mathbf{Y}_k^n\colon k \text{ is a white cell}\} \tag{166}$$

$$\mathbb{Z}_{\text{red}} := \{\mathbf{Z}_k^n\colon k \text{ is a red cell}\} \tag{167}$$

$$\mathbb{Z}_{\text{white}} := \{\mathbb{Z}_k\colon k \text{ is a white cell}\}. \tag{168}$$

Moreover, for each Tx-cooperation round $j = 1, \ldots, \mathsf{D}_{\text{Tx}}$ define the Tx-cooperation message set

$$\mathbb{T}^{(j)}_{\text{white}\to\text{red}} := \Big\{T^{(j)}_{k\to k'}\colon k \text{ is a white cell},\ k' \text{ is a red cell}\Big\}, \tag{169}$$

where message sets $\mathbb{T}^{(j)}_{\text{red}\to\text{red}}$, $\mathbb{T}^{(j)}_{\text{red}\to\text{white}}$, and $\mathbb{T}^{(j)}_{\text{white}\to\text{white}}$ are defined analogously, and for each Rx-cooperation round $j = 1, \ldots, \mathsf{D}_{\text{Rx}}$ define the Rx-cooperation message set

$$\mathbb{Q}^{(j)}_{\text{white}\to\text{red}} := \Big\{Q^{(j)}_{k\to k'}\colon k \text{ is a white cell},\ k' \text{ is a red cell}\Big\}, \tag{170}$$

where again message sets $\mathbb{Q}^{(j)}_{\text{red}\to\text{red}}$, $\mathbb{Q}^{(j)}_{\text{red}\to\text{white}}$, and $\mathbb{Q}^{(j)}_{\text{white}\to\text{white}}$ are defined analogously.

To prove the converse, for each blocklength n fix encoding, cooperation, and decoding functions so that for sufficiently large blocklength n the probability of error does not exceed $\epsilon > 0$. We show in the following that a super-receiver observing the three items listed in the following can decode all transmitted messages $\{(M_k^{(S)}, M_k^{(F)})\colon\ k = 1, \ldots, K\}$ correctly whenever the K BSs decode them correctly in the original setup. The super-receiver's probability

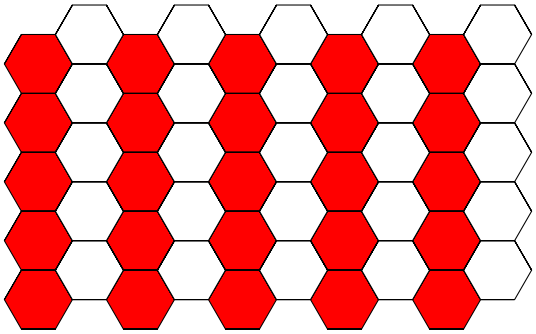

Fig. 11: Cell partitioning used for the first part of the converse bound (88).

of error thus cannot be larger than the original probability of error, which was upper-bounded by ϵ. The three items are:

1) all output signals in red cells, $\mathbb{Y}_{\text{red}}$;
2) all conferencing messages from white to red cells, $\mathbb{T}^{(1)}_{\text{white}\to\text{red}}, \ldots, \mathbb{T}^{(\mathsf{D}_{\text{Tx}})}_{\text{white}\to\text{red}}$ and $\mathbb{Q}^{(1)}_{\text{white}\to\text{red}}, \ldots, \mathbb{Q}^{(\mathsf{D}_{\text{Rx}})}_{\text{white}\to\text{red}}$; and
3) the genie-information

$$\mathbb{G} := \tilde{\mathsf{H}}_{\text{white}\to\text{white}} \tilde{\mathsf{H}}^{-1}_{\text{white}\to\text{red}} \mathbb{Z}_{\text{red}} - \mathbb{Z}_{\text{white}}, \tag{171}$$

where for each pair of colours $c, c' \in \{\text{red, white}\}$ we denote by $\tilde{\mathsf{H}}_{c,c'}$ the channel matrix from mobile users in cells of colour c to BSs in cells of colour c'. In particular, we impose that the diagonal entries of the matrix $\tilde{\mathsf{H}}_{\text{white}\to\text{red}}$ measure the channel coefficients from mobile users in a sector of a white cell to the BS of an adjacent interfering sector in a red cell. (The matrix $\tilde{\mathsf{H}}_{\text{white}\to\text{red}}$ is invertible with probability 1 because of the interference structure of the network and because all channel matrices are full rank, so the genie-information in (171) is well-defined.)

The super-receiver decodes the messages $\{M_k^{(F)}, M_k^{(S)}\}$ by means of the following seven decoding steps:

1) For each round $j = 1, \ldots, \mathsf{D}_{\text{Rx}}$, it applies the appropriate Rx-cooperation functions to the red output signals $\mathbb{Y}_{\text{red}}$ and the previous rounds' Rx-cooperation messages $\{\mathbb{Q}^{(j')}_{\text{white}\to\text{red}}\}_{j'=1}^{j-1}$ and $\{\mathbb{Q}^{(j')}_{\text{red}\to\text{red}}\}_{j'=1}^{j-1}$. This allows the super-receiver to compute the current round-j Rx-cooperation messages $\mathbb{Q}^{(j)}_{\text{red}\to\text{red}}$. (Notice that knowledge of output signals in white cells or conferencing messages sent *to* white cells are not required for this computation.)
2) It applies the appropriate decoding functions $\{g_k^{(n)}, b_k^{(n)} \colon k \text{ is a red cell}\}$ to the output signals $\mathbb{Y}_{\text{red}}$ and the Rx-cooperation messages $\{\mathbb{Q}^{(j)}_{\text{red}\to\text{red}}\}_{j=1}^{\mathsf{D}_{\text{Rx}}}$ to decode messages $\mathbb{M}_{\text{red}}$.

3) For each Tx-cooperation round $j = 1, \ldots, \mathrm{D_{Tx}}$, it applies the appropriate Tx-cooperation functions to the red messages $\mathbb{M}_{\text{red}}$ and the previous rounds' Tx-cooperation messages $\{\mathbb{T}^{(j')}_{\text{white}\to\text{red}}\}_{j'=1}^{j-1}$ and $\{\mathbb{T}^{(j')}_{\text{red}\to\text{red}}\}_{j'=1}^{j-1}$ to obtain the current round-j Tx-cooperation messages $\mathbb{T}^{(j)}_{\text{red}\to\text{red}}$.
4) It applies the encoding functions $\{f_k^{(n)}\}$ to the previously decoded messages $\mathbb{M}_{\text{red}}$ and the reconstructed Tx-cooperation messages $\{\mathbb{T}^{(j)}_{\text{white}\to\text{red}}\}_{j=1}^{\mathrm{D_{Tx}}}$ and $\{\mathbb{T}^{(j')}_{\text{red}\to\text{red}}\}_{j=1}^{\mathrm{D_{Tx}}}$ to construct input signals $\mathbb{X}_{\text{red}}$.
5) With the input and output signals sent and received in red cells, $\mathbb{X}_{\text{red}}$ and $\mathbb{Y}_{\text{red}}$, it reconstructs the output signals received at the BSs in the white cells by forming:

$$\begin{aligned}\mathbb{Y}_{\text{white}} = \tilde{\mathsf{H}}_{\text{white}\to\text{white}}\tilde{\mathsf{H}}^{-1}_{\text{white}\to\text{red}}\big(\mathbb{Y}_{\text{red}} - \tilde{\mathsf{H}}_{\text{red}\to\text{red}}\mathbb{X}_{\text{red}}\big)\\ + \tilde{\mathsf{H}}_{\text{red}\to\text{white}}\mathbb{X}_{\text{red}} - \mathbb{G}.\end{aligned} \tag{172}$$

6) For each Rx-cooperation round $j = 1, \ldots, \mathrm{D_{Rx}}$, it applies the appropriate Rx-cooperation functions to the white and red output signals $\mathbb{Y}_{\text{white}}$ and $\mathbb{Y}_{\text{red}}$ and to the observed and previously calculated Rx-cooperation messages $\{\mathbb{Q}^{(j')}_{\text{white}\to\text{red}}\}_{j'=1}^{j-1}$ and $\{\mathbb{Q}^{(j')}_{\text{red}\to\text{white}}\}_{j'=1}^{j-1}$, $\{\mathbb{Q}^{(j')}_{\text{red}\to\text{red}}\}_{j'=1}^{j-1}$, $\{\mathbb{Q}^{(j')}_{\text{white}\to\text{white}}\}_{j'=1}^{j-1}$, to compute the current round-j Rx-cooperation messages $\mathbb{Q}^{(j)}_{\text{red}\to\text{white}}$ and $\mathbb{Q}^{(j)}_{\text{white}\to\text{white}}$.
7) It applies the appropriate decoding functions $\{g_k^{(n)}, b_k^{(n)}\colon k \text{ is a white cell}\}$ to the output signals $\mathbb{Y}_{\text{white}}$ and the observed or reconstructed Rx-cooperation messages $\{\mathbb{Q}^{(j)}_{\text{red}\to\text{white}}\}_{j=1}^{\mathrm{D_{Rx}}}$ and $\{\mathbb{Q}^{(j)}_{\text{white}\to\text{white}}\}_{j=1}^{\mathrm{D_{Rx}}}$ so as to decode messages $\mathbb{M}_{\text{white}}$.

The above arguments imply that any $2K$-tuple $(R_1^{(F)}, \ldots, R_K^{(F)}, R_1^{(S)}, \ldots, R_K^{(S)})$ that is achievable over the original network from mobile users to BSs is also achievable over the network from mobile users to the super-receiver. So, by Fano's inequality:

$$\begin{aligned}&K(\bar{R}_K^{(F)} + \bar{R}_K^{(S)}) - \epsilon_n\\ &\le \frac{1}{n} I\big(M_1^{(F)}, \ldots, M_K^{(F)}, M_1^{(S)}, \ldots, M_K^{(S)}; \mathbb{Y}_{\text{red}}, \mathbb{T}^{(1)}_{\text{white}\to\text{red}}, \ldots, \mathbb{T}^{(\mathrm{D_{Tx}})}_{\text{white}\to\text{red}}, \mathbb{Q}^{(1)}_{\text{white}\to\text{red}}, \ldots, \mathbb{Q}^{(\mathrm{D_{Rx}})}_{\text{white}\to\text{red}}, \mathbb{G}\big)\\ &= \frac{1}{n} I\big(M_1^{(F)}, \ldots, M_K^{(F)}, M_1^{(S)}, \ldots, M_K^{(S)}; \mathbb{Y}_{\text{red}}\big)\\ &\quad + \frac{1}{n} I\big(M_1^{(F)}, \ldots, M_K^{(F)}, M_1^{(S)}, \ldots, M_K^{(S)}; \mathbb{T}^{(1)}_{\text{white}\to\text{red}}, \ldots, \mathbb{T}^{(\mathrm{D_{Tx}})}_{\text{white}\to\text{red}}, \mathbb{Q}^{(1)}_{\text{white}\to\text{red}}, \ldots, \mathbb{Q}^{(\mathrm{D_{Rx}})}_{\text{white}\to\text{red}} \big| \mathbb{G}, \mathbb{Y}_{\text{red}}\big)\\ &\quad + \frac{1}{n} I\big(M_1^{(F)}, \ldots, M_K^{(F)}, M_1^{(S)}, \ldots, M_K^{(S)}; \mathbb{G}\big|\mathbb{Y}_{\text{red}}\big),\end{aligned} \tag{173}$$

where ϵ_n is a function that tends to zero as $n \to \infty$.

We notice that the first summand in (173) has DoF at most $\mathsf{L} \cdot |\mathcal{I}_{\text{red}}|$, where $\mathcal{I}_{\text{red}} := \{k\colon \text{cell } k \text{ is red}\}$; the second summand in (173) has DoF at most $4|\mathcal{I}_{\text{white}}| \cdot (\mu_{\text{Tx}} + \mu_{\text{Rx}})$, where $\mathcal{I}_{\text{white}} := \{k\colon \text{cell } k \text{ is white}\}$; and the third summand in (173) has zero DoF because, for any N:

$$I(M_1^{(F)}, \ldots, M_K^{(F)}, M_1^{(S)}, \ldots, M_K^{(S)}; \mathbb{G}|\mathbb{Y}_{\text{red}}) \leq h(\mathbb{G}) - h(\mathbb{G}|\mathbb{Z}_{\text{red}}) \tag{174}$$

$$= h(\mathbb{G}) - h(\mathbb{Z}_{\text{white}}), \tag{175}$$

which is finite and does not grow with power P, irrespectively of the chosen encoding, cooperation, and decoding functions. Dividing (173) by $1/2\log(1+\mathsf{P})$ and taking the limit $\mathsf{P} \to \infty$, we obtain the following bound on the DoF:

$$K \cdot (\mathsf{S}^{(F)} + \mathsf{S}^{(S)}) \leq \mathsf{L}|\mathcal{I}_{\text{red}}| + 4|\mathcal{I}_{\text{white}}| \cdot (\mu_{\text{Tx}} + \mu_{\text{Rx}}). \tag{176}$$

Dividing the above by K and letting $K \to \infty$ establishes the desired bound after noticing that

$$\overline{\lim_{K\to\infty}} \frac{|\mathcal{I}_{\text{red}}|}{K} = \overline{\lim_{K\to\infty}} \frac{|\mathcal{I}_{\text{white}}|}{K} = 1/2. \tag{177}$$

We now prove the second upper bound

$$\mathsf{S}^{(F)} + \mathsf{S}^{(S)} \leq \mathsf{L} \cdot \left(1 - \frac{1}{2 + 2\mathsf{D}}\right). \tag{178}$$

To prove the converse, fix a sequence (in the blocklength n) of encoding, cooperation, and decoding functions with D_{Tx} and D_{Rx} Tx- and Rx-cooperation rounds with vanishing probability of error as the blocklength increases.

Fix now a blocklength n and partition the set of cells $\{1, \ldots, K\}$ into red, purple, blue, and white cells as shown in Figure 12. That means, every $2(\mathsf{D}+1)$-th column has only white cells, all columns in the middle of two white columns have only red cells, the D_{Tx} columns to the left and right of red columns have only purple cells, and all remaining columns consist of only blue cells.

The sets

$$\mathcal{I}_{\text{red}} := \{k\colon \text{cell } k \text{ is red}\}, \tag{179}$$

$$\mathcal{I}_{\text{white}} := \{k\colon \text{cell } k \text{ is white}\}, \tag{180}$$

$$\mathcal{I}_{\text{blue}} := \{k\colon \text{cell } k \text{ is blue}\}, \tag{181}$$

$$\mathcal{I}_{\text{purple}} := \{k\colon \text{cell } k \text{ is purple}\}, \tag{182}$$

then satisfy the following limiting behaviours:

$$\lim_{K\to\infty} \frac{|\mathcal{I}_{\text{white}}|}{K} = \frac{1}{2(\mathrm{D}+1)}, \tag{183a}$$

$$\lim_{K\to\infty} \frac{|\mathcal{I}_{\text{blue}}| + |\mathcal{I}_{\text{red}}| + |\mathcal{I}_{\text{yellow}}|}{K} = \frac{2\mathrm{D}-1}{2(\mathrm{D}+1)}. \tag{183b}$$

Define for each color $c \in \{\text{red, purple, blue, white}\}$:

$$\mathbb{M}_{\text{c}} := \{(M_k^{(F)}, M_k^{(S)})\colon \text{cell } k \text{ is of color } c\}, \tag{184}$$

$$\mathbb{X}_{\text{c}} := \{\mathbf{X}_k\colon \text{cell } k \text{ is of color } c\}, \tag{185}$$

$$\mathbb{Y}_{\text{c}} := \{\mathbf{Y}_k\colon \text{cell } k \text{ is of color } c\}, \tag{186}$$

$$\mathbb{Z}_{\text{c}} := \{\mathbf{Z}_k\colon \text{cell } k \text{ is of color } c\}. \tag{187}$$

Moreover, for each Tx-cooperation round $j = 1, \ldots, \mathrm{D}_{\text{Tx}}$ define the Tx-cooperation message set

$$\mathbb{T}^{(j)}_{\text{purple/red}\to\text{purple/red}} := \Big\{T^{(j)}_{k\to k'}\colon k \text{ is a purple or red cell and } \textit{less than} \\ j \textit{ hops away from a blue cell}, \ k' \text{ is a purple or red cell}\Big\}, \tag{188}$$

and for each Rx-cooperation round $j = 1, \ldots, \mathrm{D}_{\text{Rx}}$ define the Rx-cooperation message sets

$$\mathbb{Q}^{(j)}_{\text{blue/purple/red}\to\text{blue/purple/red}} := \Big\{Q^{(j)}_{k\to k'}\colon k \text{ is a blue or red cell and } \textit{less than} \\ j \textit{ hops away from a white cell}, \ k' \text{ is a red cell}\Big\}, \tag{189}$$

and

$$\mathbb{Q}^{(j)}_{\text{all}\to\text{white/blue}} := \Big\{Q^{(j)}_{k\to k'}\colon k \text{ is any cell}, \ k' \text{ is a white or blue cell}\Big\}. \tag{190}$$

Notice that $\mathbb{T}^{(j)}_{\text{purple/red}\to\text{purple/red}}$ contains only the round-j Tx-cooperation messages that can be propagated to a red cell within the remaining $\mathrm{D}_{\text{Tx}} - j$ Tx-cooperation rounds. In other words, it contains only Tx-cooperation messages that potentially can influence the encodings at the red Txs. Since red and blue cells are $\mathrm{D}_{\text{Tx}}+1$ cell hops apart, the Tx-cooperation messages $\mathbb{T}^{(j)}_{\text{purple/red}\to\text{purple/red}}$ in particular do not depend on the messages of blue or white cells, and as a consequence can be computed from the messages in red and purple cells. Similarly, $\mathbb{Q}^{(j)}_{\text{blue/purple/red}\to\text{blue/purple/red}}$ contains only the round-j Rx-cooperation messages that can be propagated to a red pruple cell within the remaining $\mathrm{D}_{\text{Rx}} - j$ Rx-cooperation rounds and thus serve in the decoding of red or purple messages. Since red and purple cells are at least D_{Rx} cell hops apart, the Rx-cooperation messages $\mathbb{Q}^{(j)}_{\text{blue/purple/red}\to\text{blue/purple/red}}$ do not depend on the outputs of white cells and can be computed from the outputs in blue, purple, and red cells. These properties will be crucial later on in the proof.

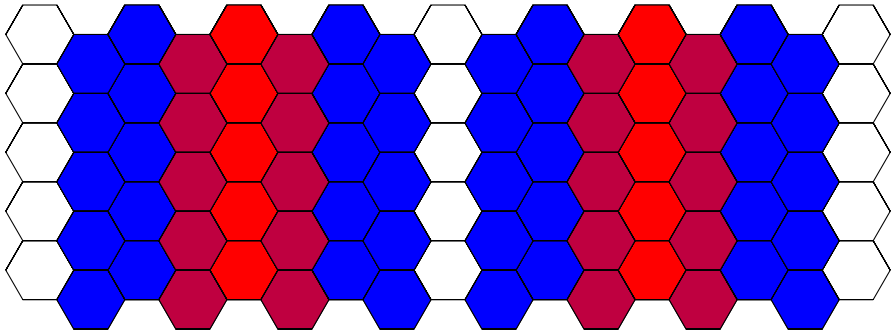

Fig. 12: Proposed cell-partitioning when $\mathrm{D} = 3$.

Notice that a super-receiver with the three items described shortly can decode all the $2K$ messages $\{M_1^{(F)}, \ldots, M_K^{(F)}, M_1^{(S)}, \ldots, M_K^{(S)}\}$ with probability of error at most ϵ. The mentioned three items are:

- all output signals in red cells, $\mathbb{Y}_{\text{red}}$;
- all output signals in blue cells, $\mathbb{Y}_{\text{blue}}$;
- the genie-information

$$\mathbb{G} := \tilde{\mathsf{H}}_{\text{white/blue/purple}\to\text{white}} \tilde{\mathsf{H}}^{-1}_{\text{white/blue/purple}\to\text{red/blue/purple}} \mathbb{Z}_{\text{red/blue/purple}} - \mathbb{Z}_{\text{white}}, \tag{191}$$

  where $\tilde{\mathsf{H}}_{\text{white/blue/purple}\to\text{white}}$ denotes the channel matrix from Txs in white, purple, or blue cells to Rxs in white cells and $\tilde{\mathsf{H}}_{\text{white/blue/purple}\to\text{red/blue/purple}}$ denotes the channel matrix from Txs in white, purple, or blue cells to Rxs in red, purple, or blue cells. In particular, we impose that the diagonal entries of the matrix $\tilde{\mathsf{H}}_{\text{white/blue /purple}\to\text{red/blue/purple}}$ indicate the channel coefficients from Txs in white, purple, or blue cells to the Rxs of adjacent interfering red, purple, or blue cells. This way, and since the channel matrices are full rank, $\tilde{\mathsf{H}}_{\text{white/purple/blue}\to\text{red/purple/blue}}$ is square (recall that we assume the same number of red and white cells) and invertible. The genie-information in (194) is thus well-defined.

Notice that if the super-receiver performs the following seven decoding steps, then it decodes all $2K$ messages $M_1^{(F)}, \ldots, M_K^{(F)}, M_1^{(S)}, \ldots, M_K^{(S)}$ correctly whenever the K BSs decode them correctly in the original setup. The super-receiver's probability of error can thus not be larger than the probability of error in the original setup.

The seven decoding steps at the super-receiver are:

1) For each Rx-cooperation round $j = 1, \ldots, \mathrm{D}_{\text{Rx}}$, it applies the appropriate Rx-cooperation functions to the output signals $\mathbb{Y}_{\text{red}}, \mathbb{Y}_{\text{purple}}$ and $\mathbb{Y}_{\text{blue}}$ and to the previously computed Rx-

cooperation messages $\{\mathbb{Q}^{(j')}_{\text{blue/purple/red}\to\text{blue/purple/red}}\}_{j'=1}^{j-1}$ so as to obtain the current round-j Rx-cooperation messages $\mathbb{Q}^{(j)}_{\text{blue/purple/red}\to\text{blue/purple/red}}$. (Notice that knowledge of output signals in white cells or conferencing messages exchanged with white cells are not required for this computation.)

2) It applies the appropriate decoding functions $\{g_k^{(n)}, b_k^{(n)}\}$ to the output signals $\mathbb{Y}_{\text{red}}$ and $\mathbb{Y}_{\text{purple}}$ and to the Rx-cooperation messages $\{\mathbb{Q}^{j}_{\text{blue/purple/red}\to\text{blue/purple/red}}\}_{j'=1}^{\text{D}_{\text{Rx}}}$ so as to decode messages $\mathbb{M}_{\text{red}}$ and $\mathbb{M}_{\text{purple}}$.

3) For each Tx-cooperation round $j = 1, \ldots, \text{D}_{\text{Tx}}$, it applies the appropriate Tx-cooperation functions to the decoded red and purple messages $\mathbb{M}_{\text{red}}$ and $\mathbb{M}_{\text{purple}}$ and to the previous rounds' Tx-cooperation messages $\{\mathbb{T}^{(j')}_{\text{purple/red}\to\text{purple/red}}\}_{j'=1}^{j-1}$to obtain the current round-j Tx-cooperation messages $\mathbb{T}^{(j)}_{\text{purple/red}\to\text{purple/red}}$.

4) It applies the encoding functions $\{f_k^{(n)}\}$ to the previously decoded messages $\mathbb{M}_{\text{red}}$ and the reconstructed Tx-cooperation messages $\{\mathbb{T}^{(j)}_{\text{purple/red}\to\text{purple/red}}\}_{j=1}^{\text{D}_{\text{Tx}}}$ to construct input signals $\mathbb{X}_{\text{red}}$.

5) It reconstructs the output signals received at the BS in the white cells $\mathbb{Y}_{\text{white}}$ as:

$$\mathbb{Y}_{\text{white}} = \tilde{\mathsf{H}}_{\text{white/blue/purple}\to\text{white}}\tilde{\mathsf{H}}^{-1}_{\text{white/blue/purple}\to\text{red/blue/purple}}(\mathbb{Y}_{\text{red/blue/purple}} - \tilde{\mathsf{H}}_{\text{red}\to\text{red/blue/purple}}\mathbb{X}_{\text{red}}) - \mathbb{G}. \tag{192}$$

6) It iteratively reconstructs all Rx-cooperation messages $\{\mathbb{Q}^{(j)}_{\text{all}\to\text{white/blue}}\}_{j=1}^{\text{D}_{\text{Rx}}}$ intended to blue or white cells.

7) It applies the appropriate decoding functions $\{g_k^{(n)}, b_k^{(n)}\}$ to the observed and reconstructed output signals $\mathbb{Y}_{\text{white}}$ and $\mathbb{Y}_{\text{blue}}$ to decode messages $\mathbb{M}_{\text{white}}$ and $\mathbb{M}_{\text{blue}}$.

The above arguments imply that any $2K$-tuple $(R_1^{(F)}, \ldots, R_K^{(F)}, R_1^{(S)}, \ldots, R_K^{(S)})$ that is achievable over the original network from mobile users to BSs is also achievable over the network from mobile users to the super-receiver. So, by Fano's inequality:

$$\begin{aligned} K(\bar{R}_K^{(F)} + \bar{R}_K^{(S)}) &\leq \frac{1}{n} I\big(M_1^{(F)}, \ldots, M_K^{(F)}, M_1^{(S)}, \ldots, M_K^{(S)}; \mathbb{Y}_{\text{red}}, \mathbb{Y}_{\text{purple}}, \mathbb{Y}_{\text{blue}}, \mathbb{G}\big) + \epsilon_n \\ &= \frac{1}{n} I\big(M_1^{(F)}, \ldots, M_K^{(F)}, M_1^{(S)}, \ldots, M_K^{(S)}; \mathbb{Y}_{\text{red}}, \mathbb{Y}_{\text{purple}}, \mathbb{Y}_{\text{blue}}\big) \\ &\quad + \frac{1}{n} I\big(M_1^{(F)}, \ldots, M_K^{(F)}, M_1^{(S)}, \ldots, M_K^{(S)}; \mathbb{G} \big| \mathbb{Y}_{\text{red}}, \mathbb{Y}_{\text{purple}}, \mathbb{Y}_{\text{blue}}\big) \\ &\quad + \epsilon_n, \end{aligned} \tag{193}$$

where ϵ_n tends to 0 as $n \to \infty$.

Notice that the first summand has MG at most $\mathsf{L}(|\mathcal{I}_{\text{red}}|+|\mathcal{I}_{\text{blue}}|)$, whereas the second summand has zero MG because

$$\begin{aligned} I(M_1^{(F)},\ldots,M_K^{(F)},M_1^{(S)},\ldots,M_K^{(S)};\mathbb{G}|\mathbb{Y}_{\text{red}},\mathbb{Y}_{\text{purple}},\mathbb{Y}_{\text{blue}}) &\le h(\mathbb{G})-h(\mathbb{G}|\mathbb{Z}_{\text{red}},\mathbb{Z}_{\text{purple}},\mathbb{Z}_{\text{blue}}) \\ &= h(\mathbb{G})-h(\mathbb{Z}_{\text{white}}), \end{aligned} \tag{194}$$

Dividing by $\log(1+\mathsf{P})$ and taking the limit $\mathsf{P}\to\infty$, we thus obtain:

$$K(\mathsf{S}^{(F)}+\mathsf{S}^{(S)}) \le \mathsf{L}(|\mathcal{I}_{\text{red}}|+|\mathcal{I}_{\text{blue}}|). \tag{195}$$

Dividing by K and letting $K\to\infty$ yields the desired bound, by (183).

APPENDIX D
PROOF OF PROPOSITION 3

We start by proving the upper bound

$$\mathsf{S}^{(F)}+\mathsf{S}^{(S)} \le \frac{\mathsf{L}}{2}+\frac{2}{3}\mu_{\text{Rx}}+\frac{4}{3}\mu_{\text{Tx}}. \tag{196}$$

For each power $\mathsf{P}>0$, fix a sequence of encoding, cooperation and decoding functions so that the average block power constraint is satisfied and for sufficiently large blocklength n, the probability of error does not exceed ϵ. Partition the network into red and white cells as depicted in Fig. 13. Define

$$\begin{aligned} \mathbb{M}_{\text{red}}^{(F)} &:= \{M_k^{(F)} : k \text{ is a mobile user in a red cell}\} \\ \mathbb{M}_{\text{red}}^{(S)} &:= \{M_k^{(S)} : k \text{ is a mobile user in a red cell}\} \\ \mathbb{X}_{\text{red}} &:= \{X_k : k \text{ is a mobile user in a red cell}\} \\ \mathbb{Y}_{\text{red}} &:= \{Y_{\tilde{k}} : \tilde{k} \text{ is a red cell}\} \\ \mathbb{Y}_{\text{white}} &:= \{Y_{\tilde{k}} : \tilde{k} \text{ is a white cell}\} \end{aligned}$$

Fix also an arbitrary pair $(\mathsf{D}_{\text{Tx}},\mathsf{D}_{\text{Rx}})$ such that $\mathsf{D}_{\text{Tx}}+\mathsf{D}_{\text{Rx}}=\mathsf{D}$. Then, for each round $j=1,\ldots,\mathsf{D}_{\text{Tx}}$, we introduce the following shortcut for transmitter conferencing messages

$$\mathbb{T}_{C_1\to C_2}^{(j)} := \{T_{k\to\ell}^{j,(n)} : k \text{ is in a cell colored in } C_1, \ell \text{ is in a cell colored in } C_2\}$$

where k and ℓ are random mobile users and C_1 and C_2 are cell colors, i.e., $C_1,C_2\in\{\text{red},\text{white}\}$. Also, for each $j'=1,\ldots,\mathsf{D}_{\text{Rx}}$, define the following shortcuts:

$$\mathbb{Q}_{C_1\to C_2}^{(j')} := \{Q_{\tilde{k}\to\ell}^{j',(n)} : \tilde{k} \text{ is a cell colored in } C_1, \ell \text{ is a cell colored in } C_2\}.$$

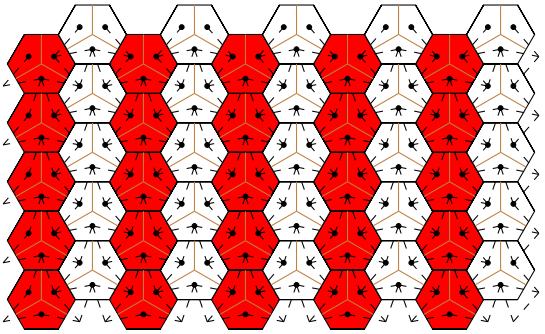

Fig. 13: Cell partitioning used for the first part of the converse bound (103).

Consider a virtual super receiver that observes $\mathbb{Y}_{\text{red}}$, $\mathbb{T}_{\text{white}\to\text{red}}$, $\mathbb{Q}_{\text{white}\to\text{red}}$ and genie information $\mathbb{G}$

$$\mathbb{G} = \mathbb{Y}_{\text{white}} - \mathsf{H}^{-1}_{\text{white}\to\text{red}}(\mathbb{Y}_{\text{red}} - \mathsf{H}_{\text{red}\to\text{red}}\mathbb{X}_{\text{red}}) - \mathsf{H}_{\text{red}\to\text{white}}\mathbb{X}_{\text{red}}, \tag{197}$$

where $\mathsf{H}_{C_1\to C_2}$ denotes the channel matrix from the mobile users in the cells of color C_1 to the basestations in the cells of color C_2. Because these matrices are square and the channel coefficients are drawn i.i.d according to a continues distribution, they are invertible. Notice that $\mathbb{G}$ satisfies

$$\lim_{\mathsf{P}\to\infty}\frac{1}{\log(1+\mathsf{P})}I(M_1,\ldots,M_{3K};\mathbb{G}|\mathbb{Y}_{\text{red}},\mathbb{T}^{(1)}_{\text{white}\to\text{red}},\ldots, \mathbb{T}^{(\text{D}_{\text{Tx}})}_{\text{white}\to\text{red}},\mathbb{Q}^{(1)}_{\text{white}\to\text{red}},\ldots,\mathbb{Q}^{(\text{D}_{\text{Rx}})}_{\text{white}\to\text{red}}) = 0, \tag{198}$$

irrespective of the fixed encoding, cooperation and decoding functions.

Consider now Algorithm 1. If the virtual super receiver follows Algorithm 1, then it decodes all the $3K$ messages $\{M_k\}$ correctly whenever the K BSs decode them correctly in the original setup.

We can therefore conclude that any tuple $(R_1,\ldots,R_{3K})$ with $R_k = R_k^{(F)} + R_k^{(S)}$ and $k = 1,\ldots,3K$, that is achievable over the original network to the BSs is also achievable over the network to the virtual super receiver. So, by Fano's inequality:

$$\begin{aligned}
3K(R^{(F)}+R^{(S)}) &\le \frac{1}{n}I(M_1,\ldots,M_{3K};\mathbb{Y}_{\text{red}},\mathbb{T}^{(1)}_{\text{white}\to\text{red}},\\
&\ldots,\mathbb{T}^{(\text{D}_{\text{Tx}})}_{\text{white}\to\text{red}},\mathbb{Q}^{(1)}_{\text{white}\to\text{red}},\ldots,\mathbb{Q}^{(\text{D}_{\text{Rx}})}_{\text{white}\to\text{red}},\mathbb{G}) + \frac{\epsilon}{n}\\
&= \frac{1}{n}I(M_1,\ldots,M_{3K};\mathbb{Y}_{\text{red}})\\
&+ \frac{1}{n}I(M_1,\ldots,M_{3K};\mathbb{T}^{(1)}_{\text{white}\to\text{red}},\ldots,\mathbb{T}^{(\text{D}_{\text{Tx}})}_{\text{white}\to\text{red}},
\end{aligned}$$

Algorithm 1

Initialization:
for $j' = 1, \ldots, \mathrm{D_{Rx}}$ **do**
  Apply the cooperation functions $\psi_{\tilde{k}\to\ell}^{j',(n)}$ to $\mathbb{Y}_{\text{red}}$ and $\{\mathbb{Q}_{\text{white}\to\text{red}}^{(j'')}\}_{j''=1}^{j'-1}$ and $\{\mathbb{Q}_{\text{red}\to\text{red}}^{(j'')}\}_{j''=1}^{j'-1}$.
  Compute $\mathbb{Q}_{\text{white}\to\text{red}}^{(j')}$ and $\mathbb{Q}_{\text{red}\to\text{red}}^{(j')}$.
end for
Apply the decoding function $g_{\tilde{k}}^{(n)}$ to $\mathbb{Y}_{\text{red}}$ and $\{\mathbb{Q}_{\text{white}\to\text{red}}^{(j')}\}_{j'=1}^{\mathrm{D_{Rx}}}$ and $\{\mathbb{Q}_{\text{red}\to\text{red}}^{(j')}\}_{j'=1}^{\mathrm{D_{Rx}}}$ to decode messages $\mathbb{M}_{\text{red}}$. This yields $\hat{\mathbb{M}}_{\text{red}}$.
for $j = 1, \ldots, \mathrm{D_{Tx}}$ **do**
  Apply the transmitter conferencing functions $\xi_{k\to\ell}^{j,(n)}$ to $\hat{\mathbb{M}}_{\text{red}}$, $\{\mathbb{T}_{\text{white}\to\text{red}}^{(j'')}\}_{j''=1}^{j-1}$ and $\{\mathbb{T}_{\text{red}\to\text{red}}^{(j'')}\}_{j''=1}^{j-1}$.
  Compute $\mathbb{T}_{\text{white}\to\text{red}}^{(j)}$ and $\mathbb{T}_{\text{red}\to\text{red}}^{(j)}$.
end for
Apply the encoding function $f_k^{(n)}$ to the decoded messages $\hat{\mathbb{M}}_{\text{red}}$, $\{\mathbb{T}_{\text{white}\to\text{red}}^{(j)}\}_{j=1}^{\mathrm{D_{Tx}}}$ and $\{\mathbb{T}_{\text{red}\to\text{red}}^{(j)}\}_{j=1}^{\mathrm{D_{Tx}}}$ to construct $\mathbb{X}_{\text{red}}$.
Reconstruct $\mathbb{Y}_{\text{white}}$ with $\mathbb{X}_{\text{red}}$, $\mathbb{Y}_{\text{red}}$, and the genie information $\mathbb{G}$.
for $j' = 1, \ldots, \mathrm{D_{Rx}}$ **do**
  Apply the cooperation functions $\psi_{\tilde{k}\to\ell}^{j',(n)}$ to $\mathbb{Y}_{\text{white}}$, $\mathbb{Y}_{\text{red}}$ and to $\{\mathbb{Q}_{\text{red}\to\text{white}}^{(j'')}\}_{j''=1}^{j'-1}$ and $\{\mathbb{Q}_{\text{white}\to\text{white}}^{(j'')}\}_{j''=1}^{j'-1}$.
  Compute $\mathbb{Q}_{\text{red}\to\text{white}}^{(j')}$ and $\mathbb{Q}_{\text{white}\to\text{white}}^{(j')}$.
end for
Apply the decoding function $g_{\tilde{k}}^{(n)}$ to $\mathbb{Y}_{\text{white}}$ and $\{\mathbb{Q}_{\text{red}\to\text{white}}^{(j')}\}_{j'=1}^{\mathrm{D_{Rx}}}$ and $\{\mathbb{Q}_{\text{white}\to\text{white}}^{(j')}\}_{j'=1}^{\mathrm{D_{Rx}}}$ to decode messages $\mathbb{M}_{\text{white}}$.
End

$$\mathbb{Q}_{\text{white}\to\text{red}}^{(1)}, \ldots, \mathbb{Q}_{\text{white}\to\text{red}}^{(\mathrm{D_{Rx}})} | \mathbb{Y}_{\text{red}}\big)$$
$$+ \frac{1}{n} I(M_1, \ldots, M_{3K}; \mathbb{G} | \mathbb{Y}_{\text{red}}, \mathbb{T}_{\text{white}\to\text{red}}^{(1)}, \ldots,$$
$$\mathbb{T}_{\text{white}\to\text{red}}^{(\mathrm{D_{Tx}})}, \mathbb{Q}_{\text{white}\to\text{red}}^{(1)}, \ldots, \mathbb{Q}_{\text{white}\to\text{red}}^{(\mathrm{D_{Rx}})}) + \frac{\epsilon}{n}, \tag{199}$$

By considering (198) and dividing (199) by $\frac{1}{2}\log(1+\mathsf{P})$ and taking the limits $\epsilon \to 0$ and $\mathsf{P} \to \infty$,

the following bound is obtained on the multiplexing gain region:

$$3K(\mathsf{S}^{(F)}+\mathsf{S}^{(S)}) \leq 3\mathsf{L}|\mathcal{I}_{\text{red}}| + 4(K-|\mathcal{I}_{\text{red}}|)(\mu_{\text{Rx}}+2\mu_{\text{Tx}}). \tag{200}$$

where $|\mathcal{I}_{\text{red}}| := \{i : \text{cell } i \text{ is red}\}$, and

$$\lim_{K\to\infty} \frac{|\mathcal{I}_{\text{red}}|}{K} = \frac{1}{2}. \tag{201}$$

Finally, by considering (201) and dividing (200) by $3K$, when $K \to \infty$ the desired bound is established. The second part of the bound (103) is proved in an analogous way to the proof of the second part of the bound (88). See Appendix C.

REFERENCES

[1] R. Kassab, O. Simeone, and P. Popovski, "Coexistence of URLLC and eMBB services in the C-RAN uplink: an information-theoretic study," in *Proc. IEEE GLOBECOM*, Abu Dhabi, United Arab Emirates, Dec 9–13, 2018.

[2] A. Matera, R. Kassab, O. Simeone, and U. Spagnolini, "Non-orthogonal eMBB-URLLC radio access for cloud radio access networks with analog fronthauling," *Entropy*, vol. 20, no. 9, pp. 661, 2018.

[3] A. Anand, G. d. Veciana, and S. Shakkottai, "Joint scheduling of URLLC and eMBB traffic in 5G wireless networks," *IEEE/ACM Trans. on Networking*, vol. 28, no. 2, pp. 477–490, Apr. 2020.

[4] H. Nikbakht, M. Wigger, W. Hachem, and S. Shamai (Shitz), " Mixed delay constraints on a fading C-RAN uplink," in *Proc. IEEE ITW 2019*, Visby, Sweden, Aug 25–28, 2019.

[5] K. M. Cohen, A. Steiner, and S. Shamai (Shitz) "The broadcast approach under mixed delay constraints," in *Proc. IEEE ISIT 2012*, Cambridge (MA), USA, July 1–6, pp. 209–213, 2012.

[6] R. Zhang, J. Cioffi, and Y.-C. Liang, "MIMO broadcasting with delay-constrained and no-delay-constrained services," in *Proc. IEEE ICC 2005*, Seoul, South Korea, May 16–20, pp. 783–787, 2005.

[7] R. Zhang, "Optimal dynamic resource allocation for multi-antenna broadcasting with heterogeneous delay-constrained traffic," *IEEE J. of Sel. Topics in Signal Proc.*, vol. 2, no. 2, pp. 243–255, Apr. 2008.

[8] W. Huleihel and Y. Steinberg, "Channels with cooperation links that may be absent," *IEEE Trans. Inf. Theory*, vol. 63, no. 9, pp. 5886–5906, Sep. 2017.

[9] E. Aktas, J. Evans, and S. Hanly, "Distributed decoding in a cellular multiple-access channel," *IEEE Trans. Wireless Comm.*, vol. 7, no. 1, pp. 241–250, Jan 2008.

[10] S. I. Bross, A. Lapidoth, and M. A. Wigger, "The Gaussian MAC with conferencing encoders," in *Proc. IEEE ISIT 2008*, Toronto, ON, Canada, pp. 2702–2706, July 2008.

[11] A. Sendonaris, E. Erkip, and B. Aazhang, "User cooperation diversity, part I: System description," *IEEE Trans. on Comm.*, vol. 51, no. 11, pp. 1927–1938, Nov 2003.

[12] A. Sendonaris, E. Erkip, and B. Aazhang, "User cooperation diversity, part II: Implementation aspects and performance analysis," *IEEE Trans. on Comm.*, vol. 51, no. 11, pp. 1939–1948, Nov 2003.

[13] A. El Gamal and V. V. Veeravalli, "Flexible backhaul design and degrees of freedom for linear interference channels", *Proc. IEEE ISIT 2014*, Hawaii, Jul. 2014.

[14] A. El Gamal, V. S. Annapureddy, and V. V. Veeravalli, "Interference channels with coordinated multi point transmission: Degrees of freedom, message assignment, and fractional reuse", *IEEE Trans. Inf. Theory*, vol. 60, pp. 3483–3498, 2014.

[15] M. Bande, A. El Gamal, and V. V. Veeravalli, "Degrees of freedom in wireless interference networks with cooperative transmission and backhaul load constraints," *IEEE Trans. Inf. Theory*, vol. 65, no. 9, pp. 5816–5832, Sep. 2019.

[16] S. Shamai (Shitz) and M. Wigger, "Rate-limited transmitter-cooperation in Wyner's asymmetric interference network," in *Proc. IEEE ISIT 2011*, St. Petersburg, Russia, Jul./Aug. 2011, pp. 425–429.

[17] A. Lapidoth, N. Levy, S. Shamai (Shitz), and M. Wigger, "Cognitive Wyner networks with clustered decoding," *IEEE Trans. Inf. Theory,* vol. 60, no. 10, pp. 6342–6367, Oct. 2014.

[18] M. Wigger, R. Timo, and S. Shamai (Shitz), "Conferencing in Wyner's asymmetric interference network: effect of number of rounds," *IEEE Trans. Inf. Theory*, vol. 63, no. 2, pp. 1199–1226, Feb. 2017.

[19] H. Nikbakht, M. Wigger, and S. Shamai (Shitz), "Multiplexing gains under mixed-delay constraints on Wyner's soft-handoff model," *Entropy*, vol. 22, no. 2, pp. 182, 2020.

[20] V. S. Annapureddy, A. El Gamal, and V. V. Veeravalli, "Degrees of freedom of interference channels with CoMP transmission and reception," *IEEE Trans. Inf. Theory*, vol. 58, no. 9, pp. 5740–5760, Sep. 2015.

[21] V. V. Veeravalli, and A. El Gamal, "Interference management in wireless networks: Fundamental bounds and the role of cooperation", *Cambridge University Press*, 2018.

[22] A. D. Wyner, "Shannon-theoretic approach to a Gaussian cellular multiple-access channel," *IEEE Trans. Inf. Theory*, vol. 40, no. 6, pp. 1713–1727, Nov. 1994.

[23] S. V. Hanly and P. A. Whiting, "Information-theoretic capacity of multi-receiver networks," *Telecommunication Systems*, vol. 1, pp. 1–42, 1993.

[24] W. Yu, T. Kwon and C. Shin, "Multicell coordination via joint scheduling, beamforming, and power spectrum adaptation," *IEEE Trans. on Wireless Comm.*, vol. 12, no. 7, pp. 1–14, July 2013.

[25] J. Chen, U. Mitra and D. Gesbert, "Optimal UAV relay placement for single user capacity maximization over terrain with obstacles," in *Proc. IEEE SPAWC 2019*, Cannes, France, pp. 1–5, July 2019.

[26] N. Levy and S. Shamai (Shitz), "Clustered local decoding for Wyner-type cellular models," *IEEE Trans. Inf. Theory*, vol. 55, no. 11, pp. 4976–4985, Nov. 2009.

[27] L. Zhou and W. Yu, "Uplink multicell processing with limited backhaul via per-base-station successive interference cancellation," *IEEE J. on Sel. Areas in Comm.*, vol. 31, pp. 1981–1993, Oct. 2013.

[28] O. Simeone, O. Somekh, H. V. Poor and S. Shamai (Shitz), "Local base station cooperation via finite-capacity links for the uplink of linear cellular networks," *IEEE Trans. Inf. Theory,* vol. 55, no. 1, pp. 190–204, Jan. 2009.

[29] O. Simeone, N. Levy, A. Sanderovich, O. Somekh, B. M. Zaidel, H. V. Poor and S. Shamai (Shitz), "Cooperative wireless cellular systems: An information-theoretic view," *Foundations and Trends in Commun. and Info. Theory, Now Publishers Inc.*, Hanover MA, vol. 8, no. 1–2, pp. 1–177, 2012.

[30] S. A. Jafar, "Interference alignment a new look at signal dimensions in a communication network," *Found. and Trends in Com. and Inf. Theory*, vol. 7, no. 1, pp. 1–134, 2011.

[31] G. Sridharan and W. Yu, "Degrees of freedom of mimo cellular networks: Decomposition and linear beamforming design," *IEEE Trans. Inf. Theory*, vol. 61, no. 6, pp. 3339–3364, June 2015.

[32] V. Ntranos, M. A. Maddah-Ali, and G. Caire, "Cellular interference alignment," *IEEE Trans. Inf. Theory*, vol. 61, no. 3, pp. 1194–1217, Mar. 2015.

[33] H. Nikbakht, M. Wigger, and S. Shamai (Shitz), "Multiplexing gain region of sectorized cellular networks with mixed delay constraints," in *Proc. IEEE SPAWC 2019*, Cannes, France, 2–5 July 2019.

[34] G. Katz, B. M. Zaidel, and S. Shamai (Shitz), "On layered transmission in clustered cooperative cellular architectures," in *Proc. IEEE ISIT 2013*, Istanbul, Turkey, Jul. 7–12, pp. 1162–1166, 2013.

[35] A. Khina, T. Philosof, and M. Laifenfeld, "Layered uplink transmission in clustered cellular networks," *arXiv:1604.01113*.

[36] J. Wang, B. Yuan, L. Huang, and S. Ali Jafar, "Sum-GDoF of 2-user interference channel with limited cooperation under finite precision CSIT," *IEEE Trans. Inf. Theory*, vol. 66, no. 11, Nov. 2020, pp. 6999–7021.

[37] S. Gelincik, M. Wigger, and L. Wang, "DoF in sectorized cellular systems with BS cooperation under a complexity constraint," in *Proc. IEEE ISWCS 2018*, Lisbon, Portugal, Aug 28–31, 2018.

[38] R. Gül, D. Stotz, S. A. Jafar, H. Bölcskei and S. Shamai, "Canonical conditions for K/2 degrees of freedom," *arXiv:2006.02310v1*, 2020.

[39] R. H. Etkin and E. Ordentlich, "The degrees-of-freedom of the K-user Gaussian interference channel is discontinuous at rational channel coefficients," *IEEE Transactions on Information Theory*, vol. 55, no. 11, pp. 4932–4946, Nov 2009.

[40] A. S. Motahari, S. Oveis-Gharan, M. A. Maddah-Ali, and A.K. Khandani, "Real interference alignment: Exploiting the potential of single antenna systems," *IEEE Transactions on Information Theory*, vol. 60, no. 8, pp. 4799–4810, Aug 2014.

[41] J. Xu, J. Zhang and J. G. Andrews, "On the accuracy of the Wyner model in cellular networks," *IEEE transactions on wireless communications*, vol. 10, no. 9, Sep. 2011, pp. 3098–3109.